6-11-82

(1)

With Alan

ABACT –
ABJDS – Jim's subroutines
Vector manipulation

AB2 – old subroutine – simulation of exp response
but wrong algorithm
integration from $\int_{\nu_j}^{\nu_{j+1}}$ instead of $\int_{\nu_j}^{\infty}$

has all stuff for doing transverse integrals analytic

AB1 – fit program
Calls SIMCOM – puts simulation into fit

AB3 – subroutines
VSCCOP
ABCCUR } dummies of things in AB2
DCUR

RESPTEST has $\int_{\nu_j}^{\infty}$ for δ-functions
CUPINT – gives current A, B, C
assuming δ-function for ν transv
TRANSP
AREAOV

Currently all for π-meals

DRESPTEST – D-exp subroutines

2) Sensitive Area Response Function for D-cup

Definitions:

$$\psi = \sqrt{v_x^2 + v_y^2} \,/\, v_z$$

$$\begin{cases} s_1 = .430 + \dfrac{.942}{1+\sqrt{1 - v_x^2/v_z^2}} + \dfrac{.198}{1+\sqrt{1+v_s^2/v_z^2}} \\ s_2 = .705 + \dfrac{.590}{1+\sqrt{1+v_s^2/v_z^2}} \\ s_3 = .495 + \dfrac{.720}{1+\sqrt{1 - v_x^2/v_z^2}} + \dfrac{.290}{1+\sqrt{1+v_s^2/v_z^2}} \end{cases}$$

$$\begin{cases} b_1^{\pm} = \dfrac{1.230 \pm 1.118}{s_1} \\ b_2^{\pm} = \dfrac{4.491 \pm 3.629}{s_2} \\ b_3^{\pm} = \dfrac{1.058 \pm .940}{s_3} \end{cases}$$

$$q_i^{(\pm)} = \frac{1}{\psi} \frac{\sqrt{(\psi^2 - (b_i^-)^2)((b_i^+)^2 - \psi^2)}}{b_i^+ \pm b_i^-}$$

$i = 1, 2, 3$

Response Function : $R_j(\psi)$

$$R_j(\psi) = \begin{cases} 1 & 0 < \psi < b_3^- \\ 1 - \frac{1}{\pi}\left[\sin^{-1} q_1^- + 0.9845_1 \psi q_1^+ - 1.21 \sin^{-1} q_1^+\right] & b_3^- < \psi < b_0 \\ \frac{1}{\pi}\left[\sin^{-1} q_1^- - 0.9845_1 \psi q_1^+ + 1.21 \sin^{-1} q_1^+\right] & b_0 < \psi < b_2^- \\ \frac{1}{\pi}\left[\sin^{-1} q_1^- - 0.9845_1 \psi q_1^+ + 1.21 \sin^{-1} q_1^+ - \sin^{-1} q_2^- - 0.3415_2 \psi q_2^+ + 1.532 \sin^{-1} q_2^+\right] & b_2^- < \psi < b_* \\ \frac{1}{\pi}\left[1.21 \sin^{-1} q_3^- - 1.4485_3 \psi q_3^+ + 1.532 \sin^{-1} q_3^+\right] & b_* < \psi < b_3^+ \end{cases}$$

where

$$b_0 = \frac{.512}{s_1}$$

$$b_* = 1.468 \sqrt{\frac{s_3 - 0.143 s_2}{s_1 s_2 s_3}}$$

$$b_3^- = \frac{.118}{s_3}$$

$$b_2^- = \frac{.862}{s_2}$$

$$b_3^+ = \frac{2.00}{s_3}$$

Main Sensor.

$$\Delta I_j = \underbrace{\sum_{i,k} W_i(\mu_x)\, W_k(\mu_y)\, Q_{ik}}_{G} \frac{A_0 T_0 \varepsilon e n \Delta v_z\, u}{\sqrt{\pi}} e^{-(u-\mu_2)^2}$$

$$W_i(\mu_e) = \frac{c_i e^{-a_i \frac{\mu_e^2}{u^2+a_i}}}{\sqrt{1+\frac{a_i}{u^2}}} \qquad (\mu_e = \mu_x, \mu_y)$$

$$Q_{ik} = \frac{1}{4}\left(\Omega_L^i - \Omega_R^i\right)\left(\Omega_U^k - \Omega_D^k\right)$$

$$\Omega_K^{e\cdot} = \frac{\Phi(z'_{Ke}) - \Phi(z_{Ke})}{z'_{Ke} - z_{Ke}}$$

$x_c = 1.01$, $x_c' = 4.94$

$$\begin{cases} z_{Le}^{(i)} = \sqrt{a_e+u^2}\,\dfrac{x_c^{(i)}}{5} - \dfrac{u}{\sqrt{a_e+u^2}}\mu_x \\ z_{Re}^{(i)} = -\sqrt{a_e+u^2}\,\dfrac{x_c^{(i)}}{5} - \dfrac{u}{\sqrt{a_e+u^2}}\mu_x \end{cases}$$

$y_0 = -2.02$, $y_0' = -3.63$

$$\begin{cases} z_{Ue}^{(i)} = \sqrt{a_e+u^2}\,\dfrac{y_0^{(i)}(\bar{x}_m)}{5} - \dfrac{u}{\sqrt{a_e+u^2}}\mu_y \\ z_{De}^{(i)} = \sqrt{a_e+u^2}\,\dfrac{y_0^{(i)}}{5} - \dfrac{u}{\sqrt{a_e+u^2}}\mu_y \end{cases}$$

$$\Phi(z) = z\,\mathrm{erf}(z) + \frac{e^{-z^2}}{\sqrt{\pi}}$$

$y_0(x) =$

$y_0'(x) =$

Main Sensor

(a) For $u^2 \gg a_i$ and $\frac{\mu_x, \mu_y}{u} \ll u$

$$z_{ic}^{(i)} \cong \frac{u}{5} x_c^{(i)} - \mu_x \gg 1 \quad \therefore \quad \Omega_L^i \approx 1 \; ; \; \Omega_R^i \approx -1$$

$$\Omega_U^{ik} \approx 1 \; ; \; \Omega_D^k \approx -1$$

$$G \approx \sum c_i e^{-a_i \mu_x^2/u^2} c_k e^{-a_k \mu_y^2/u^2}$$

$$c_2 = 1 - c_1$$

$$G \approx \sum c_i c_k e^{-\frac{a_i \mu_x^2 + a_k \mu_y^2}{u^2}} = c_1^2 e^{-a_1 \mu_b^2/u^2} + c_2^2 e^{-a_2 \mu_b^2/u^2} + c_1 c_2 \left(e^{-(a_1 \mu_x^2 + a_2 \mu_y^2)/u^2} + e^{-(a_2 \mu_x^2 + a_1 \mu_y^2)/u^2} \right)$$

$$a_1 = \frac{2.16 \times 10^{-2}}{\epsilon^{2.22}} \left(1 + 25.6 \epsilon^{1.86} \right)$$

$$a_2 = \frac{4.16 \times 10^{-3}}{\epsilon^{1.91}} \left(1 + 9.73 \epsilon^{1.68} \right)$$

$$c_1 = \frac{.141}{\epsilon^{.401}} \left(1 + .125 \epsilon^{8.92} \right)$$

$$\sum c_i c_k = c_1^2 + 2 c_1 c_2 + c_2^2 = c_1^2 + 2 c_1 (1 - c_1) + 1 - 2 c_1 + c_1^2 = 1$$

$$a_1 \mu_x^2 + a_2 \mu_y^2 = (a_1 \cos^2\varphi + a_2 \sin^2\varphi) \mu_b^2$$

$$= a_1 \mu_b^2 + (a_2 - a_1) \sin^2\varphi \, \mu_b^2$$

$$a_2 \mu_x^2 + a_1 \mu_y^2 = a_2 \mu_b^2 - (a_2 - a_1) \sin^2\varphi \, \mu_b^2$$

$$\left(\frac{a_1 + a_2}{2} + \frac{a_1 - a_2}{2} \right) \cos^2\varphi + \left(\frac{a_1 + a_2}{2} - \frac{a_1 - a_2}{2} \right) \sin^2\varphi$$

$$= \frac{a_1 + a_2}{2} + \frac{a_1 - a_2}{2} (\cos^2\varphi - \sin^2\varphi)$$

(***)

$$G \approx C_1^2 e^{-a_1 \mu_t^2/u^2} + C_2^2 e^{-a_2 \mu_t^2/u^2} + C_1 C_2 e^{-\frac{a_1+a_2}{2}\mu_t^2/u^2}\left(e^{-\frac{a_1-a_2}{2}(\cos^2\varphi - \sin^2\varphi)\mu_t^2/u^2} + e^{+(\cdots)}\right)$$

$$\cos^2\varphi - \sin^2\varphi = \frac{1+\cos 2\varphi}{2} - \frac{1-\cos 2\varphi}{2} = \cos 2\varphi$$

$$G = \left(C_1 e^{-\frac{a_1}{2}\mu_t^2/u^2}\right)^2 + \left(C_2 e^{-\frac{a_2}{2}\mu_t^2/u^2}\right)^2$$

$$+2C_1 e^{-\frac{a_1}{2}\mu_t^2/u^2}\, C_2 e^{-\frac{a_2}{2}\mu_t^2/u^2} \cosh\left(\frac{a_1-a_2}{2}\cos 2\varphi\, \mu_t^2/u^2\right)$$

$$G \cong D_1^2 + D_2^2 + 2D_1 D_2 \cosh\Delta$$

$$D_i \cong C_i e^{-\frac{1}{2}a_i \mu_t^2/u^2} \approx C_i\left(1 - \tfrac{1}{2}a_i \mu_t^2/u^2\right)$$

$$\Delta = \frac{a_1 - a_2}{2}\cos 2\varphi\, \frac{\mu_t^2}{u^2} \ll 1$$

for $u^2 \gg a_i$, $\mu_t \ll u$

$$G \approx (D_1 + D_2)^2 = \left(\underbrace{C_1 + C_2}_{1} - \tfrac{1}{2}(a_1+a_2)\mu_t^2/u^2\right)$$

$$G \approx 1 - \frac{a_1+a_2}{2}\mu_t^2/u^2$$

$$\cosh\Delta = 1 + \frac{1}{2!}\Delta^2 + \cdots$$

(b) $u^2 \ll a_i$

$$\frac{Z_{Li}^{(1)}}{R} = \left(\begin{matrix}+\\-\end{matrix}\right)\frac{a_i}{S} x_c^{(1)} - \frac{u}{\sqrt{a_i}}\mu_x$$

(****)

(c)

$Q_{ik} \approx 1$ e.g., when $\left(u^2 \gg a_i \,;\, |\vec{\mu}_t| \lesssim |u-1|\right)$

$$G = D_1^2 + D_2^2 + 2D_1 D_2 \cosh\Delta$$

$$D_i = \frac{c_i}{\sqrt{1+\frac{a_i}{u^2}}}\, e^{-\frac{a_i}{2(a_i+u^2)}\mu_t^2} \qquad (i=1,2)$$

$$\Delta = \frac{1}{2}\left(\frac{a_1}{a_1+u^2} - \frac{a_2}{a_2+u^2}\right)\mu_t^2 \cos 2\varphi$$

$$\begin{cases} \mu_x = \mu_t \cos\varphi \\ \mu_y = \mu_t \sin\varphi \end{cases} \quad \Big| \quad \cos 2\varphi = \cos^2\varphi - \sin^2\varphi$$

$$e^{-\frac{a_1\mu_t^2}{2(a_1+u^2)} + \frac{a_2\mu_t^2}{2(a_2+u^2)}} \left(e^{\frac{a_1\mu_t^2\cos^2\varphi}{2(a_1+u^2)}} + e^{-\Delta}\right)$$

$$-\alpha_1 - \alpha_2 + (\alpha_1 - \alpha_2)(\cos^2\varphi - \sin^2\varphi)$$

$$= -2\alpha_1 \sin^2\varphi - 2\alpha_2 \cos^2\varphi = -\left(\frac{a_1\mu_y^2}{a_1+u^2} + \frac{a_2\mu_x^2}{a_2+u^2}\right)$$

$$-\alpha_1 - \alpha_2 - (\alpha_1 - \alpha_2)(\cos^2\varphi - \sin^2\varphi)$$

$$= -2\alpha_1 \cos^2\varphi - 2\alpha_2 \sin^2\varphi = -\left(\frac{a_1\mu_x^2}{a_1+u^2} + \frac{a_2\mu_y^2}{a_2+u^2}\right)$$

✓

$$\bar{P}(x) = \begin{cases} 1 & 0 < |x| < 1.1 \\ \xi \dfrac{4.94 - |x|}{3.84} & 1.1 < |x| < 4.94 \end{cases}$$

$$\xi = 1.257 - 0.063|x| - 0.126\sqrt{x^2 - 5.10|x| + 6.612}$$

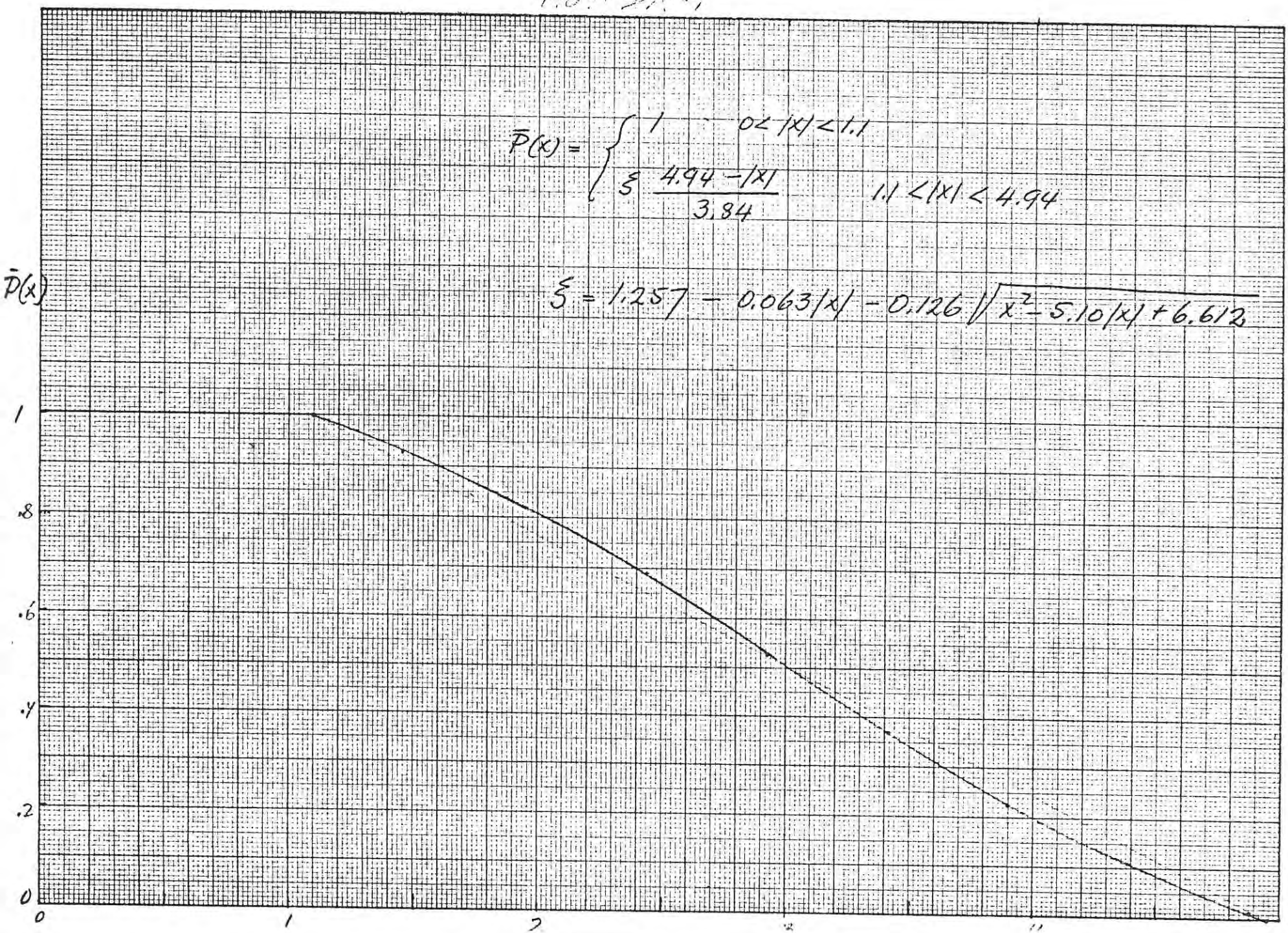

Summary — Main-Sensor Response

Transp.

$$T = T_0 \left(c_1 e^{-a_1 v_x^2/v_z^2} + c_2 e^{-a_2 v_x^2/v_z^2}\right) \times \left(c_1 e^{-a_1 v_y^2/v_z^2} + c_2 e^{-a_2 v_y^2/v_z^2}\right)$$

$$T_0 = .805^2 = 0.65$$

---

a_i, c_i are functions of $\epsilon = \sqrt{\frac{m v_z^2}{2q\phi}} - 1$

Sensitive Area Fct : $R(x,y)$

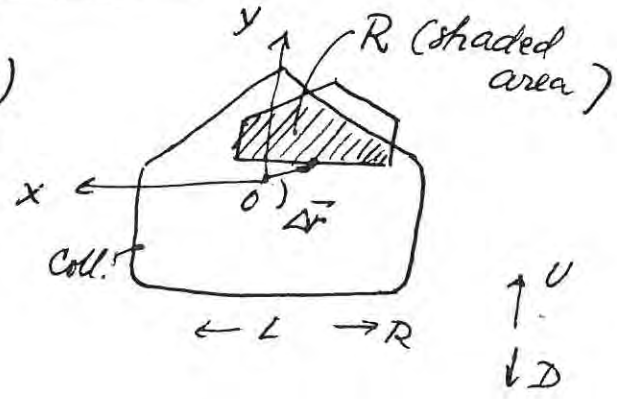

$$R(-x,y) = R(x,y)$$

$$x = \frac{\Delta x}{H} \qquad y = \frac{\Delta y}{H} \qquad H = 4.10\,cm$$

Trapizoidal Approx

R vs. y for given |x|

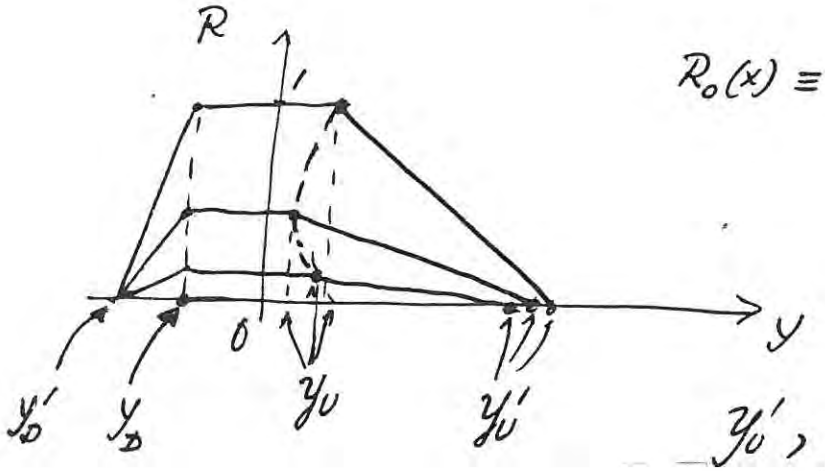

$R_0(x) \equiv R(x,0)$ given fct of x

$y_D = -2.02$

$y_D' \approx -3.63$

---

y_U', y_U given fcts of x (see graph)

x	R_0	y_0	y_0'
0	1	.707	2.32
.488	1	.512	2.46
.976	1	.205	2.53
1.46	.93	−.090	2.46
1.95	.82	−.327	2.36
2.44	.69	−.456	2.21
2.93	.53	−.444	2.05
3.41	.37	−.371	1.83
3.90	.23	−.285	1.58
4.39	.108	−.049	1.27
4.88	.012	+.51	1.0

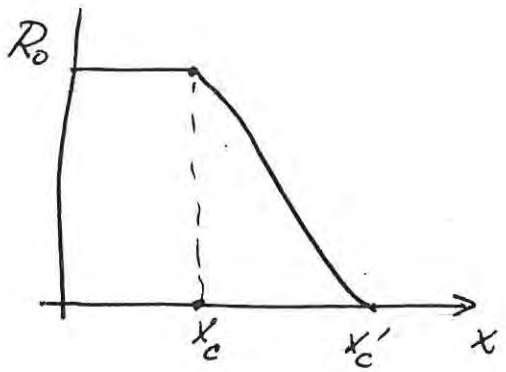

$x_c = 1.10$

$x_c' = 4.94$

$$R_0 \approx \begin{cases} 1 & 0 < |x| < x_c \\ 1.29 - .26|x| & x_c < |x| < x_c' \end{cases}$$

$$0 \le |x| \le x_c$$

or

$$R_0 \cong \begin{cases} 1 & \\ \dfrac{x_c' - |x|}{x_c' - x_c} & x_c \le |x| \le x_c' \end{cases}$$

$y_0(x) \approx$

$y_0'(x) \approx$

Mano. & Transp. functions

$c_1 + c_2 = 1$

$i,j = 1,2$

$$F_{ij} \equiv c_i c_j \, e^{-a_i v_x^2/v_z^2 - (v_x - V_x)^2/w^2 - a_j v_y^2/v_z^2 - (v_y - V_y)^2/w^2}$$

$$F_{ij} \equiv G_{ix} G_{jy} C_{ij}$$

$$C_{ij} = c_i c_j \, e^{-\frac{a_i}{u^2 + a_i}\mu_x^2 - \frac{a_j}{u^2 + a_j}\mu_y^2}$$

$$u = \frac{v_z}{w} \; ; \; \mu_{x,y} = \frac{V_{x,y}}{w} \; ; \quad (\bar{V} \text{ is wind velocity})$$

$$\begin{cases} G_{ix} \equiv e^{-\alpha_i (x - \bar{x})^2} \\ G_{jy} \equiv e^{-\alpha_j (y - \bar{y})^2} \end{cases}$$

Defs

$$\alpha_{i,j} = \frac{u^2 + a_{i,j}}{S^2} \qquad (S = S(\epsilon))$$

$$G_{ix} = \mu_x \frac{Su}{u^2 + a_i} \; ; \; G_{jy} = \mu_y \frac{Su}{u^2 + a_j}$$

$$x = S\frac{v_x}{v_z} \; ; \; y = S\frac{v_y}{v_z}$$

$$I_{ij} \equiv \iint_{-\infty}^{+\infty} R(x,y) \, G_{ix} \, G_{jy} \, dx \, dy$$

$$\iint_{-\infty}^{+\infty} F_{ij}(v_x, v_y) R \, dv_x dv_y = \frac{v_z^2}{S^2} C_{ij} \, I_{ij}$$

$$R(x,y) = R_0(x)\begin{cases} \dfrac{y-y_D'}{y_D-y_D'} & y_D' < y < y_D \\ 1 & y_D < y < y_U \\ \dfrac{y_U'-y}{y_U'-y_U} & y_U < y < y_U' \end{cases}$$

$$\bar{I}_{ij} = \int_{-x_c'}^{x_c'} R_0(x)\, G_{ix}\, dx\, J_{ij}(x)$$

$$J_{ij}(x) = \int_{y_D'}^{y_D} \frac{y-y_D'}{y_D-y_D'} G_{jy}\, dy + \int_{y_D}^{y_U} G_{jy}\, dy + \int_{y_U}^{y_U'} \frac{y_U'-y}{y_U'-y_U} G_{jy}\, dy$$

$$J_j(x) = K_j \left[-\frac{\bar{\Phi}(z_{Dj}') - \bar{\Phi}(z_{Dj})}{z_{Dj}' - z_{Dj}} + \frac{\bar{\Phi}(z_{Uj}') - \bar{\Phi}(z_{Uj})}{z_{Uj}' - z_{Uj}} \right]$$

$$\bar{\Phi}(z) \equiv z\,\mathrm{erf}(z) + \frac{1}{\sqrt{\pi}} e^{-z^2} \quad ; \quad \bar{\Phi}'(z) = \mathrm{erf}(z), \quad \bar{\Phi}(0) = \frac{1}{\sqrt{\pi}} = .564$$

$$\mathrm{erf}(z) = \frac{2}{\sqrt{\pi}} \int_0^z e^{-t^2} dt$$

$$z_{Aj} = (y_A - \sigma_{yj})\sqrt{\alpha_j} \qquad (A \Rightarrow D, U)$$

$$z_{Aj}' = (y_A' - \sigma_{yj})\sqrt{\alpha_j}$$

$$K_j = \frac{\sqrt{\pi}}{2} \frac{1}{\sqrt{\alpha_j}}$$

If $J_j(x)$ slowly varying in x:

$$\bar{I}_{ij} = J_j(\bar{x}_i)\, K_i \left[-\frac{\bar{\Phi}(z_{Li}') - \bar{\Phi}(z_{Li})}{z_{Li}' - z_{Li}} + \frac{\bar{\Phi}(z_{Ri}') - \bar{\Phi}(z_{Ri})}{z_{Ri}' - z_{Ri}} \right]$$

$$\begin{cases} x_R = -x_L = x_c \\ x_R' = -x_L' = x_c' \end{cases} \qquad z_{Bi} = (x_B - \sigma_i)\sqrt{\alpha_i} \qquad z_{Bi}' = (x_B' - \sigma_i)\sqrt{\alpha_i} \qquad (B = L, R)$$

Fig. 1 (for Main Sensor - Trapez. Approx)

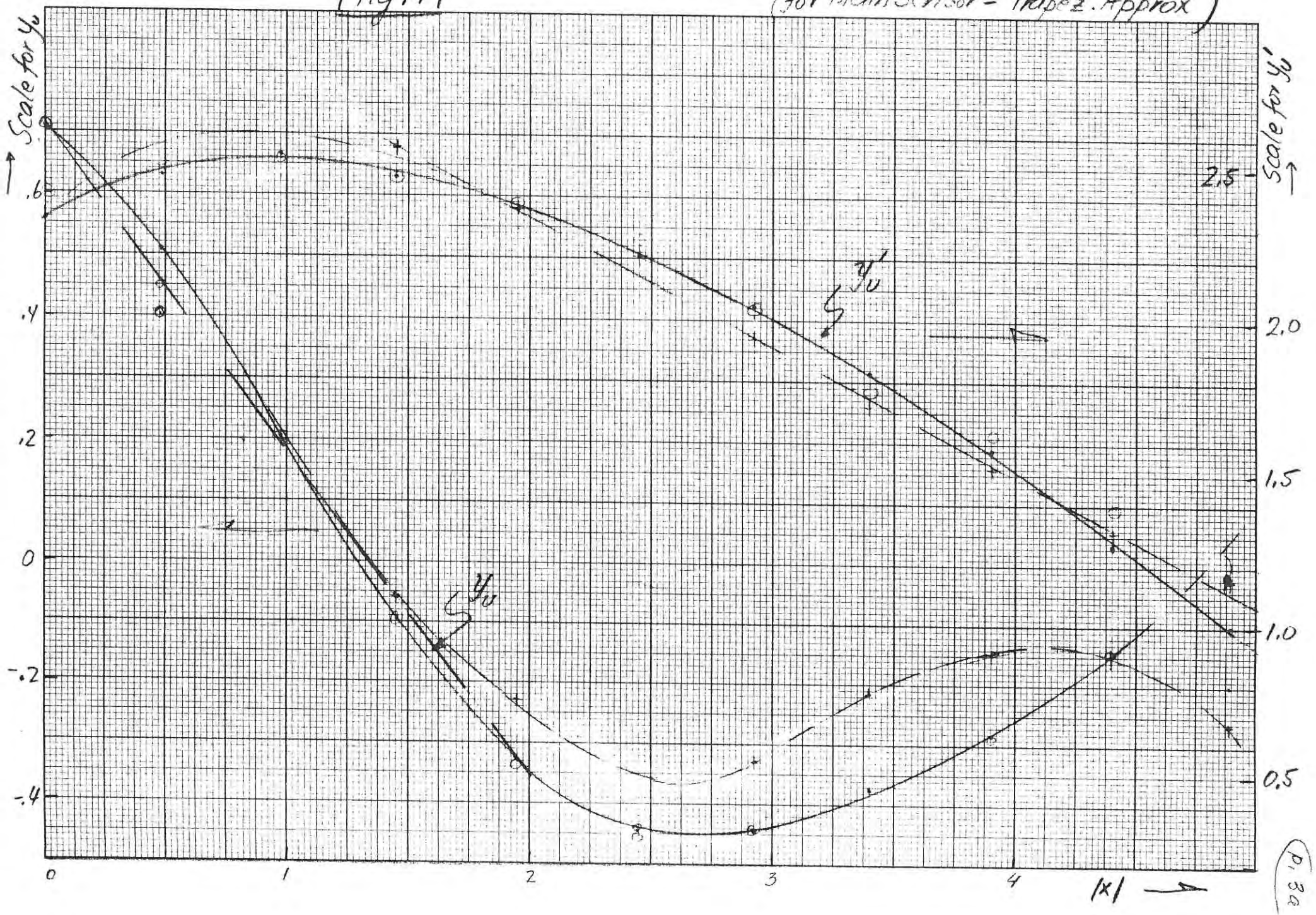

$$\bar{x}_i = \frac{1}{\sqrt{\alpha_i}} \; \frac{-\psi_i(z'_{Li}) + \psi_i(z_{Li}) + \psi_i(z'_{Ri}) - \psi_i(z_{Ri})}{\Phi(z'_{Li}) - \Phi(z_{Li}) + \Phi(z'_{Ri}) - \Phi(z_{Ri})}$$

~~$\psi_i(z) = \left(\sqrt{\alpha_i}\,\sigma_{xi}\,z - \frac{1}{2}\right) erf(z) + \frac{1}{\sqrt{\pi}}\left(z + \sqrt{\alpha_i}\,\sigma_{xi}\,e^{-z^2}\right)$~~

$$\psi_i = \sqrt{\alpha_i}\,\sigma_{xi}\left(\Phi(z) - \frac{1}{\sqrt{\pi}} e^{-z^2}\right) - \frac{1}{2} erf(z)$$

$$= \sqrt{\alpha_i}\,\sigma_{xi}\left[\Phi(z) - \frac{1}{2\sqrt{\alpha_i}\,\sigma_{xi}}\left(erf(z) + \frac{2}{\sqrt{\pi}}\sqrt{\alpha_i}\,\sigma_{xi}\,e^{-z^2}\right)\right]$$

~~for $\sigma_{xi} \to \infty$~~

~~$\bar{x}_i \simeq \sigma_{xi}$~~

$$\omega_i = \sqrt{\alpha_i}\,\sigma_{xi}$$

$$\psi_i(z) = z\,\Phi(\omega_i) + \omega_i \Phi(z) - \frac{1}{2} erf(z)$$

$$\sqrt{\alpha_i} = \frac{\sqrt{u^2 + a_i}}{s}$$

$$\sigma_{xi} = \mu_x \frac{su}{u^2 + a_i}$$

$$\begin{cases} z_{Dj} = -\dfrac{\sqrt{u^2+a_j}}{s}\,2{,}02 - \mu_y \dfrac{u}{\sqrt{u^2+a_j}} \\ z'_{Dj} = -\dfrac{\sqrt{u^2+a_i}}{s}\,3{,}63 - \mu_y \dfrac{u}{\sqrt{u^2+a_j}} \end{cases}$$

$$\begin{cases} z_{Uj} = \dfrac{\sqrt{u^2+a_j}}{s}\,y_0(x) - \mu_y \dfrac{u}{\sqrt{u^2+a_j}} \\ z'_{Uj} = \dfrac{\sqrt{u^2+a_i}}{s}\,y'_0(x) - \mu_y \dfrac{u}{\sqrt{u^2+a_j}} \end{cases}$$

$$\begin{cases} z_{(L}^{R)i} = \pm\dfrac{\sqrt{u^2+a_i}}{s}\,1{,}01 - \mu_x \dfrac{u}{\sqrt{u^2+a_i}} \\ z'^{(R}_{L)i} = \pm\dfrac{\sqrt{u^2+a_i}}{s}\,4{,}94 - \mu_x \dfrac{u}{\sqrt{u^2+a_i}} \end{cases}$$

$$\overline{|x_\sigma|} \equiv \frac{\int_{-\infty}^{+\infty} |x| e^{-\alpha(x-\sigma)^2} dx}{\int_{-\infty}^{+\infty} e^{-\alpha(x-\sigma)^2} dx} = \frac{\Phi(\sigma\sqrt{\alpha})}{\sqrt{\alpha}}$$

$$\Phi(z) = z\,\mathrm{erf}(z) + \frac{1}{\sqrt{\pi}} e^{-z^2}$$

$\mathcal{J} = \frac{1}{1+\epsilon^2}$; $\epsilon = \sqrt{\frac{1}{\mathcal{J}} - 1}$ D-cup (pos. ions)

GSG Fit ; $P = [c e^{-a_1 \psi} + (1-c) \times e^{-a_2 \psi}] \cos k\psi$

$\mathcal{J}=$	ϵ	C	a_1	a_2	S_1	K
.5	1	.82	.54	5.5	1.056	.439
.6	.816	.837	.59	6.0	1.075	.455
.7	.655	.85	.644	7.7	1.098	.475
.8	.500	.839	.677	7.7	1.129	.502
.9	.333	.81	.72	7.1	1.178	.547
.95	.229	.78	.773	6.9	1.219	.585
.97	.176	.761	.824	6.9	1.244	.610
.98	.143	.744	.87	7.25	1.261	.627
.99	.101	.697	.93	7.4	1.284	.650

$K = .394 S_1^2$ $\quad S_1 = .495 + \frac{.720}{1+\sqrt{1-\mathcal{J}}} + \frac{.290}{1+\sqrt{1+\mathcal{J}/N}}$

$(N = 3.03)$

$\beta = 30°$

Re: Non-Uniform Sensitive Area Response

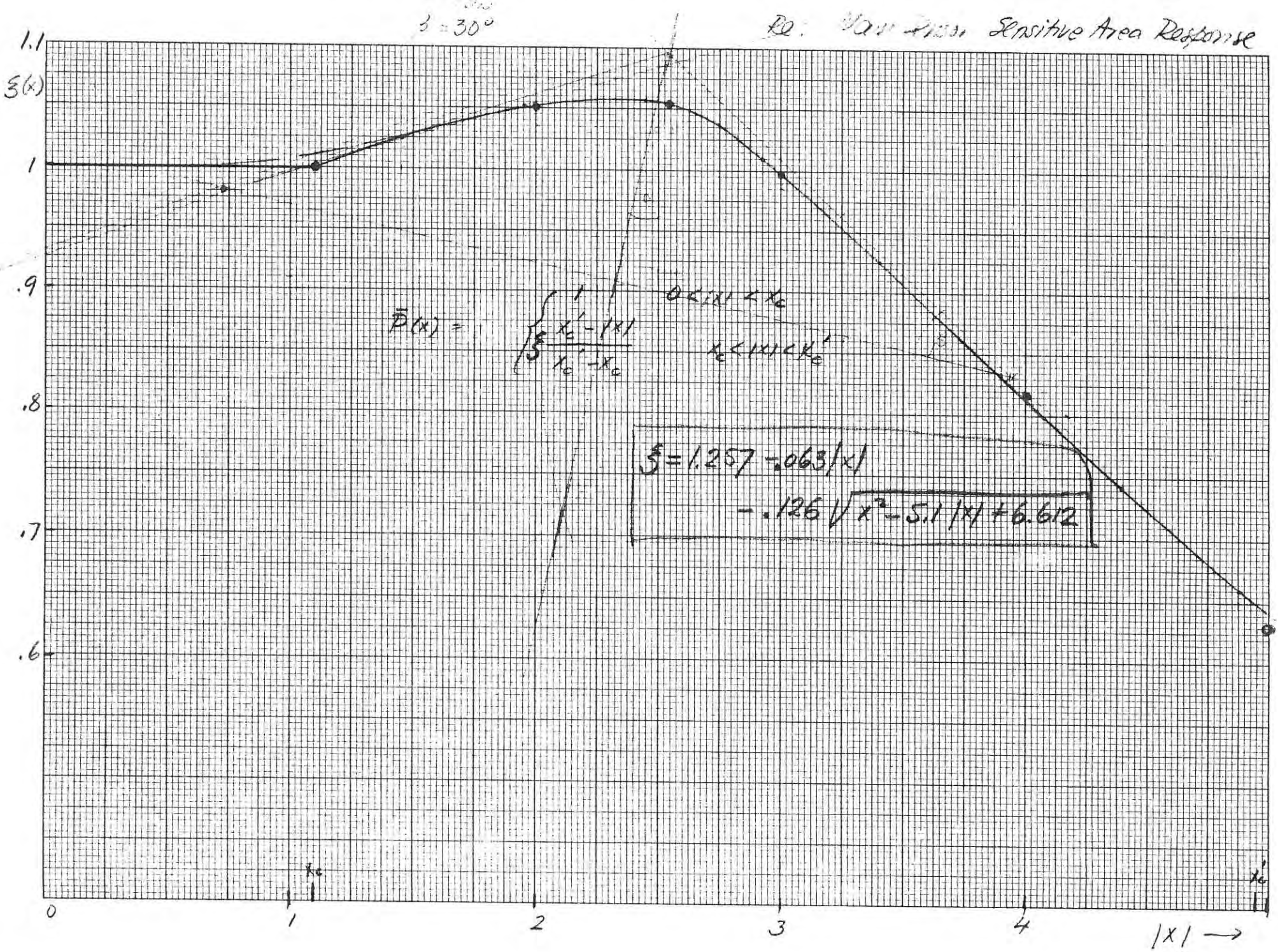

$$P(x,y) = \bar{P}(x)\begin{cases} \dfrac{y-y_0'}{y_0-y_0'} \\ 1 \\ \dfrac{y_0'-y}{y_0'-y_0} \end{cases}$$

$$\bar{P}(x) = \begin{cases} 1 & 0<|x|<1.10 \\ h(x) & 1.10<|x|<4.95 \end{cases}$$

x	$h(x)$	$\xi(x)$
$x_c = 1.1$	1	1
1.46	.93	1.026
1.95	.82	1.052
2.44	.69	1.058
2.93	.53	1.010
3.41	.37	.925
3.90	.227	.832
4.39	.108	.743
4.88	.012	.660
$x_c' = 4.95$	0	~

$$h = \frac{-|x|+x_c'}{x_c'-x_c}\xi(x) \qquad \begin{cases} x_c = 1.10 \\ x_c' = 4.95 \end{cases} \quad x_c'-x_c = 3.85$$

Analytical Studies of the Response of ~~Voyager~~ PLS ~~Plasma~~ Sensors on Voyagers I and II.

The design and physical properties of the four M.I.T. ~~Plasma~~ sensors that ~~are part of the~~ constitute the Voyager Plasma Science Experiment (PLS) have been reported elsewhere (see, e.g., ...) Here we shall confine our discussion to one specific aspect of the ~~data~~ analysis of data acquired by the PLS sensors, namely, a construction of analytical expressions for the sensor response functions ~~of the sensor~~ that are both, accurate for all possible directions ~~of flow~~ and magnitudes of the plasma bulk velocity, and, at the same time, are sufficiently simple as to allow a certain number of analytical integrations needed for deducing the desired five plasma parameters (i.e., the bulk velocity, the thermal speed ~~and anisotropies~~ and, the number densities of a given ion species ~~ions~~, etc.). Such two stringent requirements appear to be indispensable in the case of the studies of the plasma flow in the Jovian magnetosphere. (The anticipated measurements in the Saturnian environment will undoubtedly impose similar requirements on our data analysis). The reason for it is as follows: The preliminary analysis

of the Jovian magnetospheric plasma (see, e.g., ... and Belcher & McNutt, ...) have shown that the plasma as a whole does not corotate rigidly about the Jovian spin axis; moreover, the bulk velocity seems to exhibit variable directions and magnitudes depending on the location of the spacecraft relative to the Jovian magnetic dipole coordinates and thus whether the spacecraft is on the day or night side of the plasma disk. This latter flow feature could be ascertained thus far only qualitatively because of the complex nature of the response of the PLS sensors to flow directions that not nearly parallel to the collector normal of a given sensor. Nonetheless, since substantial ion currents are observed throughout the magnetosphere on three of the four detectors [e.g., the configuration of the three main sensors (A,B,C cups) and the azimuthal orientation of the side-sensor (the D-cup) are such as to during the inbound leg of Voyager 1 favor the B,C,D combination for reliable data acquisition]. Therefore, we have, at least in principle, enough information to obtain the five macroscopic parameters for each ion species identified in the differential energy spectrum. Since many such determinations are desired throughout the flight, the crux of the matter is to

accomplish this in an expeditious manner within a reasonable span of time and without prohibitive ~~[illegible]~~ computer costs. ~~[illegible]~~ one can show that, If the ~~[illegible]~~ two aforementioned requirements on the construction of the response functions are fulfilled, ~~the~~ a complete data analysis program can be brought to fruition.

2 With this objective in mind we began, almost two years ~~ago~~ ago, a comprehensive study of ~~the~~ analytical characteristics of the response functions of the main and side sensors obtained beforehand in a rigorous manner by a combination of numerical techniques and ~~by~~ theoretical considerations. The design of the cups is such that (except for a large Mach number flow entering ~~[illegible]~~ within a narrow cone of the cup normal) such studies become enormously lengthy and complex in detail. The sources of complexity are different for the D-cup from those for the A,B,C cups. Both sets, however the D-cup and the ABC-cluster, require the knowledge of ~~are characterized by~~ ~~[illegible]~~ three distinct aspects of their response:

(1) ~~a complete knowledge of~~ the path ~~[illegible]~~ of a charged particle between the aperture and the collector must be ascertained for variety of initial conditions and all values of the voltages used at the modulator grids.

(2) the transparency of each grid as a function

of the energy, ~~and~~ the ~~direction~~ angle of entrance of the impinging particles, ~~as well as the~~ and the modulator and suppressor voltages, must be calculated.

(3) The size of the sensitive area of the collector plate of a given sensor must be determined. (The "sensitive area" is defined as that portion of the collector area that will be struck by a parallel monoenergetic beam of ~~specified ion~~ of given ion species that enters the aperture from a specified direction.)

The knowledge of these three functions (the "path function", the "transparency", and the "sensitive area function") allows one to relate the contribution of a given ion species to the measured current to the distribution function of that species. One has schematically:

$$\Delta I_a^{(n)} = Z_a e A_0 T_0 \left\{ \int_{v_{z,n}}^{\infty} v_z dv_z \iint f_a(\vec{v}) R_n(\vec{v}) dv_x dv_y - \int_{v_{z,n+1}}^{\infty} dv_z \iint f_a(\vec{v}) R_{n+1}(\vec{v}) dv_x dv_y \right\}$$

where the symbols have the following meaning: $\Delta I_a^{(n)}$ is the electric current due to ion species of kind "a" when the detector operates between the n^{th} and $(n+1)^{th}$ steps of the modulator voltage; $v_{z,n}$ and $v_{z,n+1}$ are the corresponding normal (cutoff) components of the ion velocity; $Z_a e$ is ion charge, A_0 and T_0 are, respectively,

the sensitive area and the transparency at normal incidence; f_a is the distribution function of the ion of kind "a", $R_n(\bar{v})$ is the response function for the n^{th} step of the threshold voltage; ~~(Note that R_n is normalized to unity for normal incidence)~~, and, finally, v_x, v_y indicate the ion velocity components in the plane of the collector. Note that R_n and R_{n+1} are the products of the transparency and the sensitive area functions, normalized to unity at normal incidence. Figures 1 and 2 show typical shapes of these functions for a main sensor and the side sensor, respectively. The coordinate x, y are related to v_x, v_y by $x = S_n(v_z) v_x$, $y = S_n(v_z) v_y$, where $S_n(v_z)$ is the aforementioned path function. Figure 3 shows the sensitive area response function of a main sensor (without the effects of the transparency). A comparison between Figures 1 and 3 allows one to see that, at large-angle incidence, the transparency and the sensitive area effects are equally important and, what is critical for magnetospheric data analysis — the response functions can be far removed from their nominal unity values at normal incidence.

The figures show clearly the complex behavior of $R_n(\bar{v})$ as functions of v_x, v_y and v_z. On the other hand, the expression

for $\Delta I_a^{(n)}$ suggests that it would highly desirable to construct mathematical expressions for R_n's simple enough so that the two-dimensional integrals in the (v_x, v_y) plane could be carried out analytically, if the form of f_a is assumed to be known (e.g., for Convected maxwellian f_a's).

After a long search using a variety of empirical forms for $R_n(\bar{v})$ we have converged on a representation of R_n's that is sufficiently simple and accurate to satisfy our requirements. It would be inappropriate to go into details here, except to mention that, for main sensors, R_n's involve linear combinations of the expressions of the type $S_n v_i e^{-a_n v_i^2/v_z^2}$ and $e^{-b_n v_i^2/v_z^2}$, where $v_i = (v_x, v_y)$ and a_n, b_n are suitable functions of v_z and the modulator voltage steps. The accuracies achieved by such representations are a few percent or better for the entire (v_x, v_y) plane provided that the distribution functions do not refer to an extremely cold (very high mach number) plasma. Similar expressions for R_n of the side sensor has also been found; it is somewhat simpler than those for the main sensors because the the side-sensor exhibits (to a high approximation) an axial symmetry with respect to its normal.

Armed with such integrable response functions we were able to obtain analytical expressions of $\Delta I_a^{(n)}$ for the M-mode operation of the detectors (Recall that, in the M-mode, $(v_{z,n+1} - v_{z,n}) \ll v_{z,n}$).

Although they are fairly lengthy, they are perfectly manageable, even computable by hand. The computer time needed to evaluate a complete energy-spectrum in the M-mode amounts to, at most, a few seconds, which is orders of magnitude shorter than the time needed to evaluate $\Delta I_a^{(n)}$ in direct integrations over a given distribution function. (Note that in a direct-integration simulation program one faces a five-dimensional integral: 3 integrations in the $\vec{v}$-space and 2 integrations involving the sensitive area in the collector plane).

In summary, we are able to state that, having found an analytical representation of the PLS sensors' response, we are in the position to find routinely the five desired macroscopic ion parameters in the Jovian environment.

(S. Olbert, A. Barnett)

Positive Ions

D-cup response function $P = GR = P(\bar{\xi}; N)$

(For $N = \frac{\phi_0}{|\phi_s|} = 3.03$) ; $\bar{\xi} = \frac{\phi_n}{\phi_0} = \frac{1}{1+\bar{\epsilon}^2}$

Use for:

M-Mode ($\bar{\xi} = .98$) : $P = (.744 e^{-.87\psi} + .256 e^{-7.25\psi}) \cos(.625\psi)$

L-Mode ($\bar{\xi} \approx .835$) : $P = (.83 e^{-.69\psi} + .17 e^{-7.5\psi}) \cos(.515\psi)$

$\psi = \frac{v_t^2}{\bar{v}_z^2}$; $\frac{1}{2} A m_p \bar{v}_z^2 = Ze\bar{\phi}_n$

	ψ_{max}	$\sqrt{\psi_{max}}$	$\bar{\epsilon}$
M-mode	2.51	1.58	.143
L-mode	3.053	1.75	.445

Angular orientation of grids in D-cup (side sensor)

Grid name	#	Voyager I α_j	Voyager II α_j'	Symbol	Rel. Voltage in ⊕ Mode
Aperture	1	0°	0°	A	0
⊕ Modulator	2	$\alpha_M = 68°$	$\alpha_M = 68°$	M_+	variable, ϕ_n
⊖ —	3	62°	62°	M_-	0
Ground	4	50°	80°	G	0
Back-out	5	55°	55°	B	0
Ground	6	40°	24°	G	0
Suppressor 1	7	$\alpha_s = 0°$	$\alpha_s = 10°$	S_1	-95^V
— 2	8	4°	0°	S_2	0

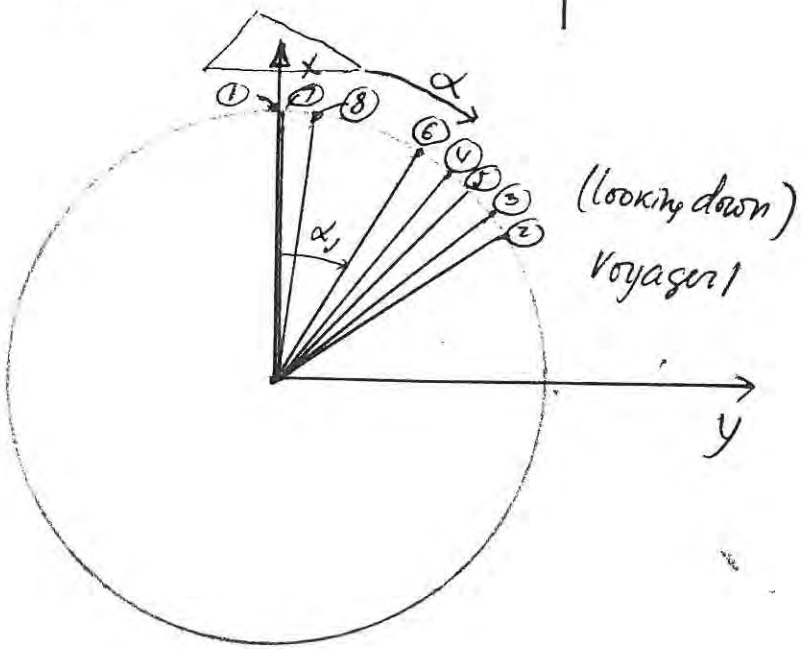

Fitting $y_0(x)$

$$y = \frac{A\cos(kx+\gamma)}{1+\alpha x} \qquad \varphi = kx+\gamma$$

	x	y
x_1 =	.25	.62
x_0 =	1.3	0
x_m =	2.7	-.45
at	2.7	y is min

$$\frac{y'}{y} = -k\tan\varphi - \frac{\alpha}{1+\alpha x}$$

$$\alpha = -(1+\alpha x_m)k\tan\varphi_m$$

$$\alpha = -\frac{k\tan\varphi_m}{1+kx_m\tan\varphi_m} \qquad 1+\alpha x_m = \frac{1}{1+kx_m\tan\varphi_m}$$

$$\varphi_0 \equiv kx_0+\gamma = \frac{\pi}{2}$$

$$\varphi_m = kx_m+\gamma = \varphi_0 + k(x_m-x_0) = \frac{\pi}{2} + 1.4k$$

$$\varphi_1 = kx_1+\gamma = \frac{\pi}{2} + 1.05k$$

$$\frac{A\cos\varphi_m}{1+\alpha x_m} = -.45$$

$$\frac{A\cos\varphi_1}{1+\alpha x_1} = .62$$

$$\alpha = -A(1+kx_m\tan\varphi_m) \qquad A(1+kx_m\tan\varphi_m)\cos\varphi_m = -.45$$

$$1+\alpha x_1 = 1 - \frac{kx_1\tan\varphi_m}{1+kx_m\tan\varphi_m} = \frac{1+k(x_m-x_1)\tan\varphi_m}{1+kx_m\tan\varphi_m}$$

$$A(1+kx_m\tan\varphi_m)\cos\varphi_1 = .62(1+2.45\tan\varphi_m)$$

$$\frac{\cos\varphi_1}{\cos\varphi_m} = \frac{-.62}{.45}(1+2.45\tan\varphi_m)$$

$$\cos\varphi_1 = -1.38(\cos\varphi_m + 2.45\sin\varphi_m)$$

$$\cos\varphi_1 = \sin(1.05k)$$

$$\sin(1.05k) = 1.38\sin(1.4k) - 3.38\cos(1.4k)$$

$1.4k = \beta$

$$\sin(\tfrac{3}{4}\beta) = 1.38\sin(1.4\beta) - 3.38\cos(1.4\beta)$$

β	RHS	LHS = $\sin(.75\beta)$	β	RHS	LHS
70	.141	.793	81.2	.847	
80	.772	.866	81.4	.859	
83	.958	.885	81.7	.878	.877
81	.834	.872			

RHS

$\beta = 81.69$

$\boxed{k = 1.018}$

$$\gamma = \frac{\pi}{2} - 1.05k - k.25 = \frac{\pi}{2} - 1.30k = .247 \rightarrow 14.17^\circ$$

$$\varphi_m = 171.66^\circ \qquad \tan\varphi_m = -.1466 \qquad \cos\varphi_m = -.989$$

$$\alpha = \frac{1.018 \times .1466}{1 + 2.7 \times 1.018 \times .1466} = .250$$

$$A = \frac{.45}{.989}(1 + .250 \times 2.7) = .762$$

$$y_0 = \frac{.762\cos(1.018x + .247)}{1 + .25x} \rightarrow \frac{.762\cos(58.33^\circ x + 14.15^\circ)}{1 + .25x}$$

~~= .739~~

.041

Fitting y_0'

Try parabola $\qquad y = y_m + p(x - x_m)^2 \qquad y_m = 2.52 \quad x_m = 1.95$

$x = 2 : y_0' = 2.36 \rightarrow 2.38$ ~~$p = \frac{.16}{1.05^2} = .145$~~

$x = 4 : y_0' = 1.51 \rightarrow 1.37$

$x = 3 : y_0' = 2 \leftarrow 2 \qquad p = \frac{2.52 - 2}{2.05^2} = .124$

For $x_m = 1$, $y_m = 2.50$

$x = 3 : \quad p = \frac{0.50}{4} = .125$

$$y_0' = 2.50 - .125(x-1)^2$$

9/26/84

Steve's Notes

"Response Fct in Side Sensor ; Positive Ions, m-mode"

$$\frac{I}{I_0} = e^{-F} \quad ; \quad F = -\left\{ 12 \ln \frac{1 - c\sqrt{1+\psi^2}}{1-c} + 2 \ln \frac{1 - c\sqrt{1+\frac{\psi^2}{1-\xi_m^2}}}{1-c} \right.$$

$$\left. + 2 \ln \frac{1 - c\sqrt{1+\psi^2/1+\xi_B^2}}{1-c} \right.$$

$$\psi^2 = \frac{v_t^2}{v_z^2} \overline{\cos^2 \varphi} \qquad \psi^2 << 1 \Rightarrow \frac{1 - c\sqrt{1+\psi^2}}{1-c} = 1 - \frac{c}{2(1-c)} \psi^2$$

$$\epsilon = \sqrt{\frac{1}{\xi} - 1}$$

Main Sensor $\quad \bar{P}(x) = \begin{cases} 1 & 0 < x < 1.1 \\ \frac{4.94 - |x|}{3.84} & ; \; 1.1 < |x| < 4.94 \end{cases}$

$$\xi = 1.257 - 0.063|x| - 0.126\sqrt{x^2 - 5.10|x| + 6.612}$$

Main sensor

$$T = T_0 \left(c_1 e^{-a_1 v_x^2/v_z^2} + c_2 e^{-a_2 v_x^2/v_z^2} \right) \left(c_1 e^{-a_1 v_y^2/v_z^2} + c_2 e^{-a_2 v_y^2/v_z^2} \right)$$

a_i, c_i are functions of $\epsilon \equiv \sqrt{\frac{m v_z^2}{2 q \phi} - 1}$

$$\boxed{c_1 + c_2 = 1}$$

10/3/84

Main reason - from letter to Ed (8-11-80)

$$G_j(\psi) = c_j e^{-a_j \psi^2} + (1-c_j) e^{-b_j \psi^2}$$

ψ = either $v_x / v_{\bar{z}j}$ or $v_y / v_{\bar{z}j}$

10/12/84

Grid Transparency

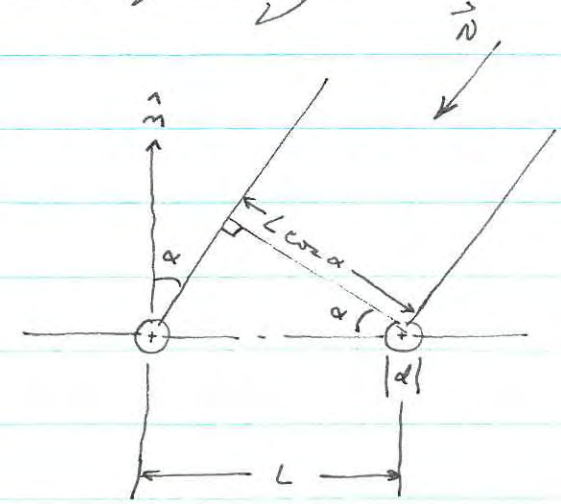

$$\text{Probability of collision} = \frac{\text{grid area}}{\text{open area}} = \frac{d}{L\cos\alpha - d} \quad (L\cos\alpha > d)$$

$$\Rightarrow \cos\alpha > \frac{d}{L}$$

$$\Rightarrow \text{Transparency} = 1 - \frac{d}{L\cos\alpha - d}$$

$$= 1 - \frac{d}{L}\left(\frac{1}{\cos\alpha - d/L}\right)$$

$$= 1 - c\left(\frac{1}{\cos\alpha - c}\right) \quad \text{where } c \equiv \frac{d}{L} = \frac{1}{42}$$

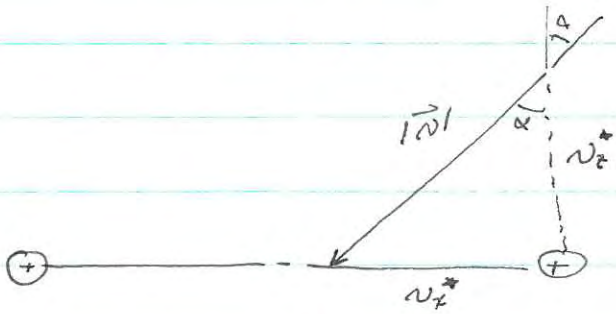

$$\Rightarrow \cos\alpha = \frac{N_z^*}{\sqrt{N_x^{*2} + N_z^{*2}}}$$

Must have $\cos\alpha > \frac{d}{L} = c$

$$v_z^{*2} = v_z^2 - \frac{2e\phi}{Amp} \qquad T = 1 - c\sqrt{1 + \frac{v_x^2}{v_z^2 - \frac{2e\phi}{Amp}}}$$

for $T \geq 0$ otherwise $T = 0$

$$1 + \tan^2\alpha = \sec^2\alpha \qquad \tan\alpha = \frac{v_x^*}{v_z^*}$$

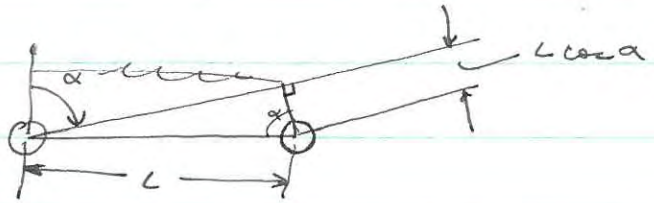

Total material $L\cos\alpha$

Material going through $L\cos\alpha - d$

$$\Rightarrow T = \frac{L\cos\alpha - d}{L\cos\alpha} \qquad A = \frac{d}{L\cos\alpha}$$

$$\boxed{T = 1 - \frac{d}{L\cos\alpha}}$$

for $L\cos\alpha > d$

$$T = 1 - c\sec\alpha \qquad \cos\alpha > \frac{d}{L} = c$$

Otherwise $T = 0$

$$\Rightarrow T = 1 - c\sqrt{1 + \frac{v_x^{*2}}{v_z^{*2}}}$$

$$\cos\alpha > \frac{d}{L} = c$$

$$\sec^2\alpha < \frac{1}{c^2}$$

$$\sqrt{\tan^2\alpha + 1} = \boxed{\sqrt{1 + \frac{v_x^{*2}}{v_z^{*2}}} < \frac{1}{c}}$$

10/12/84

Main Sensor Response

$$\left|\frac{S_x}{h}\right| > X_n' \Rightarrow A_x = 0$$

$$X_n' = 4.94$$

$$\frac{S_y}{h} < Y_n' = -3.62 \Rightarrow A_y = 0$$

$$\frac{S_y}{h} > Y_n' \Rightarrow A_y = 0$$

$$Y_n'_{max} = 2.50$$

$$\text{So} \quad \left|\frac{S_x}{h}\right|, \left|\frac{S_y}{h}\right| \geq 5 \Rightarrow A_x, A_y = 0$$

$$\frac{S_x}{h} = S\frac{\nu_x}{\nu_z}$$

$$\frac{S_y}{h} = S\frac{\nu_y}{\nu_z}$$

Shift function

$$S = 0.743 \frac{\nu_z^2}{\nu_h^2}\left[1 - \sqrt{1 - \frac{\nu_h^2}{\nu_z^2}}\right] + \frac{0.093}{\sqrt{1 - \frac{\nu_h^2}{\nu_z^2}}} + 0.392 \frac{\nu_z^2}{\nu_x^2}\left[\sqrt{1 + \frac{\nu_x^2}{\nu_z^2}} - 1\right]$$

$\nu_z \geq \nu_h$

$$\nu_z = \nu_h \Rightarrow \quad S = 0.743 + \frac{0.093}{0} \Rightarrow S \to \infty$$

10/12/84

$\nu_t \gg \nu_h, \nu_a$

$$\Rightarrow S = 0.743 \frac{\nu_t^2}{\nu_h^2}\left[1 - 1 + \frac{1}{2}\frac{\nu_h^2}{\nu_t^2}\right] + 0.093\left(1 + \frac{1}{2}\frac{\nu_h^2}{\nu_t^2}\right)$$

$$+ 0.392 \frac{\nu_t^2}{\nu_a^2}\left[1 + \frac{1}{2}\frac{\nu_a^2}{\nu_h^2} - 1\right]$$

$$= 0.743\left(\frac{1}{2}\right) + 0.093 + 0.392\left(\frac{1}{2}\right)$$

$$\cong 0.66$$

$v_t \geq v_k$

$$S = 0.743 \frac{v_t^2}{v_k^2}\left[1-\sqrt{1-\frac{v_k^2}{v_t^2}}\right] + \frac{0.093}{\sqrt{1-\frac{v_k^2}{v_t^2}}} + 0.392 \frac{v_t^2}{v_2^2}\left[\sqrt{1+\frac{v_{R_2}^2}{v_t^2}}-1\right]$$

$$\left(\frac{v_t}{v_k}\right)^2 \equiv x$$

$$\left(\frac{v_t}{v_2}\right)^2 = \left(\frac{v_t}{v_k}\right)^2 \cdot \left(\frac{v_k}{v_2}\right)^2$$

$$= x \cdot y \qquad y \equiv \left(\frac{v_k}{v_2}\right)^2$$

(From conversation w/ Stan)
Early October, 1984

(1)

Tethered satellite paper going

---

for isotropic response $\frac{1}{\sqrt{a^2+\psi}} e^{-\psi^2}$

i.e. $w >> |\vec{v}|$

Ψ problem worrying Stan

beam at large angle ψ to primary for use for Ψ

May be something wrong in code

Check the 2nd integration over energy function integral

Look for $\frac{0-0}{0-0}$ — limiting forms

(2)

Plot a_j, b_j, c_j and try to fit

get a family of curves that look like

sawtooth curves

Try plot on log-log paper – try to get previous functions which are analytic.

---

to get T to exponential plot on different graph papers.

Graphical procedure only

Yn and Yn' – pieced straight

can get within 20% probably (from Stan)

10/12/84

(2)

Integrals of the form

$$I_1 = \int_0^a x e^{-\alpha x^2} I_0(\beta x)\, dx$$

$$I_2 = \int_0^a x^2 e^{-\alpha x^2} I_0(\beta x)\, dx$$

$$\int_0^\infty e^{-a^2 t^2} I_\nu(bt)\, dt = \frac{\sqrt{\pi}}{2a} e^{\frac{b^2}{8a^2}} I_{\frac{1}{2}\nu}\left(\frac{b^2}{8a^2}\right)$$

$$\frac{1}{z}\frac{d}{dz}\left[I_0(z)\right] = \frac{1}{z} I_1(z)$$

$$\Rightarrow \frac{d}{dz} I_0(z) = I_1(z)$$

$$\left(\frac{1}{z}\frac{d}{dz}\right) z I_1(z) = I_0(z)$$

$$\frac{d}{dz}\left[z I_1(z)\right] = z I_0(z)$$

$$\frac{\partial}{\partial b}\left[\int_0^\infty e^{-a^2 t^2} I_1(bt)\, dt\right] = \int_0^\infty e^{-a^2 t^2} \frac{\partial}{\partial b}\left[b I_1(bt)\right] dt$$

$$= \int_0^\infty e^{-a^2 t^2} \frac{d}{d(bt)}\left[bt\, I_1(bt)\right] dt$$

$$= \int_0^\infty e^{-a^2 t^2} bt\, I_0(bt)\, dt$$

$$= b \int_0^\infty e^{-a^2 t^2} t\, I_0(bt)\, dt$$

10/12/84

(3)

$$\frac{1}{b}\frac{\partial}{\partial b}\left[b\,\frac{\sqrt{\pi}}{2a}\,e^{\frac{b^2}{8a^2}}\,I_{1/2}\left(\frac{b^2}{8a^2}\right)\right]$$

$$I_{1/2}(z) = \frac{1}{\sqrt{\frac{\pi}{2z}}}\,\frac{\sinh z}{z}$$

$$= \sqrt{\frac{2z}{\pi}}\,\frac{1}{z}\sinh z$$

$$= \sqrt{\frac{2}{\pi z}}\sinh z$$

$$\Rightarrow \frac{1}{b}\frac{\partial}{\partial b}\left[\frac{b}{2a}\sqrt{\pi}\,e^{\frac{b^2}{8a^2}}\sqrt{\frac{2}{\pi}}\,\frac{\sqrt{8}a}{b}\sinh\left(\frac{b^2}{8a^2}\right)\right]$$

$$= \frac{1}{b}\frac{\partial}{\partial b}\left[\frac{\cancel{b}}{\cancel{2a}}\,\frac{\cancel{4}a}{\cancel{b}}\,e^{\frac{b^2}{8a^2}}\,\frac{1}{\cancel{2}}\left(e^{\frac{b^2}{8a^2}} - e^{-\frac{b^2}{8a^2}}\right)\right]$$

$$= \frac{1}{b}\frac{\partial}{\partial b}\left[e^{\frac{b^2}{4a^2}} - 1\right]$$

$$= \frac{1}{b}\,e^{\frac{b^2}{4a^2}}\,\frac{2b}{4a^2}$$

$$= \frac{1}{2a^2}e^{\frac{b^2}{4a^2}}$$

$$\Rightarrow \int_0^\infty e^{-a^2t^2}\,t\,I_0(bt)\,dt = \frac{1}{2a^2}e^{\frac{b^2}{4a^2}}$$

10/13/84

①

$$S = 0.743 \frac{v_t^2}{v_h^2}\left[1-\sqrt{1-\frac{v_h^2}{v_t^2}}\right] + 0.093 \frac{1}{\sqrt{1-\frac{v_h^2}{v_t^2}}} + 0.340$$

$$+ 0.392 \frac{v_t^2}{v_a^2}\left[\sqrt{1+\frac{v_a^2}{v_t^2}} - 1\right]$$

$\therefore \quad S = S\left(\frac{v_t}{v_h}, \frac{v_t}{v_a}\right)$ $\qquad \frac{v_t^2}{v_a^2} = \left(\frac{v_t}{v_h}\right)^2 \left(\frac{v_h}{v_a}\right)^2 = \frac{\chi}{\alpha}$

$\frac{v_t}{v_h} \geq 1$ $\qquad$ or $\quad S = S\left(\left[\frac{v_t}{v_h}\right]^2, \left[\frac{v_a}{v_h}\right]^2\right)$

$\left(\frac{v_t}{v_h}\right)^2 \equiv \chi \qquad \left(\frac{v_a}{v_h}\right)^2 \equiv \alpha$

$\Rightarrow \quad S = S(\chi, \alpha)$

$$= 0.743\,\chi\left[1-\sqrt{1-\frac{1}{\chi}}\right] + 0.093 \frac{1}{\sqrt{1-\frac{1}{\chi}}} + 0.340$$

$$+ 0.392\,\chi \frac{1}{\alpha}\left[\sqrt{1+\frac{\alpha}{\chi}} - 1\right]$$

$$\frac{dS}{d\chi} = 0.743\left[\left[1-\sqrt{1-\frac{1}{\chi}}\right] + \chi(-1)\frac{1}{2}\frac{1}{\sqrt{1-\frac{1}{\chi}}}(-1)\left(-\frac{1}{\chi^2}\right)\right]$$

$$+ 0.093\left(-\frac{1}{2}\right)\frac{1}{\left(1-\frac{1}{\chi}\right)^{3/2}}\frac{1}{\chi^2}$$

$$+ 0.392\left[\frac{1}{\alpha}\left[\sqrt{1+\frac{\alpha}{\chi}} - 1\right] + \frac{\chi}{\alpha}\frac{1}{2}\frac{1}{\sqrt{1+\frac{\alpha}{\chi}}}\left(-\frac{1}{\chi^2}\right)\right]$$

10/13/84

(2)

$$S' = 0.743\,x\left(1-\sqrt{1-\frac{1}{x}}\right) + 0.093\frac{1}{\sqrt{1-\frac{1}{x}}} + 0.340$$

$x - 1$

$\sqrt{1-\frac{1}{x}} - 2$

x	S'
1.001	4.003
1.01	1.950
1.1	1.219
1.5	0.972
2	0.907
5	0.836
10	0.819
20	0.812
100	0.806
1000	0.805
1.0001	10.376
1.00001	30.4890

$$S'(2) = (0.743)(2)\left(1-\sqrt{\tfrac{1}{2}}\right) + 0.340$$

$$+ 0.093\sqrt{2}$$

$$= 0.907$$

$$S'(10) = 7.43\left(1-\sqrt{\tfrac{9}{10}}\right) + 0.340$$

$$+ 0.093\frac{1}{\sqrt{\frac{9}{10}}}$$

$$= 0.819$$

$x = 1+\epsilon^2$

$$\Rightarrow \sqrt{1-\frac{1}{x}} = \sqrt{1-\frac{1}{1+\epsilon^2}}$$

$$\simeq \sqrt{1-(1-\epsilon^2)}$$

$$\simeq \epsilon$$

$$\Rightarrow S'(1+\epsilon^2) \simeq 0.743 + 0.093\frac{1}{\epsilon} + 0.340$$

$$\simeq 1.083 + \frac{0.093}{\epsilon}$$

$x = 1.0001 = 1+(10^{-2})^2$

$\Rightarrow S' \simeq 10.383$

$$1-\sqrt{1-\frac{1}{x}} \simeq 1-\left(1-\frac{1}{2x}\right) \simeq \frac{1}{2x}$$

$$S' \simeq 0.743\left(\frac{1}{2}\right) + 0.093 + 0.340$$

$$\simeq 0.8045$$

10/13/84

(2)

$$2\overline{)930}\quad 465$$
$$8$$
$$13$$
$$12$$
$$10$$

$$\frac{\frac{1}{x}}{1-\frac{1}{x}} = \frac{1}{x-1}$$

$$\frac{dS}{dx} = 0$$

$$\Rightarrow 0 = 0.743\left\{1 - \sqrt{1-\frac{1}{x}} - \frac{1}{2}\frac{1}{x}\frac{1}{\sqrt{1-\frac{1}{x}}}\right\}$$

$$- 0.0465\,\frac{1}{\sqrt{1-\frac{1}{x}}}\,\frac{1}{x}\,\frac{1}{x-1}$$

$$+\frac{0.392}{\alpha}\left\{\sqrt{1+\frac{\alpha}{x}} - 1 - \frac{1}{2x}\frac{1}{\sqrt{1+\frac{\alpha}{x}}}\right\}$$

Look at $f = \frac{x}{\alpha}\left[\sqrt{1+\frac{\alpha}{x}} - 1\right]$

$$x = 1 \Rightarrow f = \frac{1}{\alpha}\left[\sqrt{1+\alpha} - 1\right]$$

$$\alpha \ll 1 \Rightarrow f \simeq \frac{1}{\alpha}\left(1 + \frac{1}{2}\alpha - 1\right)$$
$$\simeq \frac{1}{2}$$

$$\alpha \gg 1 \Rightarrow f \simeq \frac{1}{\alpha}\sqrt{\alpha}$$
$$\simeq \frac{1}{\sqrt{\alpha}}$$

③ 10/13/84

$x = 1 + \epsilon^2 \qquad \epsilon^2 \ll 1$

$$\Rightarrow \quad \sqrt{1-\frac{1}{x}} \simeq \sqrt{1-\frac{1}{1+\epsilon^2}}$$
$$\simeq \sqrt{1-(1-\epsilon^2)}$$
$$\simeq \sqrt{\epsilon^2}$$
$$\simeq \epsilon$$

Tagamet 3. 5.5 mg/kg × 7 kg = 38.5

232-1758

Chlorpromazine .5 mg × 7 = 3.5 mg 3.5 mg

$$\Rightarrow 0 = 0.743 \left\{ 1 - \epsilon - \frac{1}{2}(1-\epsilon^2)\frac{1}{\epsilon} \right\}$$
$$-0.0465 (1-\epsilon^2)\frac{1}{\epsilon^2}\frac{1}{\epsilon} \}$$

$$0 = 0.743 \left\{ 1 - \epsilon - \frac{1}{2\epsilon} + \frac{1}{2}\epsilon \right\}$$
$$-0.0465 \left(\frac{1}{\epsilon^3} - \frac{1}{\epsilon} \right)$$

$$\Rightarrow 0 \simeq 0.743\left(-\frac{1}{2\epsilon}\right) - 0.0465\frac{1}{\epsilon^3} + 0.0465\left(\frac{1}{\epsilon}\right)$$

$x = 1 + \epsilon^2$

$$S = 0.743(1+\epsilon^2)\left(1-\sqrt{1-\frac{1}{1+\epsilon^2}}\right) + 0.093\frac{1}{\sqrt{1-\frac{1}{1+\epsilon^2}}} + 0.340$$

$$\begin{array}{r} 743 \\ 340 \\ \hline 1083 \end{array}$$

$$= 0.743\left(1-\sqrt{1-1+\epsilon^2}\right) + 0.093\frac{1}{\sqrt{1-(1-\epsilon^2)}} + 0.340$$

$$S = 0.743(1-\epsilon) + 0.093\frac{1}{\epsilon} + 0.340$$

$$S = 1.083 + 0.093\frac{1}{\epsilon}$$

10/13/84

(4)

$$S = S' + 0.392 \times \frac{1}{\alpha}\left[\sqrt{1+\frac{\alpha}{x}} - 1\right]$$

$$\frac{x}{\alpha} \gg 1 \Rightarrow \frac{x}{\alpha}\left[1 + \frac{1}{2}\frac{\alpha}{x} - 1\right]$$

$$\frac{x}{\alpha} \ll 1 \Rightarrow \frac{x}{\alpha}\sqrt{\frac{\alpha}{x}} \simeq \sqrt{\frac{x}{\alpha}}$$

$$\left(\frac{x}{\alpha}\right)_{min} = \left(\frac{v_t}{v_c}\right)^2_{min} = \frac{10}{95}$$

$$\Rightarrow S_{min} = 0.8045 + 0.392\,(0.236)$$

$$\Rightarrow \boxed{S_{min} = 0.897}$$ minimum value for the shift function in the main sensor

---

Reference (2.22e)

$$S = 0.495 + \frac{1}{2}(0.720) + 0.290\,(0.236)$$

$$\Rightarrow \boxed{S'_{min} = 0.923}$$

$$\Rightarrow 0.9 \leq \frac{v_x}{v_t} \leq 5$$

$$\text{Or } \frac{v_x}{v_t}, \frac{v_y}{v_t} \leq 5.5$$

10/13/84
(5)

$$T = \left(1 - c\sqrt{1+\frac{v_x^2}{v_z^2}}\right)^5 \left(1 - c\sqrt{1+\frac{v_x^2}{v_z^2}\frac{1}{1-\frac{1}{\gamma}}}\right)^3 \left(1 - c\sqrt{1+\frac{v_x^2}{v_z^2}\frac{1}{1+\frac{v_y^2}{v_x^2}}}\right)$$

$$\times \frac{v_y}{v_z} \cdots$$

$\gamma = 1.1 \Rightarrow \frac{1}{1-\frac{1}{1.1}} = 11$

$(S' = 1.95)$

$$5 = 1.95\,\frac{v_x}{v_z}$$

$$\Rightarrow \frac{v_x}{v_z} = 2.56$$

$$\Rightarrow \sqrt{1+\left(\frac{v_x}{v_z}\right)^2 \frac{1}{1-\frac{1}{\gamma}}} = 8.563$$

$$\left[1 - \frac{1}{42}(2.748)\right]^5 \left[1 - \frac{1}{42}\,8.563\right]^3 = 0.3597$$

$$1 - \frac{5}{42}(2.748) - \frac{3}{42}(8.563) = 0.0612$$

$\frac{v_x}{v_z} = 1$

$$\left(1 - \frac{1}{42}\sqrt{2}\right)^5 = 0.8426$$

$$1 - \frac{5\sqrt{2}}{42} = 0.8316$$

$$1 - \frac{1}{42}\left(1+\frac{1}{2}\right) = 0.9643$$

Interesting cases are $v_x/v_z,\ v_y/v_z > 1$

$$\left(1 - c\sqrt{1+\frac{v_x^2}{v_z^2}}\right)^5 = e^{\ln\left[1 - c\sqrt{1+\frac{v_x^2}{v_z^2}}\right]^5}$$

$$= e^{5\ln\left[1 - c\sqrt{1+\frac{v_x^2}{v_z^2}}\right]}$$

$$= e^{-5c\sqrt{1+\frac{v_x^2}{v_z^2}}}$$

$$\simeq e$$

$$= 0.8451$$

10/13/84

(4)

$$(1-c\sqrt{1+x})^5 = e^{\ln(1-c\sqrt{1+x})^5}$$

$$= e^{5\ln(1-c\sqrt{1+x})}$$

$$f = \ln(1-c\sqrt{1+\alpha x})$$

$$\frac{df}{dx} = \frac{1}{1-c\sqrt{1+\alpha x}}(-c)\frac{1}{2}\frac{1}{\sqrt{1+\alpha x}}\alpha$$

$$= -\frac{c\alpha}{2}\frac{1}{\sqrt{1+\alpha x}}\frac{1}{1-c\sqrt{1+\alpha x}}$$

$$\left.\frac{df}{dx}\right|_{x=0} = -\frac{c\alpha}{2}\frac{1}{1-c}$$

$$\frac{d^2f}{dx^2} = -\frac{c\alpha}{2}\frac{1}{\sqrt{1+\alpha x}}\left[(-1)\left(\frac{1}{1-c\sqrt{1+\alpha x}}\right)^2(-c)\frac{1}{2}\frac{1}{\sqrt{1+\alpha x}}\alpha\right]$$

$$-\frac{c\alpha}{2}\frac{1}{1-c\sqrt{1+\alpha x}}\left(-\frac{1}{2}\right)\frac{1}{(1+\alpha x)^{3/2}}\alpha$$

$$\left.\frac{d^2f}{dx^2}\right|_{x=0} = -\frac{c\alpha}{2}\left[\frac{-1}{(1-c)^2}\left(\frac{-c\alpha}{2}\right)\right] - \frac{c\alpha}{2}\frac{1}{1-c}\left(-\frac{\alpha}{2}\right)$$

$$= -\frac{c\alpha}{2}\left[\frac{c\alpha}{2}\frac{1}{(1-c)^2} - \frac{\alpha}{2}\frac{1}{1-c}\right]$$

$$= -\frac{c\alpha^2}{4}\left[\frac{c}{(-c)^2} - \frac{1}{1-c}\right]$$

$$1 - \frac{c}{1-c} = \frac{1-c}{1-c} - \frac{c}{1-c}$$

$$= \frac{1-2c}{1-c}$$

$$= -\frac{c}{1-c}\frac{\alpha^2}{4}\left[\frac{c}{1-c} - 1\right]$$

$$= \frac{c}{1-c}\frac{\alpha^2}{4}\frac{1-2c}{1-c}$$

10/13/84

(7)

$$f = \ln\left(1 - c\sqrt{1+\alpha x}\right)$$

$$x = \frac{c\alpha}{2}\frac{1}{1-c}$$

$$= \ln(1-c) - \frac{c\alpha}{2}\frac{1}{1-c}x + \frac{c}{1-c}\frac{\alpha^2}{4}\frac{1-2c}{1-c}\frac{x^2}{4} + \cdots$$

$$\left(1 - c\sqrt{1+\alpha x}\right)^5 = e^{5\ln\left[1 - c\sqrt{1+\alpha x}\right]}$$

$$= e^{5\ln(1-c) + -\frac{5c\alpha}{2}\frac{1}{1-c}x + \frac{c}{1-c}\frac{\alpha^2}{4}\frac{1-2c}{1-c}\frac{x^2}{2} + \cdots}$$

$\alpha = 1$

$$\Rightarrow \left(1 - c\sqrt{1+x}\right)^5 \simeq (1-c)^5\, e^{-\frac{5}{2}\frac{c}{1-c}x + \frac{1}{8}\frac{c}{1-c}\frac{1-2c}{1-c}x^2}$$

$$= 0.8865\, e^{-0.0610x + 0.00297x^2}$$

For $x = 1$

$$(1-c)^5 = 0.8865$$

$$(1-c)^5 e^{-5/2\frac{c}{1-c}x} = 0.8340x$$

$$(1-c)^5 e^{-5/2\frac{c}{1-c}x + 1/8\frac{c}{1-c}\frac{1-2c}{1-c}x^2} = 0.8365x$$

10/13/84

(8)

$$\left(1 - c\sqrt{1+x}\right)^5$$

$$0.8865\, e^{-0.0610x}$$

$$e^{-0.119\sqrt{x}}$$

$$e^{-5c\sqrt{1+x}}$$

x	0.1	0.5	1	2	10	50
	0.88128	0.8625	0.8426	0.8101	0.6628	0.3932
	0.8811	0.8599	0.8340	0.7847	0.4817	0.0420
	0.9631	0.9193	0.8878	0.8451	0.6864	0.4311
	0.8826	0.8643	0.8451	0.8137	0.6738	0.4273

<1% <0.4% 8%

$x = 2$ $\quad \frac{0.8101 - 0.7847}{0.8101} \times 100 = 3.13\%$

$\left(1 - \frac{1}{42}\sqrt{6}\right)^5 = 0.7405$

$x = 5$ $\quad \frac{0.7405 - 0.6535}{0.7405} \times 100 = 11.7\%$

$0.8865 e^{-(0.0610)5} = 0.6535$

$\frac{c}{1-c} = \frac{\frac{1}{42}}{1-\frac{1}{42}} = \frac{1}{41}$ $\quad x = 0.5$ $\quad 0.30\%$

$$(1-c)^5 e^{\frac{5c}{1-c}} e^{-\frac{5c\sqrt{1+x}}{1-c}} = 1.00146\, e^{-\frac{5}{41}\sqrt{1+x}}$$

$x \to$ 0.1 0.5 1 2

0.88123 0.86252 0.84282 0.81078

$x \to$ 10 50

0.66931 0.41919

6% error

10/13/84

1

Summary

$$I_k = I_k^* - I_{k+1}^*$$

$$I_k^* = A_0 Z^* e \int_{-\infty}^{\infty} dv_x \int_{-\infty}^{\infty} dv_y \int_{v_k}^{\infty} dv_z \, v_z f(\vec{v}) R(\vec{v}, v_k)$$

$$R(\vec{v}, v_k) = \frac{TA}{A_0}$$

$$T = G\left(\left[\frac{v_x}{v_z}\right]^2, \left[\frac{v_z}{v_k}\right]^2, \left[\frac{v_z}{v_e}\right]^2\right) G\left(\left[\frac{v_y}{v_z}\right]^2, \left[\frac{v_z}{v_k}\right]^2, \left[\frac{v_z}{v_e}\right]^2\right)$$

$$G(x, \alpha, \beta) = \left(1 - c\sqrt{1 + x^*}\right)^5 \left(1 - c\sqrt{1 + \frac{x}{1 - \frac{1}{\alpha}}}\right)^3 \left(1 - c\sqrt{1 + \frac{x}{1 + \frac{1}{\beta}}}\right)$$

Or $G(x, \alpha_0, \beta_0) = \left(1 - c\sqrt{1 + x^{max}}\right)^5 \left(1 - c\sqrt{1 + \alpha_0 x}\right)^3 \left(1 - c\sqrt{1 + \beta_0 x}\right)$

$$\alpha_0 \equiv \frac{1}{1 - \frac{1}{\alpha}} = \frac{\alpha}{\alpha - 1} \qquad \beta_0 \equiv \frac{1}{1 + \frac{1}{\beta}} = \frac{\beta}{\beta + 1} \qquad c = \frac{1}{42}$$

$$A = A_x\left(S\frac{v_x}{v_z}\right) A_y\left(S\frac{v_x}{v_z}, S\frac{v_y}{v_z}\right)$$

$$S = S\left(\frac{v_z}{v_k}, \frac{v_z}{v_2}\right)$$

10/13/84

2

$$G = (1 - c\sqrt{1+x})^5 (1 - c\sqrt{1+\alpha x})^3 (1 - c\sqrt{1+\beta x})$$

$$= e^{\ln(1-c\sqrt{1+x})^5} e^{\ln(1-c\sqrt{1+\alpha x})^3} e^{\ln(1-c\sqrt{1+\beta x})}$$

$$= e^{5\ln(1-c\sqrt{1+x})} e^{3\ln(1-c\sqrt{1+\alpha x})} e^{\ln(1-c\sqrt{1+\beta x})}$$

$$= e^{-5c\sqrt{1+x}} e^{-3c\sqrt{1+\alpha x}} e^{-c\sqrt{1+\beta x}}$$

$$= e^{-5/2 \frac{c}{1-c} x} e^{-\frac{3}{2}\alpha \frac{c}{1-c} x} e^{-\frac{1}{2}\beta \frac{c}{1-c} x} (1-c)^9$$

$$= (1-c)^9 e^{-\frac{1}{2}\frac{c}{1-c} x [5 + 3\alpha + \beta]}$$

Alan used $T = T_0 \sum_{i=1}^{2} c_i e^{-a_i \frac{v_x^2}{v_0^2}} \sum_{j=1}^{2} c_j e^{-a_j \frac{v_y^2}{v_0^2}}$

$T_0 = (1-c)^{18}$ $\quad c_1 + c_2 = 1$

$$\Rightarrow G = c_1 e^{-a_1 x} + (1-c_1) e^{-a_2 x}$$

$$\frac{c}{1-c} = \frac{1}{\alpha_2} \frac{1}{1 - \frac{1}{\alpha_2}} = \frac{1}{\alpha_2} \frac{1}{\frac{\alpha_2 - 1}{\alpha_2}} = \frac{1}{\alpha_2 - 1} = \frac{1}{\alpha_1}$$

10/13/84

3

So one could set $\boxed{c_1 = 1}$, a_2 arbitrary

$$a_1 = \frac{1}{2}\frac{c}{1-c}(5+3\alpha+\beta)$$

$$= \frac{1}{2}\frac{c}{1-c}\left(5+3\frac{1}{1-\frac{v_{tk}^2}{v_t^2}}+\frac{1}{1+\frac{v_{ta}^2}{v_t^2}}\right)$$

$$a_1 = \frac{\frac{1}{2}\frac{1}{a_2}}{1-\frac{1}{a_2}}\left(5+3\frac{1}{1-\frac{v_k^2}{v_t^2}}+\frac{1}{1+\frac{v_a^2}{v_t^2}}\right)$$

$$\frac{\frac{1}{a_2}}{1-\frac{1}{a_2}} = \frac{1}{a_2-1} = \frac{1}{a_1}$$

$$\boxed{a_1 = \frac{1}{a_2}\left(5+3\frac{1}{1-\frac{v_k^2}{v_t^2}}+\frac{1}{1+\frac{v_a^2}{v_t^2}}\right)}$$

10/16/84

(1)

$$f(\vec{v}) = \frac{n}{\pi^{3/2} w^3} e^{-(v_x - V_x)^2/w^2 - (v_y - V_y)^2/w^2 - (v_z - V_z)^2/w^2}$$

$$I_k = I_k^* - I_{k+1}^*$$

$$I_k^* = A_0 \frac{Z^* e n}{\pi^{3/2} w^3} \int_{v_k}^{\infty} dv_z \, v_z \, e^{-(v_z - V_z)^2/w^2}$$

$$\times \int_{-\infty}^{\infty} dv_x \, e^{-(v_x - V_x)^2/w^2} \; G\left(\left[\frac{v_x}{v_z}\right]^2, \left[\frac{v_z}{v_k}\right]^2, \left[\frac{v_z}{v_a}\right]^2\right) A_x\left(S \frac{v_x}{v_z}\right)$$

$$\times \int_{-\infty}^{\infty} dv_y \, e^{-(v_y - V_y)^2/w^2} G\left(\left[\frac{v_y}{v_z}\right]^2, \left[\frac{v_z}{v_k}\right]^2, \left[\frac{v_z}{v_a}\right]^2\right) A_y\left(S \frac{v_x}{v_z}, S \frac{v_y}{v_z}\right)$$

$$S = S\left(\left[\frac{v_z}{v_k}\right]^2, \left[\frac{v_z}{v_a}\right]^2\right)$$

$$S(\alpha, \beta) \equiv 0.743 \alpha \left(1 - \sqrt{1 - \tfrac{1}{\alpha}}\right) + \frac{0.093}{\sqrt{1 - \frac{1}{\alpha}}} + 0.392 \beta \left(\sqrt{1 + \tfrac{1}{\beta}} - 1\right) + 0.340$$

$$G(\eta, \xi, S) \equiv \left(1 - c\sqrt{1 + \eta}\right)^5 \left(1 - c\sqrt{1 + \eta \frac{1}{(1 - \frac{1}{\xi})}}\right)^3 \left(1 - c\sqrt{1 + \eta \frac{1}{(1 + S)}}\right)$$

10/16/84

(2)

$$A_x(X) = \begin{cases} \dfrac{X + 4.94}{3.84} & -4.94 < X < -1.10 \\ 1 & -1.10 < X < 1.10 \\ \dfrac{X - 4.94}{-3.84} & 1.10 < X < 4.94 \\ 0 & X < -4.94 \text{ and } X > 4.94 \end{cases}$$

$$A_y(X,Y) = \begin{cases} \dfrac{Y - 2.02}{-1.60} & -3.62 < Y < -2.02 \\ 1 & -2.02 < Y < Y_m(X) \\ \dfrac{Y - Y_m(X)}{Y_m'(X) - Y_m(X)} & Y_m(X) < Y < Y_m'(X) \\ 0 & Y < -3.62 \text{ and } Y > Y_m'(X) \end{cases}$$

$(\sim 1.0 < Y_m'(X) < \sim 2.6)$

10/16/84

(3)

If $S\frac{v_x}{v_z} > 4.94$ the integrand is zero in the v_x integration. If we have a sufficiently good approximation for GA_x with $\alpha S\frac{v_x}{v_z} < 4.94$ then the same mathematical approximation will suffice for GA_y (since A_y cuts off for even smaller values in its argument).

We want to look at

$$GA_x = \left(1-c\sqrt{1+\frac{v_x^2}{v_z^2}}\right)^5\left(1-c\sqrt{1+\frac{v_x^2}{v_z^2}\frac{1}{1-\frac{v_y^2}{v_z^2}}}\right)^3\left(1-c\sqrt{1+\frac{v_x^2}{v_z^2}\frac{1}{1+\frac{v_y^2}{v_z^2}}}\right)$$

$$\times\begin{cases} 1 & 0 < S\frac{v_x}{v_z} < 1.10 \\ \dfrac{S\frac{v_x}{v_z}-4.94}{3.84} & 1.10 < S\frac{v_x}{v_z} < 4.94 \end{cases}$$

versus $(1-c)^9 \exp\left[-\frac{1}{2}\frac{c}{1-c}\left(5+\frac{3}{1-\frac{v_y^2}{v_z^2}}+\frac{1}{1+\frac{v_y^2}{v_z^2}}\right)\frac{v_x^2}{v_z^2}\right]$

$$\times\begin{cases} 1 & 0 < S\frac{v_x}{v_z} < 1.10 \\ \dfrac{S\frac{v_x}{v_z}-4.94}{3.84} & 1.10 < S\frac{v_x}{v_z} < 4.94 \end{cases}$$

where $S = 0.743\frac{v_z^2}{v_y^2}\left(1-\sqrt{1-\frac{v_y^2}{v_z^2}}\right) + 0.093\frac{1}{\sqrt{1-\frac{v_y^2}{v_z^2}}}$

$$+ 0.392\frac{v_z^2}{v_x^2}\left(\sqrt{1+\frac{v_x^2}{v_z^2}}-1\right) + 0.340$$

10/16/84

(4)

Define the following $c \equiv \frac{1}{42} = 0.02381$

$(1-c)^9 = 0.80503$

$\frac{1}{2}\frac{c}{1-c} = \frac{1}{82} = 0.01220$

$\nu_2 = 134.9$

$$46.08 \leq \nu_K \leq 1{,}059$$

and $\nu_z > \nu_K$

$$S \equiv 0.743 \left(\frac{\nu_z}{\nu_K}\right)^2 \left(1 - \sqrt{1 - \left[\frac{\nu_K}{\nu_z}\right]^2}\right) + 0.093 \frac{1}{\sqrt{1 - \left[\frac{\nu_K}{\nu_z}\right]^2}}$$

$$+ 0.392 \left(\frac{\nu_z}{\nu_2}\right)^2 \left(\sqrt{1 + \left[\frac{\nu_2}{\nu_z}\right]^2} - 1\right) + 0.340$$

Consider values of ν_x such that

$$0 < \nu_x < 4.94 \left(\frac{\nu_z}{S}\right)$$

Over this range we want to compare the real transparency function

$$G_R \equiv \left(1 - c\sqrt{1 + \left[\frac{\nu_x}{\nu_z}\right]^2}\right)^5 \left(1 - c\sqrt{1 + \left[\frac{\nu_x}{\nu_z}\right]^2 \frac{1}{1 - \left[\frac{\nu_K}{\nu_z}\right]^2}}\right)^3 \left(1 - c\sqrt{1 + \left[\frac{\nu_x}{\nu_z}\right]^2 \frac{1}{1 + \left[\frac{\nu_2}{\nu_z}\right]^2}}\right)$$

with the approximation

$$G_A \equiv (1-c)^9 \exp\left[-\frac{1}{2}\frac{c}{1-c}\left(5 + \frac{3}{1 - \left[\frac{\nu_K}{\nu_z}\right]^2} + \frac{1}{1 + \left[\frac{\nu_2}{\nu_z}\right]^2}\right)\left(\frac{\nu_x}{\nu_z}\right)^2\right]$$

10/16/84
(5)

In the expression for $A_y(X, Y)$ we need

$$A_y(X, Y) = \frac{Y - Y_m(x)}{Y_m'(x) - Y_m(x)} = \frac{Y}{Y_m'(x) - Y_m(x)} - \frac{Y_m(x)}{Y_m'(x) - Y_m(x)}$$

(from Stan's tabulated values of Y_m and Y_m')

X	$\frac{1}{Y_m' - Y_m}$	$\frac{Y_m}{Y_m' - Y_m}$
0	0.620	0.438
0.488	0.513	0.263
0.976	0.430	0.088
1.46	0.392	−0.035
1.95	0.379	−0.124
2.44	0.375	−0.171
2.93	0.401	−0.178
3.41	0.454	−0.168
3.90	0.536	−0.153
4.39	0.758	−0.037
4.88	2.041	1.041

10/16/84

V

$$1 - c\sqrt{1+x} = e^{\ln(1-c\sqrt{1+x})}$$

$$\ln(1-c\sqrt{1+x}) = -c\sqrt{1+x} - \tfrac{1}{2}c^2(1+x)$$

$$= -c\left(1+\tfrac{1}{2}x\right) - \tfrac{1}{2}c^2(1+x)$$

$$= -c\left(1+\tfrac{1}{2}c\right) - c\left(\tfrac{1}{2}x\right) - \tfrac{1}{2}c^2 x$$

$$= -c\left(1+\tfrac{1}{2}c\right) - \left(\tfrac{1}{2}c + \tfrac{1}{2}c^2\right)x$$

$$\sqrt{1+x} = 1 + \tfrac{1}{2}x - \tfrac{1}{8}x^2 + \cdots$$

$$\left(1-c\sqrt{1+x^2}\right)^5 = \left(1+cx-cx-c\sqrt{1+x^2}\right)^5$$

$$= \left(1+cx-c\left[x+\sqrt{1+x^2}\right]\right)^5$$

$$= \left(1+cx-c\sinh^{-1}x\right)^5$$

$$= e^{5\ln\left(1+cx-c\sinh^{-1}x\right)}$$

$$\simeq e^{5c\left[x-e^{\sinh^{-1}x}\right]}$$

$$\simeq e^{5c\left(x-e^{x}\right)}$$

Compare with above $5c(\sqrt{x}-e^{\sqrt{x}})$

$e^{[-20]}$

x	
0.1	0.8819
0.5	0.8545
1	0.8150
2	
10	0.0945

6-11-82
(2)

TEST3 – not interesting; debug stuff

AB2A – old stuff $\int_{v_j}^{v_{j+1}}$

ABRD – DATARD – make data out of
a data file TEST1 DATA
~~image~~ image of a summary tape
(Hoge made it).
SIMCOM – plug into fit routine
(PARM, LARRY, ARRY1, WRAY)
New version does only one species – v_x, v_y, v_z, w, n
Calls CPINT etc. and gives back counts in
required channels – array LCHAN selects channels
to be simulated – logical flags

ABRD2 – Currently being used for fitting
protons in monenen.

Logic set up to save time — must input consecutive channels
in each cup – can only have one set of consecutive channels.

12-27-82

See LNS listing JDSPERS1 — Used in routine JSUREST

In JDS PC under ASRESP2

ASRESP(V, WS, ZS, AS, MODE, CURRL, RESP(4)) from 0. to 1.

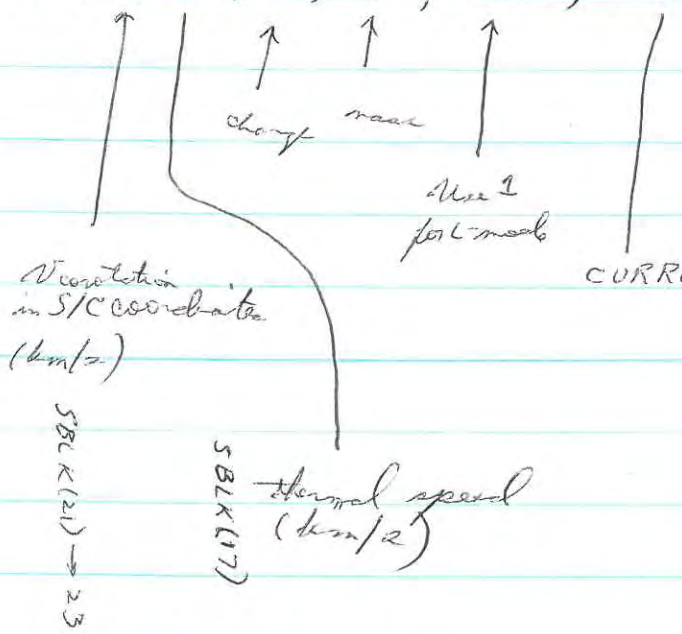

DATSAT in Task

RESP is the normalized flux — uses Area main = 65.
Area D = 56.24

Assume density of $1.0\ cm^{-3}$

In PMODEL, CPRESP finds the response for a given velocity vector — used in integration scheme

DO 6000 LOOPS

9/4/93
RLM ①

We can try to evaluate the integral

$$\int_0^\delta x e^{-\alpha x^2} I_0(\beta x)\, dx$$ by repeated integration by parts. Depending upon how we proceed with the expansion we can find two alternate forms

$$(I)\quad \int_0^\delta x e^{-\alpha x^2} I_0(\beta x)\, dx = \frac{1}{2\alpha} e^{\beta^2/4\alpha} - \frac{e^{-\alpha\delta^2}}{2\alpha} \sum_{n=0}^{\infty} \left(\frac{\beta}{2\alpha\delta}\right)^n I_n(\beta\delta)$$

and

$$(II)\quad \int_0^\delta x e^{-\alpha x^2} I_0(\beta x)\, dx = \frac{e^{-\alpha\delta^2}}{2\alpha} \sum_{n=1}^{\infty} \left(\frac{2\alpha\delta}{\beta}\right)^n I_n(\beta\delta)$$

where the $I_n(x)$ are modified Bessel functions. Note that if $\delta \to \infty$ (I) gives

$$\int_0^\infty x e^{-\alpha x^2} I_0(\beta x)\, dx = \frac{1}{2\alpha} e^{\beta^2/4\alpha}$$

For reference, we note that the generating function for the modified Bessel functions is

$$e^{\frac{1}{2}z\left(t+\frac{1}{t}\right)} = \sum_{k=-\infty}^{\infty} t^k I_k(z) \quad ; \quad I_k(z) = I_{-k}(z)$$

although this is apparently of no help to us here.

Finally, we also note that

$$\int_0^\infty x^2 e^{-\alpha x^2} I_0(\beta x)\, dx = -\frac{2}{2\alpha} \int_0^\infty e^{-\alpha x^2} I_0(\beta x)\, dx$$

and $$\int_0^\infty e^{-\alpha x^2} I_0(\beta x)\, dx = \frac{1}{2}\sqrt{\frac{\pi}{\alpha}}\, e^{\beta^2/8\alpha} I_0\left(\beta^2/8\alpha\right)$$

For the indefinite integral there is one special case in which

$$\beta = 2\alpha\delta \quad \text{or} \quad \delta = \frac{\beta}{2\alpha}$$

From the generating function we have

$$e^{z\cos\theta} = I_0(z) + 2\sum_{k=1}^{\infty} I_k(z)\cos(k\theta)$$

Put $\theta = 0 \Rightarrow \cos\theta = \cos k\theta = 1$

$$\therefore e^{z} = I_0(z) + 2\sum_{k=1}^{\infty} I_k(z)$$

Or $$\sum_{k=1}^{\infty} I_k(z) = \left[e^{z} - I_0(z)\right]\frac{1}{2}$$

Hence $$\int_0^{2\alpha/\beta} x e^{-\alpha x^2} I_0(\beta x)\,dx = \frac{e^{-\alpha\delta^2}}{4\alpha}\left(e^{\beta\delta} - I_0(\beta\delta)\right)$$

Abstract

The Response Function of Modulator Grid Faraday Cup Plasma Instruments

by Alan Barnett and Stanislaw Olbert

Modulator grid Faraday cup plasma analyzers are a very useful tool for making in situ measurements of space plasmas. One of their great attributes is that their simplicity permits their angular response function to be calculated theoretically. In this paper, we derive an expression for this response function by computing the trajectories of the charged particles inside the cup. We use the Voyager Plasma Science Experiment as a specific example. Two approximations to the "rigorous" response function useful for data analysis are discussed.

The theoretical formulas were tested by multi-sensor analysis of solar wind data. The tests indicate that the formulas represent the true cup response function for all angles of incidence with a maximum error of only a few percent.

1. Introduction

A useful tool for making in situ measurments of space plasmas is the Modulator Grid Faraday cup. In this paper we discuss the operation of this type of instrument and derive an expression for its response function. An instrument consisting of an array of four Faraday cups which was flown on the Voyager missions to the outer planets[1] is shown in Figure 1. Although the formulas which we quote describe the Voyager instrument, the method we use can easily be applied to any Faraday cup.

The response function of the cup is defined as the ratio of the particle flux reaching the collector to the particle flux incident on the aperture when the incident particles are a collimated, monoenergetic beam. We compute the response function by studying the trajectories of the particles inside the cup. In Section 2 we describe the model of the cup which we use and the nature of the approximations which we have to make.

We show that the response function can be written as a product of two terms, the "sensitive area" and the grid transparency. The sensitive area term is computed from a straightforward study of the trajectories, while statistical arguments are required to determine the grid transparency term. These terms are derived in detail, and explicit expressions for them are given for the case of the Voyager instruments, in Sections 3 and 4.

Once the response function is known, one can use it to analyze data. The collector current from a plasma described by a known distribution function can be computed by performing an integration over velocity space. The problem of data analysis, therefore, becomes the problem of solving an integral equation for the distribution function. A very useful approximate method for solving the integral equation is to use a parameterized model for the

distribution function, and then find the "best fit" values for the parameters. In order to do this, one must be able to perform the velocity space integration. Certain further approximations which permit the integration over the components of velocity perpendicular to the cup normal to be performed analytically for the case where the distribution function is a convected maxwellian are described in Section 5.

Once we have computed the response function, we want to test it. In order to do this, one would like to have a very narrow test beam. Unfortunately, it is very difficult to make such a beam in the lab. We have used the calm solar wind at about 4 AU as our test beam. Analysis of data from Voyager 1 taken when the spacecraft was rotating (Voyager is a three axis stablized spacecraft) causing the solar wind to enter the cups at large angles indicates that our expressions are an excellent represention of the true response functions of the cups for all energies and angles of incidence. This analysis is discussed in Section 6.

2. The Physics of the Modulator Grid Faraday Cup

In this section, we analyze the physics of the Faraday cup and present the model which we use to compute the response function, using the Voyager PLS instrument as an example. Throughout this paper, we will consider the measurement of positive ions. For electrons, the analysis which we present can be modified in a straightforward manner, although in that case the emmission of secondaries must be considered.

As can be seen from Figure 1, the PLS instrument consists of 4 Faraday cups. Three of them, called the A, B, and C cups are arrayed about an axis af symmetry and have pentagonally shaped apertures and collectors. The fourth

cup, called the D-cup, is circular in shape (a more conventional design) and points 88° from the main sensor symmetry axis. The geometry will be very important for understanding the test of the response function.

A cross-section of one of the PLS instrument's main sensor cups is shown in Figure 2. The cup consists of an aperture stop, eight parallel grids and a collector plate mounted in a metal housing. A top view of a cup is shown in Figure 3. Fig. 3 also defines a coordinate system which we call cup coordinates ($\hat{z}$ is the inward pointing cup normal). Notice that the collector is much larger than the aperture, a fact which gives this cup a much larger field of view than a conventional cup.

During operation, the collector plate and all of the grids except the modulator grids and the suppressor grid are grounded to the spacecraft. The suppressor grid is kept at -95 V to shield the collector from the plasma electrons and to return any secondary electrons to the collector. The instrument is used by applying a square wave positive voltage to the modulator grids and measuring the collector current. Since more particles are repelled when the retarding potential is increased, the current waveform is an inverted square wave as shown in Figure 4. We call the upper and lower limiting modulator voltages ϕ_k and ϕ_{k+1}, respectively, and the corresponding collector currents I_k^* and I_{k+1}^*. The signal I_k is the amplitude of the current step, given by

$$I_k = I_k^* - I_{k+1}^* \qquad 1$$

We wish to determine collector current as a function of the modulator voltage and the plasma distribution function. To a first approximation, the signal consists of all of the incident particles for which the z-component of velocity (v_z) is between v_k and v_{k+1}, where v_k is related to ϕ_k by

$$v_k = (2Z^* e\phi_k / A^* m)^{1/2} \qquad 2$$

where m_p is the proton mass, A^* is the mass of the ion in AMU, Z^* is the charge state of the ion, and e is the proton charge. To obtain a better approximation, we need to study the motion of the charged particles inside the cup.

The total electric current incident on the aperture (I_{ap}) is due to ionic species a is

$$I_{ap} = Z_a^* e \iint_{\text{Aperture}} dx\, dy \int_{-\infty}^{\infty} dv_x \int_{-\infty}^{\infty} dv_y \int_{0}^{\infty} v_z\, f_a(\vec{v})\, dv_z \qquad 3$$

where dx dy is an area element in the aperture and $f_a(\vec{v})$ is the distribution function of ion species a. For the total current, one must sum over all species. In the remainder of this paper, we will supress the subscript a.

Not all of the particles incident on the aperture reach the collector. In principle, given the initial position and velocity of a particle, one can calculate its trajectory and thereby determine whether or not it will reach the collector. We can therefore formally write for the collector current

$$I_k^* = Z^* e \iint_{\text{Aperture}} dx\, dy \int_{-\infty}^{\infty} dv_x \int_{-\infty}^{\infty} dv_y \int_{0}^{\infty} v_z\, f(\vec{v})\, H(\vec{v},x,y,\phi_k) dv_z \qquad 4$$

where $H(\vec{v},x,y,\phi_k)$ equal to one if the trajectory of a particle incident on the aperture at the position x,y with velocity $\vec{v}$ reaches the collector, and is equal to zero otherwise. In practice, Equation 4 is useless in this form because the precision with which we can calculate the particle trajectories is insufficient to permit us to accurately predict whether or not a given incident particle will collide with one of the grids. We can, however, compute the <u>probability</u> that a particle will collide with a grid. If we denote by A_{ap} the area of the aperture, and by $R(\vec{v},\phi_k)$ the probability that an incident particle with velocity $\vec{v}$ has of reaching the collector (which is the same as the fraction of particles of a uniform beam of particles with velocity

$\vec{v}$ which reaches the collector), we can rewrite the Equation 4 as

$$I_k^* = Z^* e A_{ap} \int_{-\infty}^{\infty} dv_x \int_{-\infty}^{\infty} dv_y \int_{0}^{\infty} v_z \, f(\vec{v}) \, R(\vec{v},\phi_k) dv_z \qquad 5$$

We call $R(\vec{v},\phi_k)$ the response function of the detector.

To determine R, we use the following model of the cup. We assume that the electrostatic potential inside the cup depends only on z, and that it is a linear function of distance between any two adjacent grids. (The model potential for the Voyager PLS main sensor cups is shown in Figure 5.) This approximation neglects the fine structure of the fields near the grid wires and the fringing fields near the edges of the grids. If the distance between the grids is much greater than the spacing between the wires and the grid spacing is much smaller than the linear dimensions of the grid, this approximation should be adequate.

In our model field, we can calculate the particle trajectories exactly. The particle trajectory between any two grids is either a straight line or a parabola. If we now assume that the probability of a particle striking a grid (a possibility not included in our trajectory calculation) does not depend on the position where the particle enters the cup, we can write R as a product of two terms and a normalization constant

$$R(\vec{v},\phi_k) = T(\vec{v},\phi_k) \, A(\vec{v},\phi_k)/A_{ap} \qquad 6$$

where T is the transparency of the grids (the probability that a particle does <u>not</u> collide with a grid), A is the "sensitive area" (the area of the aperture for which incident particles will strike the collector).

3. The Sensitive Area

We discuss first the sensitive area. Consider an incident beam of particles of velocity $\vec{v}$. If v_z is less than v_k, defined by Equation 2, then the particle will be repelled by the modulator voltage, so R will be 0. We therefore must change, in Equation 5, the lower limit of integration over v_z from zero to v_k.

If v_z is greater than v_k, then in the collector plane the beam will have the shape of the aperture, but its position will be displaced because of the components of the particle velocity transverse to the cup normal direction, as shown in Figure 6. We define a two-dimensional vector $\vec{S}$, also shown in Figure 6, to be the displacement of the aperture image from a perpendicular projection of the aperture into the plane of the collector. One can calculate from the equations of motion that the "shift vector" $\vec{S}$ is given by

$$S_x = S^* h \frac{v_x}{v_z} \qquad 7a$$

$$S_y = S^* h \frac{v_y}{v_z} \qquad 7b$$

where h is the distance between the aperture and the collector, and S^*, called the shift function, depends only upon v_z, the cup geometry, and the grid voltages. For the Voyager main sensor cups, the shift function is given explicitly by

$$S^* = .743\left(\frac{[1-(1-\frac{v_k^2}{v_z^2})^{1/2}]}{(v_k^2/v_z^2)}\right) + .093\left(\frac{1}{1-(v_k^2/v_z^2)}\right)^{1/2} + .392\left(\frac{[(1+\frac{v_s^2}{v_z^2})^{1/2}-1]}{(v_s^2/v_z^2)}\right) + .340 \qquad 8$$

Once the shift vector is known, the sensitive area can be computed in a straightforward manner using a geometrical construction. For cups with

cylindrical symmetry, the sensitive area depends only on the magnitude of $\vec{S}$, and the functional dependence can be expressed simply in closed form. For the Voyager main sensor, on the other hand, this functional dependence is complicated. As there are 16 separate regions where the dependence is different (see Figure 7), an exact analytical representation is cumbersome. A plot of the sensitive area (normalized to unity for normal incidence) as a function of S_y/h, with S_x/h as a parameter, is shown in Figure 8.

4. The Grid Transparency

We now consider the grid transparency. The transparency of a single grid is defined as the probability of an incident particle traversing the plane of the grid without colliding with the wires (all particles which strike the wires are assumed to be absorbed). We model a grid as a planar structure consisting of two perpendicular sets of parallel cylindrical wires. The transparency of the grid will be the product of the transparencies of each set of wires considered separately.

Consider a set of wires which run in the $\hat{y}$-direction (as before, $\hat{z}$ is taken to be normal to the plane of the grid). Since the transparency of these wires does not depend upon v_y, we only need to consider the projection of the particle motion into the x-z plane. The probability of a particle colliding with one of the wires is simply the ratio of the area of the wires to the area of the gaps between the wires projected into a plane perpendicular to the particle velocity vector. As can be seen from Figure 9, the probability of collision is proportional to sec α, where α is the angle between the projection of the particle velocity into the x-z plane and the z- axis. The same line of reasoning can be applied to the set of wires which runs in the

$\hat{x}$-direction. Using the computed trajectories in our simplified cup model to compute the value of α for each grid, and noting that the probability of a particle reaching the collector plane without colliding with a grid is simply the product of the probabilities of it successfully traversing each individual grid, we can write the grid transparency term as the following product

$$T=\prod_i [1-c(1+\frac{v_x^2}{v_z^2-\frac{2e\phi_i}{Am_p}})^{1/2}][1-c(1+\frac{v_y^2}{v_z^2-\frac{2e\phi_i}{Am_p}})^{1/2}] \qquad 9$$

where ϕ_i is the voltage on the i-th grid and c is the ratio of the wire diameter to the wire spacing.

For the voyager main sensor, c=1/42 and the sets of wires in the different grids are parallel. Since each cup has three modulator grids, one suppressor grid, and five grounded grids (see Fig. 1), the transparency is given explicitly by

$$T=[1-c(1+\frac{v_x^2}{v_z^2})^{1/2}]^5[1-c(1+\frac{v_x^2}{v_s^2-v_k^2})^{1/2}]^3[1-c(1+\frac{v_x^2}{v_z^2-v_s^2})^{1/2}]\times$$
$$[1-c(1+\frac{v_y^2}{v_z^2})^{1/2}]^5[1-c(1+\frac{v_y^2}{v_z^2-v_k^2})^{1/2}]^3[1-c(1+\frac{v_y^2}{v_z^2-v_s^2})^{1/2}] \qquad 10$$

The subscript s refers to the suppressor grid; v_s is defined in a manner analogous to the definition of v_k in Equation 2

$$v_s=(2Z^*e\phi_s/A^*m_p)^{1/2} \qquad 11$$

where ϕ_s is the voltage on the suppressor grid. Note that, for the Voyager main sensor cups, at normal incidence $T=T_o=(1-c)^{18}=0.65$.

5. Further Approximations

In order to use our results to analyze data, one must evaluate the integrals of Equation 5 for a parameterized distribution function, and use the data to obtain "best fit" values for the parameters. It is possible to do all of the integrations numerically, but a much faster running computer code can be written if some of the integrations can be done analytically. In this section we outline two approximation schemes which permit analytical, closed form evaluation of the integrations over v_x and v_y. The details of the schemes are given in ref 2.

For the complicated geometry of the Voyager PLS main sensor, a suitable analytic expression for the sensitive area (Figure 8) must first be found. We used a family of trapezoids, plotted in Figure 10. The formulas for these trapezoids are

$$A=A_x(S_x/h)A_y(S_x/h,S_y/h) \qquad 12$$

$$A_x=\frac{(S_x/h)+X'_r}{X'_r-X_r} \qquad -X'_r<S_x/h<X_r \qquad 12a$$

$$A_x=1 \qquad -X_r<S_x/h<X_r \qquad 12b$$

$$A_x=\frac{(S_x/h)-X'_r}{X'_r-X_r}\ \xi(-S_x/h) \qquad X_r<S_x/h<X'_r \qquad 12c$$

$$A_x=0 \qquad \text{Otherwise} \qquad 12d$$

$$A_y=\frac{(S_y/h)+Y_d}{Y'_d-Y_d} \qquad Y'_d<S_y/h<Y_d \qquad 12e$$

$$A_y=1 \qquad -Y_d<S_y/h<Y_d \qquad 12f$$

$$A_y=\frac{(S_y/h)-Y_u(S_x)}{Y'_u(S_x)-Y_u(S_x)} \qquad Y_u(S_x)<S_y/h<Y'_u(S_x) \qquad 12g$$

$$A_y=0 \qquad \text{Otherwise} \qquad 12h$$

with

$$X_r = 1.10 \tag{13a}$$

$$X_r' = 4.94 \tag{13b}$$

$$Y_d = -2.02 \tag{13c}$$

$$Y_d' = -3.62 \tag{13d}$$

$$Y_u = \frac{.762\ \cos\{1.018(S_x/h)+.247\}}{1+0.25(S_x/h)} \tag{13e}$$

$$Y_u' = 2.50-0.125[(S_x/h)-1]^2 \tag{13f}$$

All of the quantities defined by Equations 12a-h and 13a-f are dimensionless. Y_u and Y_u' are plotted in Figure 11. Figure 12 shows a 3-D plot of $A(\vec{S}/h)$. The values of X_r, X_r', Y_d, Y_d', Y_u, and Y_u' were chosen so as to match the volume of the solid of Fig. 12 as closely as possible with the volume of the solid representing the true area overlap. Figure 13 shows a 3-D plot of $R(S_x/h, S_y/h)$, computed using the "trapezoidal approximation" for A and Eq. 10 for T.

We shall now proceed to describe two different approximation schemes. In both cases, the plasma distribution function will be assumed to be a convected maxwellian

$$f(\vec{v}) = \frac{n_o}{w^3 \pi^{3/2}} \exp\{-(\vec{v}-\vec{V})^2/w^2\} \tag{14}$$

where $\vec{V}$ is the plasma bulk velocity, w is the thermal speed, and n_o is the particle number density. For the case where V >> w, we have a well collimated beam. In this case, we can approximate the dependence of f on v_x and v_y by a product of delta functions

$$f(\vec{v}) = \frac{n_o}{w\sqrt{\pi}}\, \delta(v_x-V_x)\ \delta(v_y-V_y)\ \exp\{-(v_z-V_z)^2/w^2\} \tag{15}$$

The delta functions permit the integrations over v_x and v_y to be computed

trivially, leaving only the numerical integration over v_z. This approximation was used to experimentally test the response function, as described in the following section.

For the more general case where the bulk velocity is not much greater than the thermal speed, we must change the form of the expression for the grid transparency. It is possible to approximate Equation 9 by an expression of the form

$$T = [\sum_{i=1}^{2} c_i \exp\{-a_i (\frac{v_x}{v_z})^2\}] [\sum_{j=1}^{2} c_j \exp\{-a_j (\frac{v_y}{v_z})^2\}] \qquad 16$$

where the a's and c's are functions of the grid voltages and v_z only. The values of the a's and c's must be determined by a numerical fitting procedure. This approximation permits the desired integrals to be evaluated numerically with the aid of the saddle point method.

For a cylindrically symmetrical cup, a similar approximation scheme can be used. This case is much simpler, since the response function does not depend upon the azimuthal angle of incidence of the particles. (Except for a small effect due to the rectangular structure of grids themselves. If the grids are mounted such that the wires of a given grid are not parallel to the wires of the other grids, this effect will be minimized.) The sensitive area can be approximated by a single trapezoid, and the grid transparency term contains one sum of gaussians, rather than the product of two sums of gaussians. The integration over azimuth angle then yields a modified Bessel function, which can be approximated by a sum of exponentials to permit analytic evaluation of the integral over the magnitude of the tangential velocity.

6. Experimental Test of the Response Function

In order to test our theoretical response function, we have analyzed data taken by Voyager 1 during a cruise maneuver. Voyager is a three-axis stablized spacecraft, and most of the time it is oriented such that the main sensor symmetry axis, which is parallel to the spacecraft's main antenna, is pointed toward the Earth. Since the angular separation between the Earth and the sun, as viewed from the outer solar system, is small, the solar wind direction was usually almost parallel to the main sensor symmetry axis. In this configuration the "unity response" approximation to the cup response (all incident particles which are not stopped by the modulator voltage reach the collector, but the aperture area is corrected for the transparency of the grids at normal incidence) is good. During the cruise maneuver, however, the spacecraft performed a series of rotations, some of which involved rotating the main antenna away from the Earth.

The data were taken over a period of 90 minutes on 14 September, 1978, when Voyager 1 was 4.1 AU from the sun. The solar wind bulk speed during the maneuver varied between 368 and 378 km/sec, while the thermal speed varied between 14 and 20 km/sec. Data were taken simultaneously in all four cups. Two such spectra are shown in Figures 14 and 15. The figures consists of $I_k/(\phi_{k+1}-\phi_k)$ plotted versus v_k for each cup. The staircases are the data, while the smooth curves are the "best fit" simulations. The fits are excellent, correctly reproducing the location, height, and shape of each peaks in all of the cups in which there is a signal. For the spectra of Figure 14, the angles between the bulk velocity and the cup normals for the A, B, C, and D cups were 38°, 72°, 56° and 124°, respectively, while for the spectrum of Fig. 15 the angles were 67°, 34°, 52°, and 56°, respectively.

As an illustration of the extent to which we are actually testing our response function using this process, consider Figures 16 and 17. Figure 16 is the same spectrum as Figure 14, except that the smooth curve is a simulation using the parameters derived from the fit of Fig. 14 with the assumption of unity response. Notice that although the peaks are all in the right place due to the effect of the sharply peaked distribution function, the heights and shapes are all wrong. It should be pointed out that the current in the B cup of this spectrum is only about 4% of what the current would be if the same beam were at normal incidence.

An even more striking example is shown in Fig. 17. While the measurements were being taken, the spacecraft was rotating at a rate of one rotation every 33 minutes. Since the instrument takes .24 seconds to measure a single channel, and the same channel is measured simultaneoussly in all four cups, the peak in the B-cup (channel 46) was measured about 5 seconds later than the peak in the A-cup (channel 24) was measured. During that time, the spacecraft rotated about $.9^{\circ}$. For the fit shown in Fig. 15, this rotation was compensated for, while for the fit shown in Fig 17 the effect of this small rotation was neglected. Our theoretical response function is sufficiently good that failure to account for this rotation of less than 1° made the fit noticably worse!

The quality of the fits to the data taken during the cruise maneuver has convinced us that our theoretical response function represents the true response function of the Voyager PLS experiment within a few percent for all angles of incidence. We further believe that this knowledge makes the Voyager PLS experiment the best understood plasma instrument ever flown.

References

[1]Bridge,H.S., J.W. Belcher, R.J. Butler, A.J. Lazarus, A.M. Mavretic, J.D. Sullivan, G.L. Siscoe, and V.M. Vasyliunas; Sp. Sci. Rev. 21:259-287 1977

[2]Barnett,A.S; NASA technical report CSR-TR-84-1 1984

[3]We would like to thank Herb Bridge, John Belcher, and Alan Lazarus for helpful discussions.

This work was supported under JPL Contract 953733 and NASA contract NSG 22-009-015.

Figure Captions

Figure 1 The Voyager PLasma Science (PLS) Experiment.

Figure 2 Cross section of a PLS main sensor cup.

Figure 3 PLS main sensor Aperture and Collector Areas. Note direction of axes for cup coordinates: $\hat{z}$ points into the cup.

Figure 4 Modulator Voltage and Collector Current Versus Time.

Figure 5 Model Potential Versus z for a PLS main sensor cup.

Figure 6 Definition of the Shift Vector. The figure shows the outline of the collector of one of the main sensor cups, with the image of the aperture in the collector superposed on it. An incident monoenergetic beam of particles will have the shape of the aperture as it travels through the cup. The shift vector $\vec{S}$ is the vector which lies in the collector plane and points from the point directly underneath the center of the long side of the aperture to the corresponding point on the image of the aperture in the incident beam.

Figure 7 The Sensitive Area of a Main Sensor Cup. The figure shows the 16 distinct regions in which there is a different functional dependence of the sensitive area on the shift vector.

Figure 8 Main Sensor Sensitive Area Versus S_y/h.

Figure 9 Geometry for Grid Transparency Calculation. A beam of particles incident on a grid of parallel, cylindrical wires is shown. α is the angle between the beam direction and the normal to the plane of the grid, L is the distance between the centers of two adjacent wires, and d is the wire diameter. The wires run in the $\hat{y}$-direction, and the $\hat{z}$-direction is normal to the grid plane, with $+\hat{z}$ making an acute angle with the direction of the incident beam.

Figure 10 Main Sensor Sensitive Area Versus S_y/h (Trapezoidal Approximation). Compare with Figure 8.

Figure 11 Y_u and Y'_u Versus S_x/h.

Figure 12 3-D Plot of the Sensitive Area Versus S_x and S_y in the Trapezoidal Approximation.

Figure 13 3-D Plot of the Full Response Function, computed using the trapezoidal approximation for the sensitive area and the "exact" expression for the grid transparency.

Figure 14 Reduced Distribution Function Versus Velocity for Cruise Maneuver Spectrum 1. The staircases are the data, while the smooth curve is the fit.

Figure 15 Reduced Distribution Function Versus Velocity for Cruise Maneuver Spectrum 2. The staircases are the data, while the smooth curve is the fit.

Figure 16 Reduced Distribution Function Versus Velocity for Cruise Maneuver Spectrum 1. The staircases are the data, while the smooth curve is a simulation done assuming "unity" response using the plasma parameters determined from the fit which is plotted in Figure 14. Note that the locations of the peaks in the simulation are correct, but their heights and shapes are wrong.

Figure 17 Reduced Distribution Function Versus Velocity for Cruise Maneuver Spectrum 2. The staircases are the data, while the smooth curve is the fit. The change in the orientation of the spacecraft between the time of the peaks in the different cups was <u>not</u> compensated for. Compare to Figure 15.

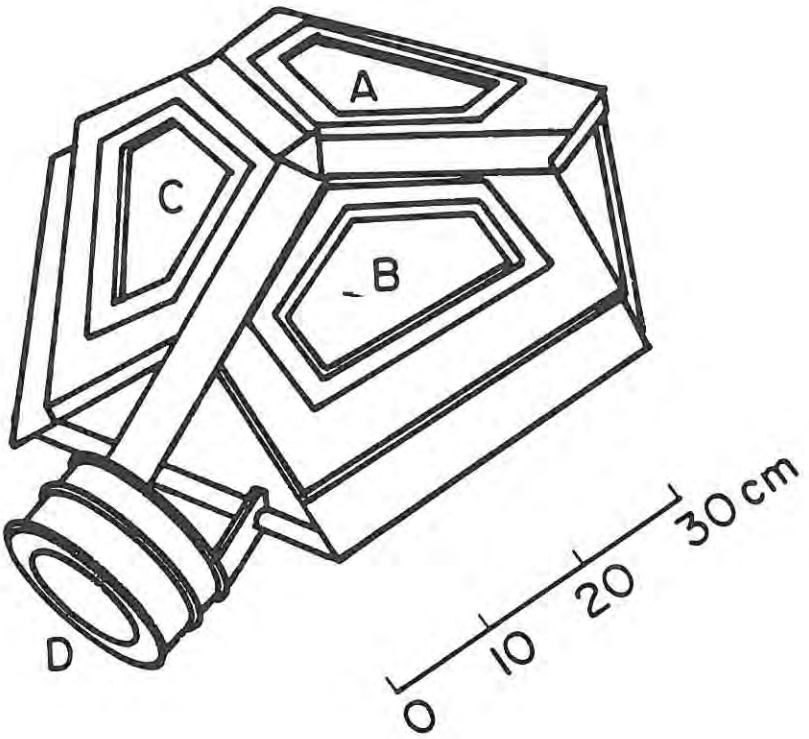

Figure 1

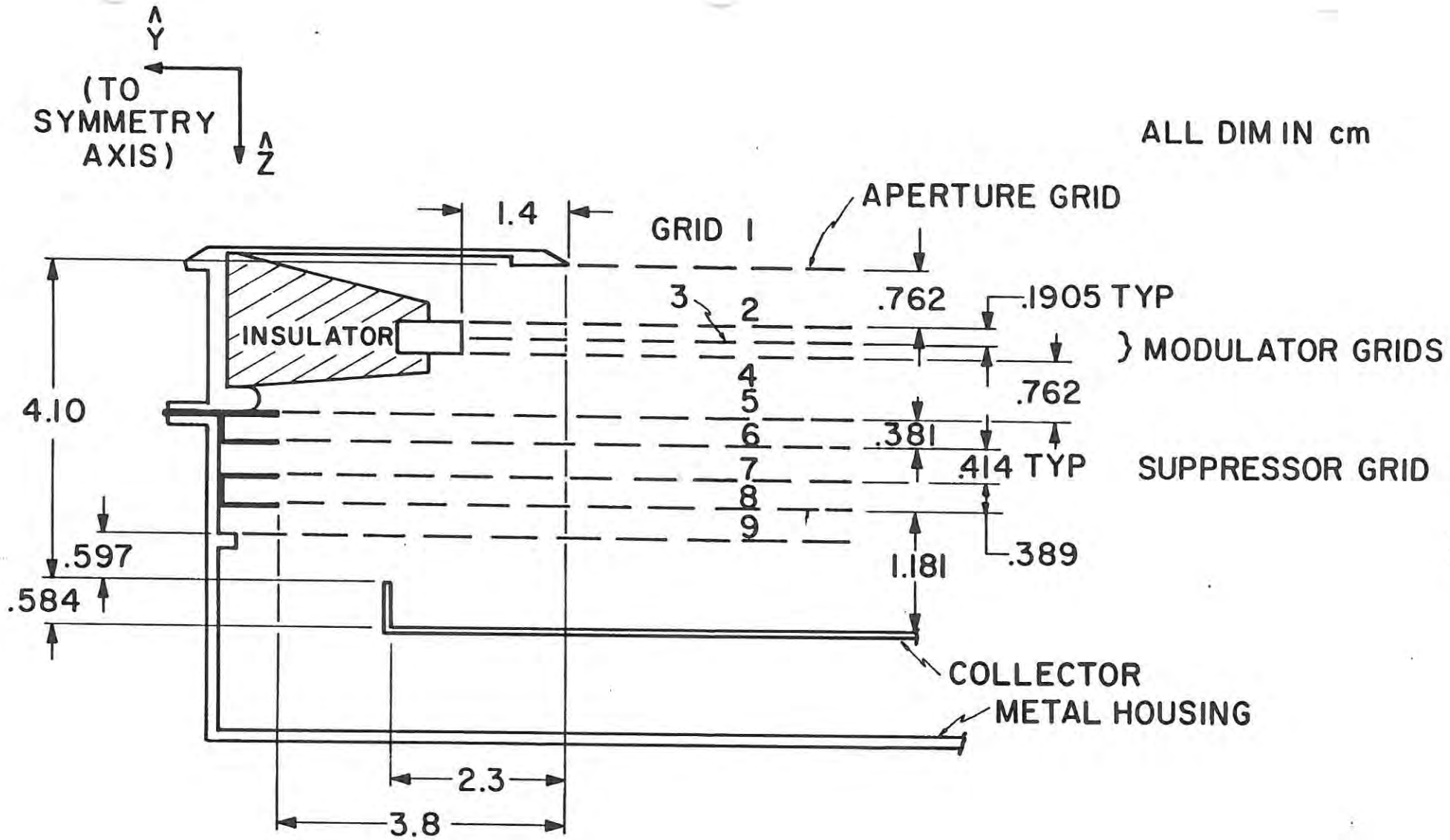

MAIN SENSOR
VERTICAL CUT OF UPPER SEGMENT

Figure 2

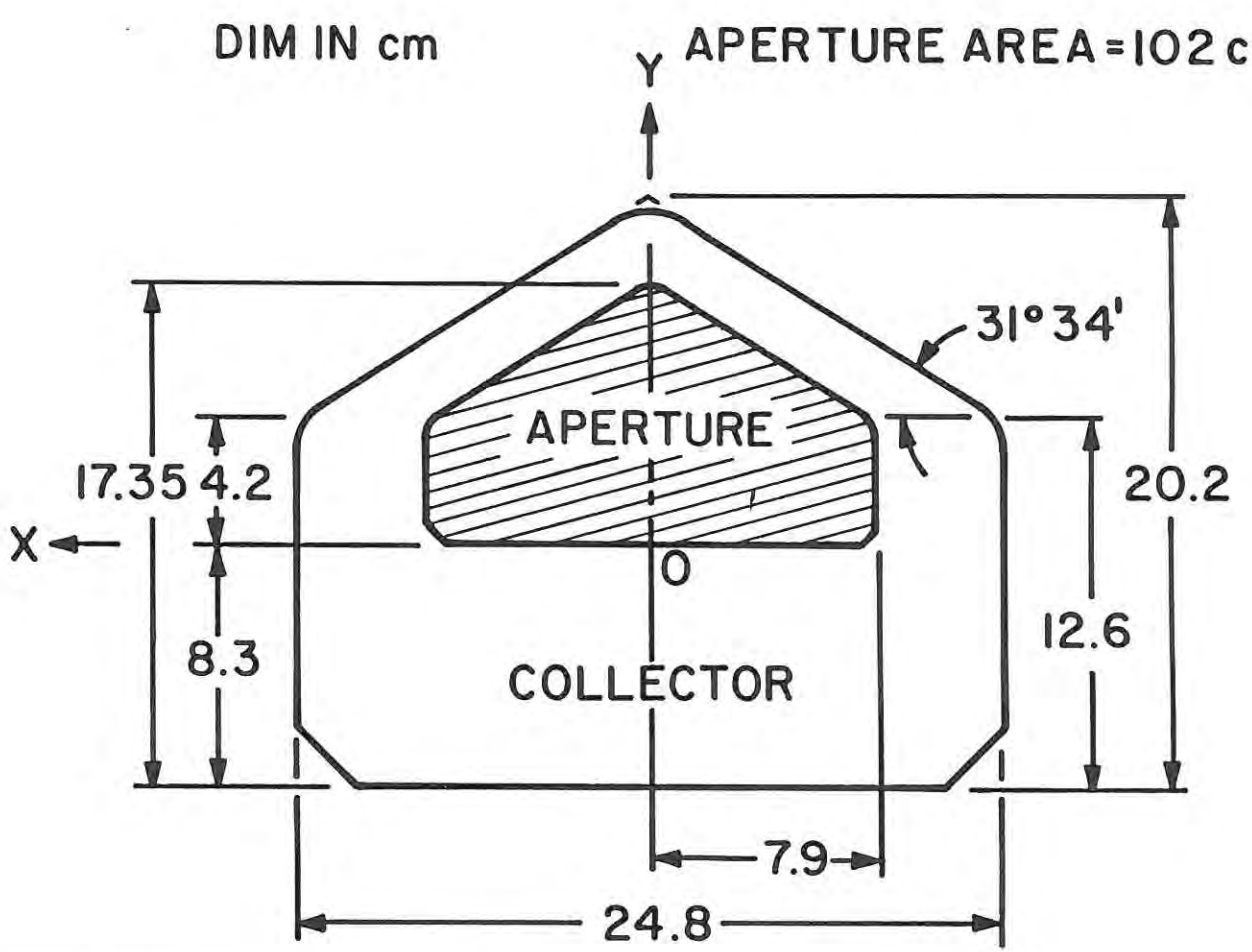

MAIN SENSOR (APERTURE AND COLLECTOR AREAS)

Figure 3

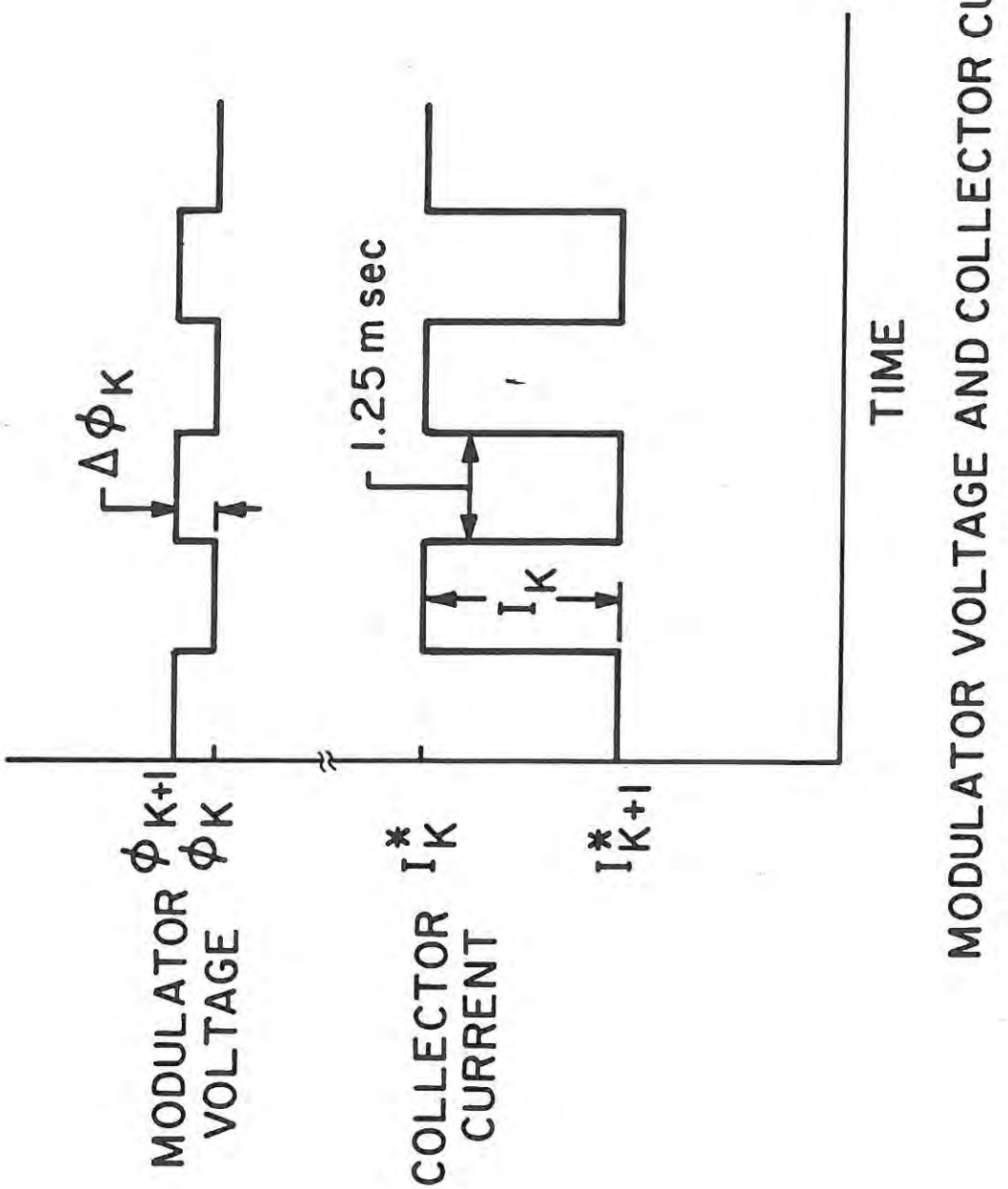

MODULATOR VOLTAGE AND COLLECTOR CURRENT
vs
TIME

Figure 4

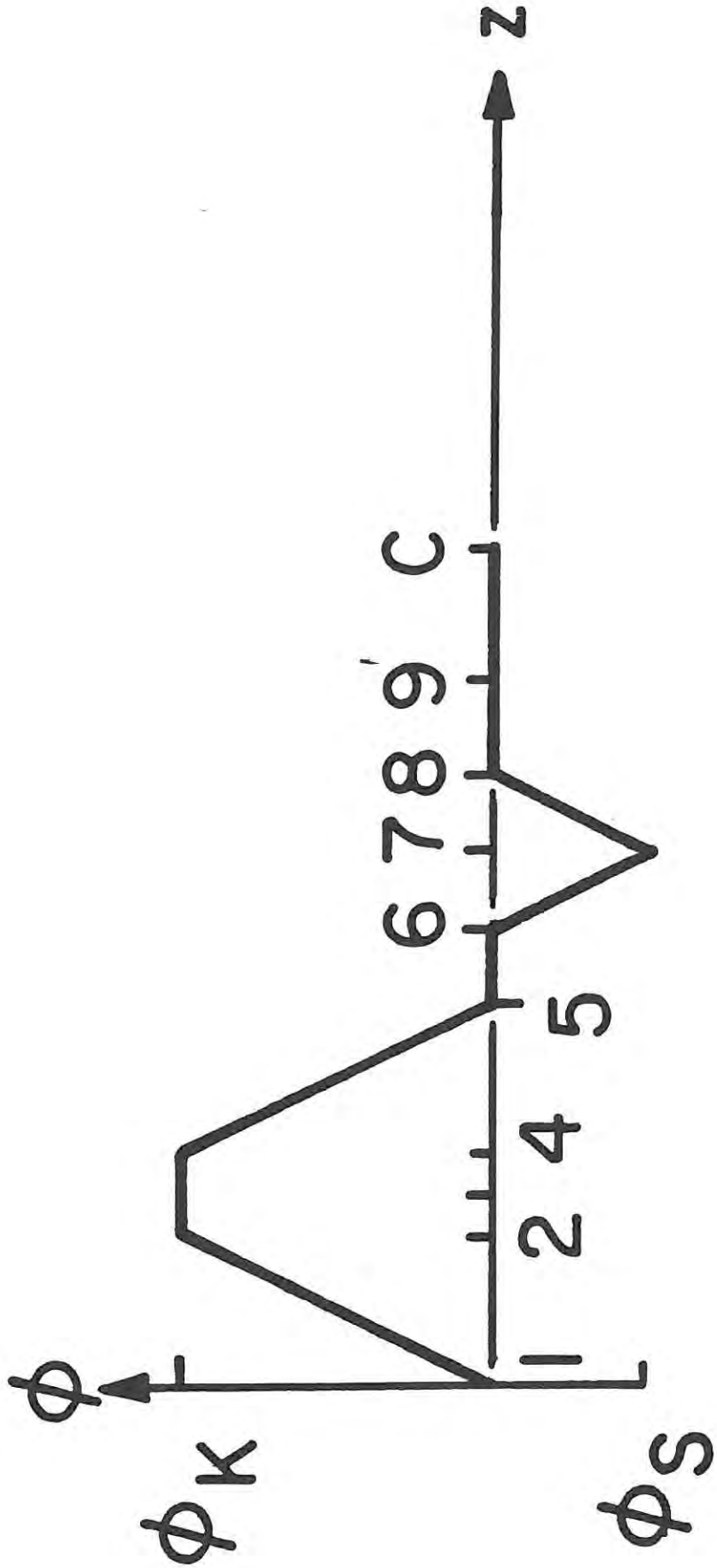

Figure 5

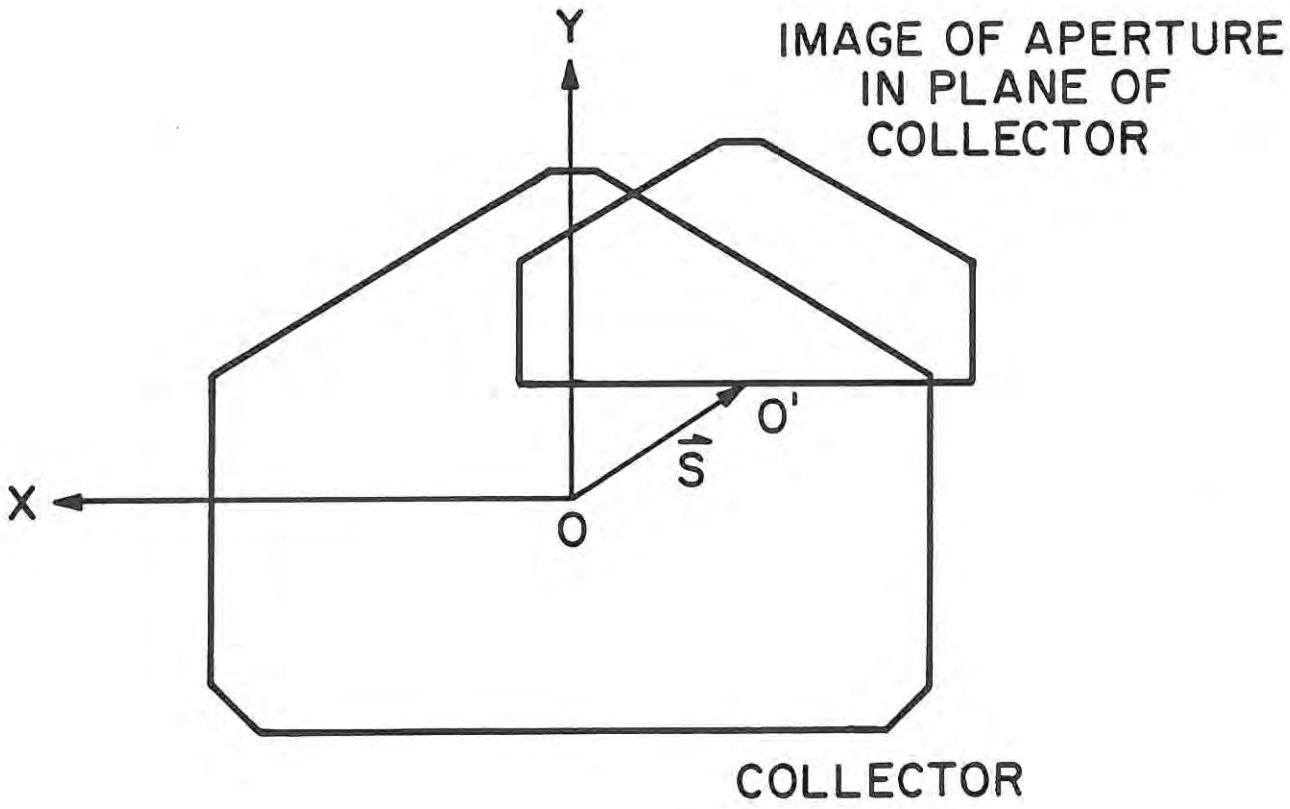

DEFINITION OF SHIFT VECTOR

Figure 6

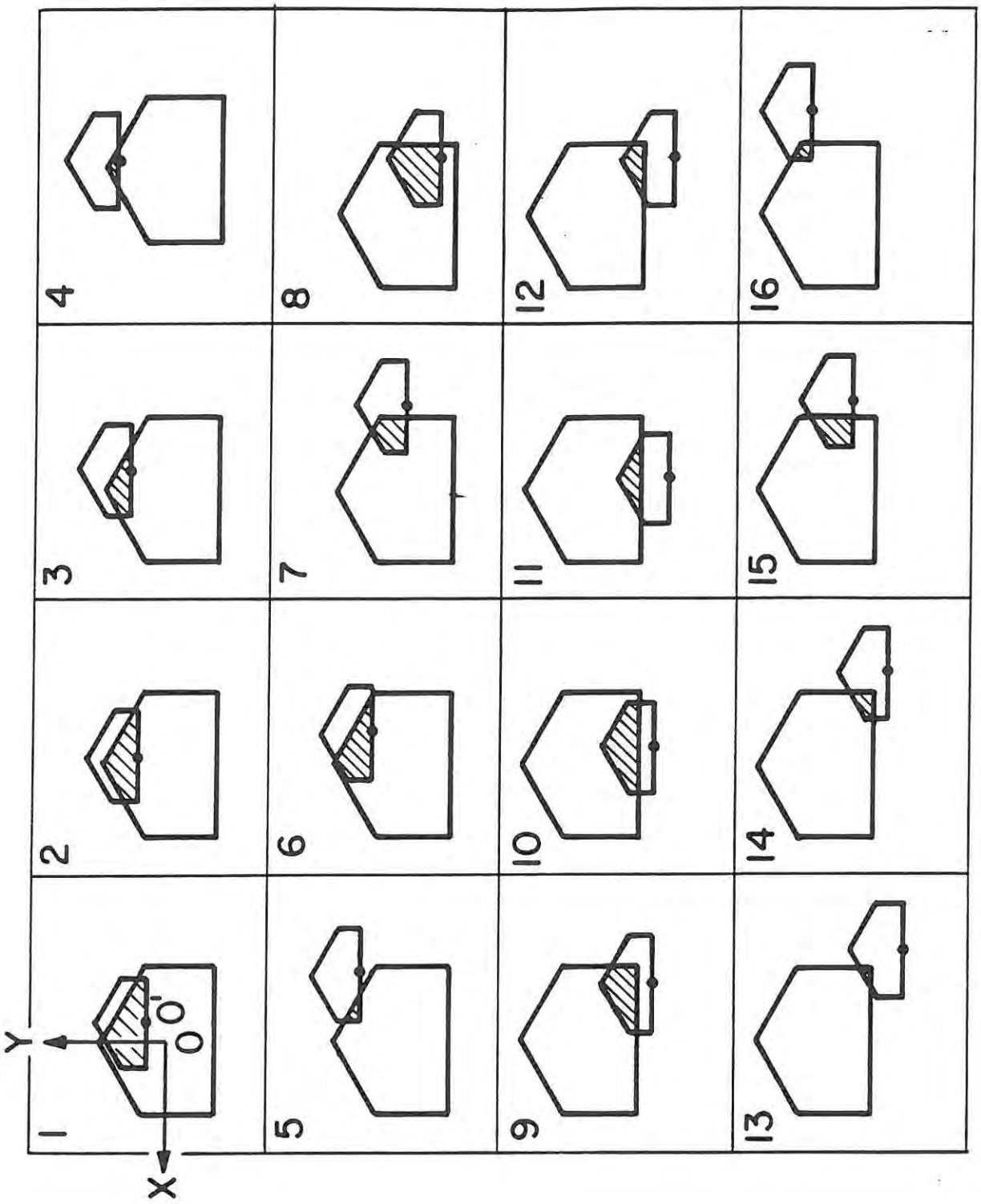

Figure 7

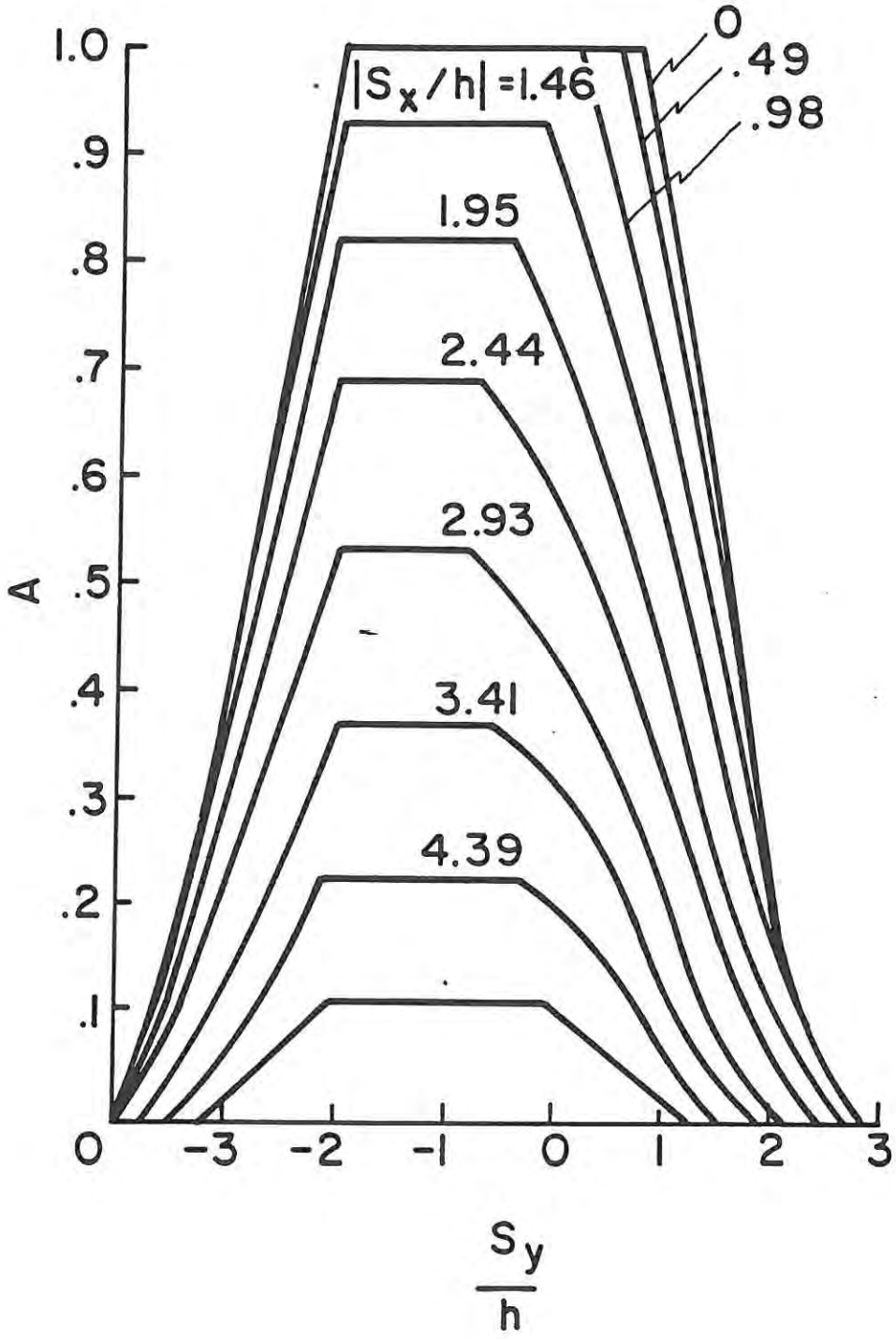

MAIN SENSOR SENSITIVE AREA vs S_y/h

Figure 8

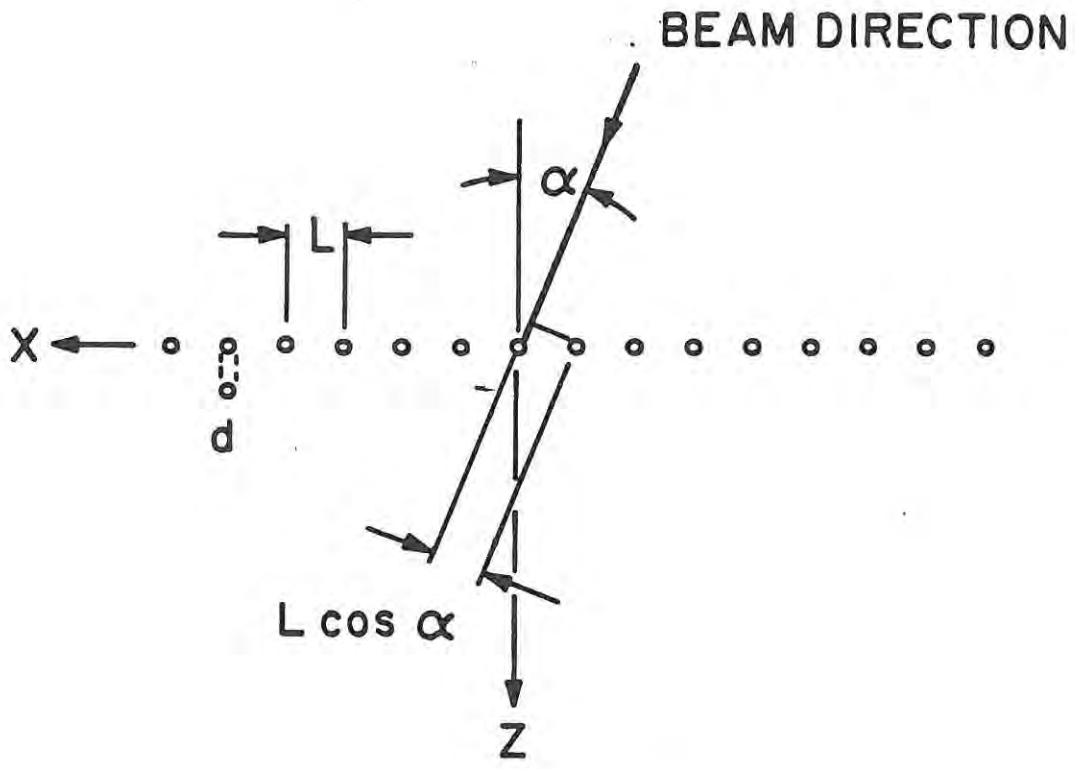

GEOMETRY FOR GRID TRANSPARENCY

Figure 9

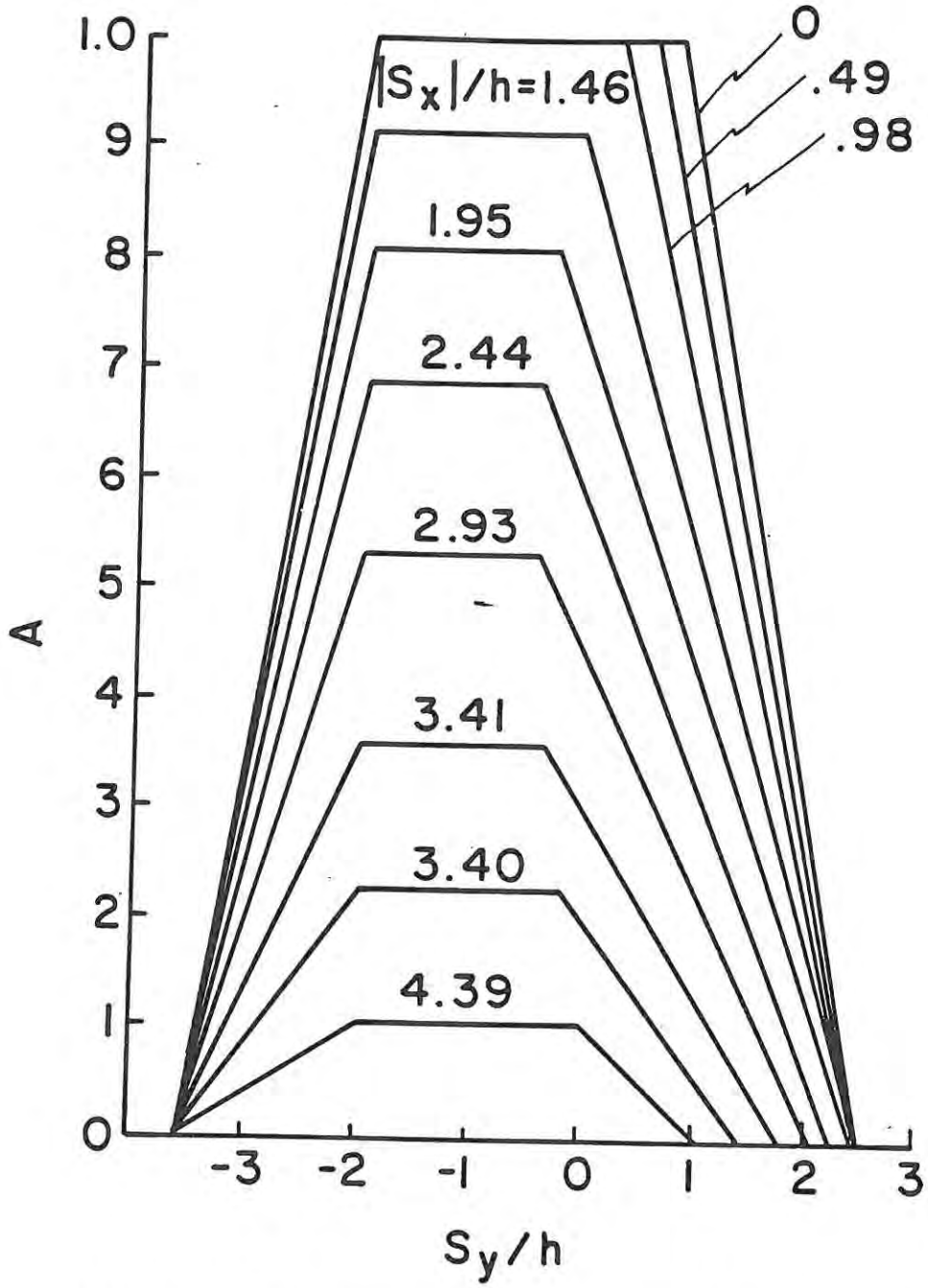

MAIN SENSOR SENSITIVE AREA vs S_y/h

(TRAPEZOIDAL APPROXIMATION)

Figure 10

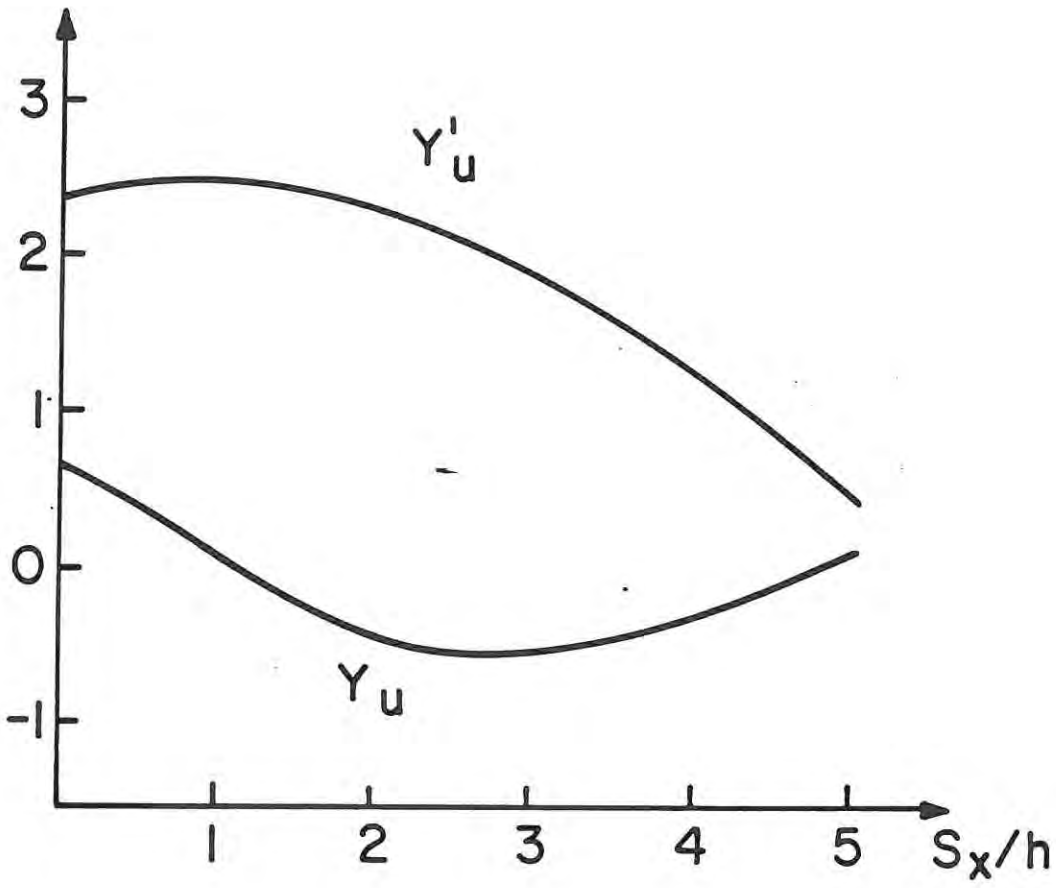

Figure 11

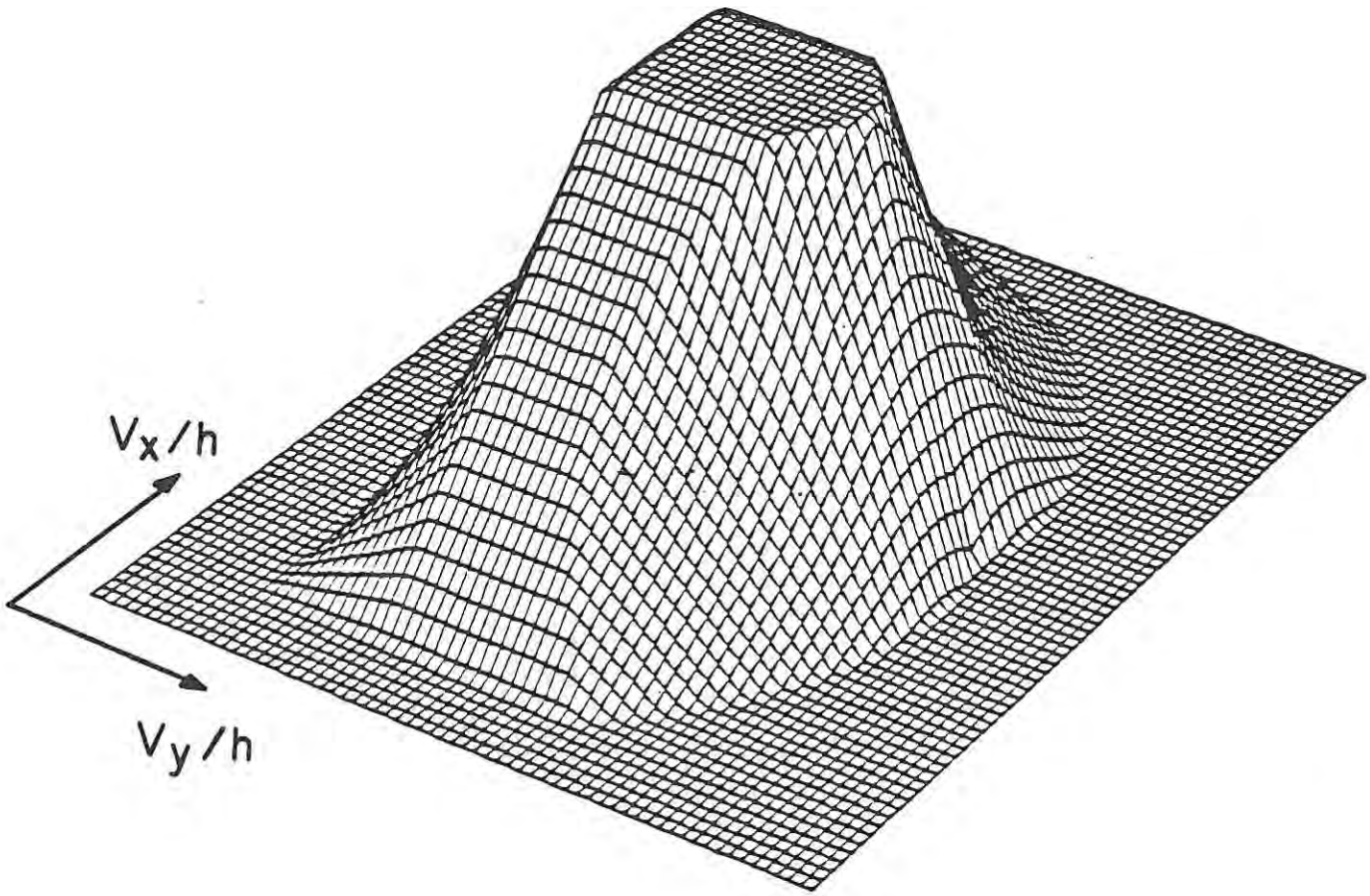

Figure 12

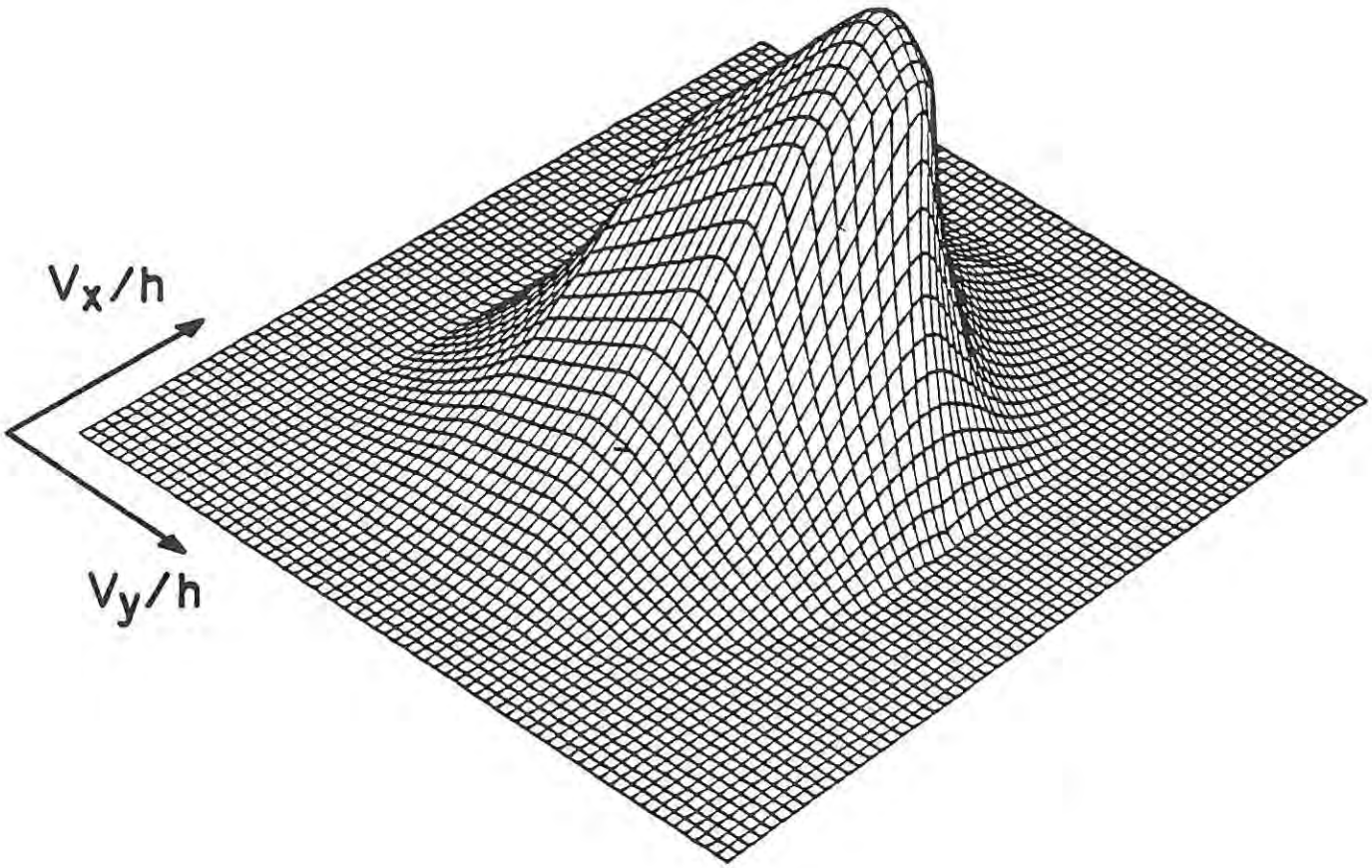

Figure 13

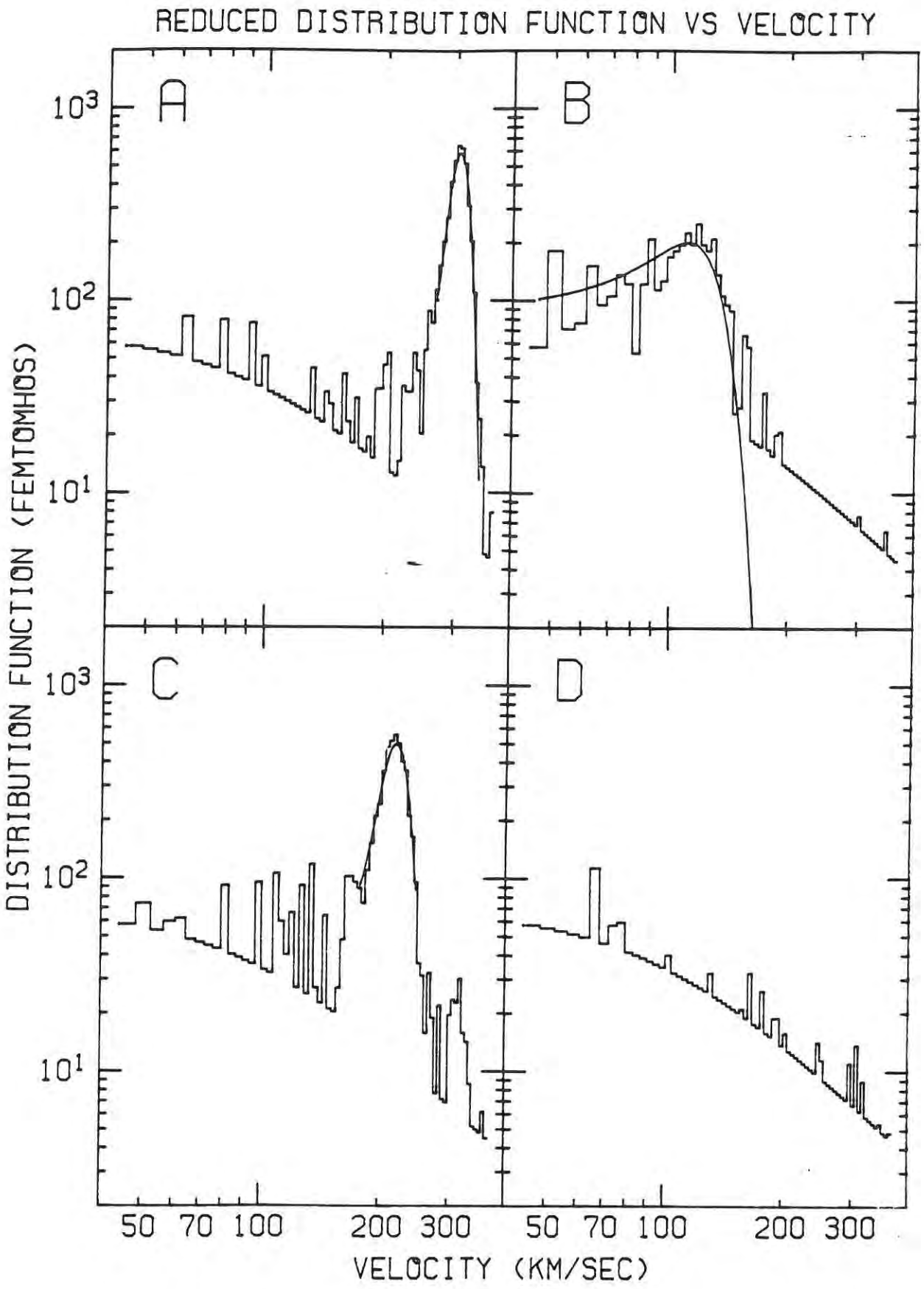
REDUCED DISTRIBUTION FUNCTION VS VELOCITY
A
B
C
D
10^3
10^2
10^1
DISTRIBUTION FUNCTION (FEMTOMHOS)
50 70 100 200 300
50 70 100 200 300
VELOCITY (KM/SEC)

Figure 14

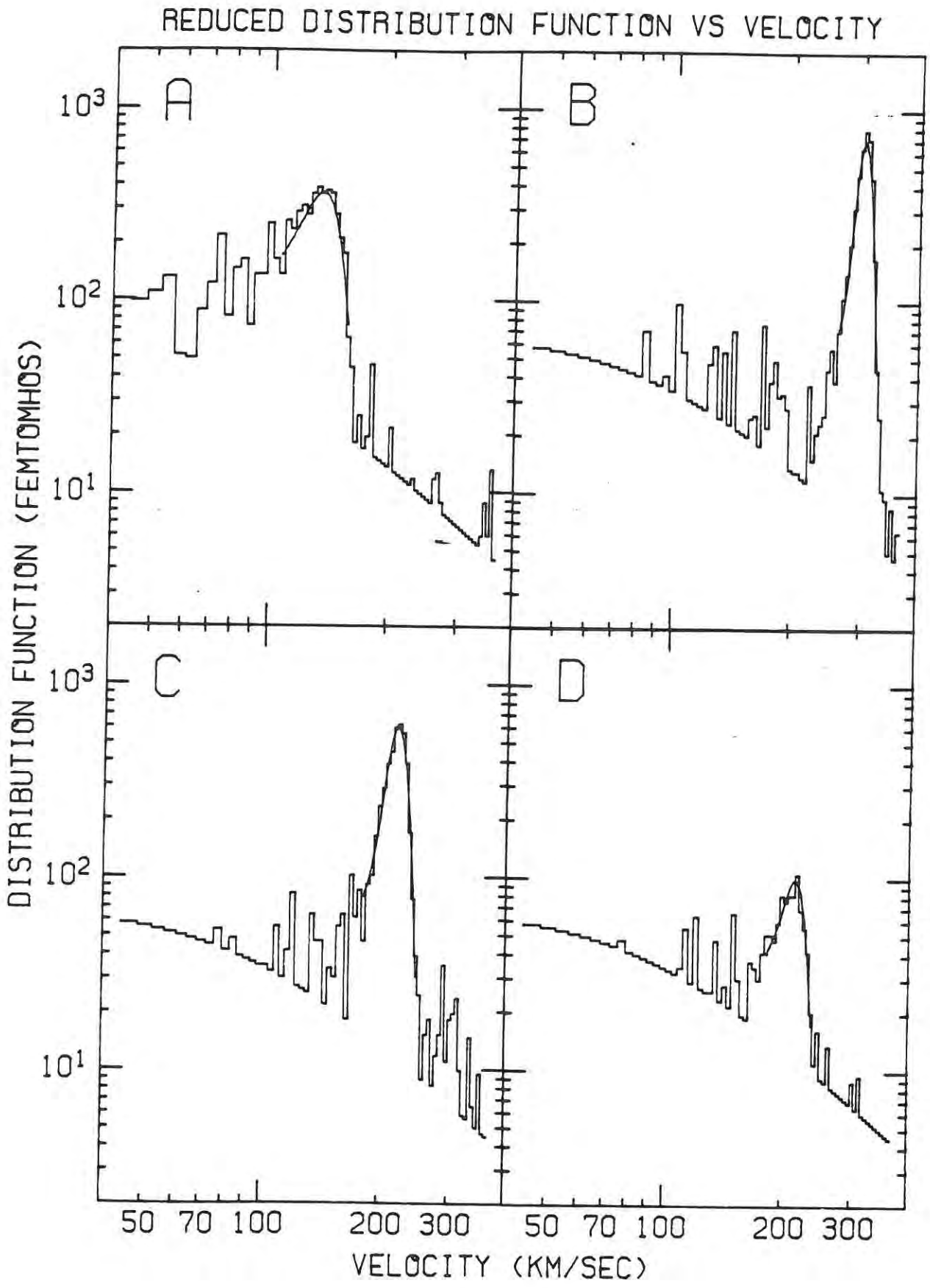
REDUCED DISTRIBUTION FUNCTION VS VELOCITY
A
B
C
D
10^3
10^2
10^1
DISTRIBUTION FUNCTION (FEMTOMHOS)
50 70 100 200 300
50 70 100 200 300
VELOCITY (KM/SEC)

Figure 15

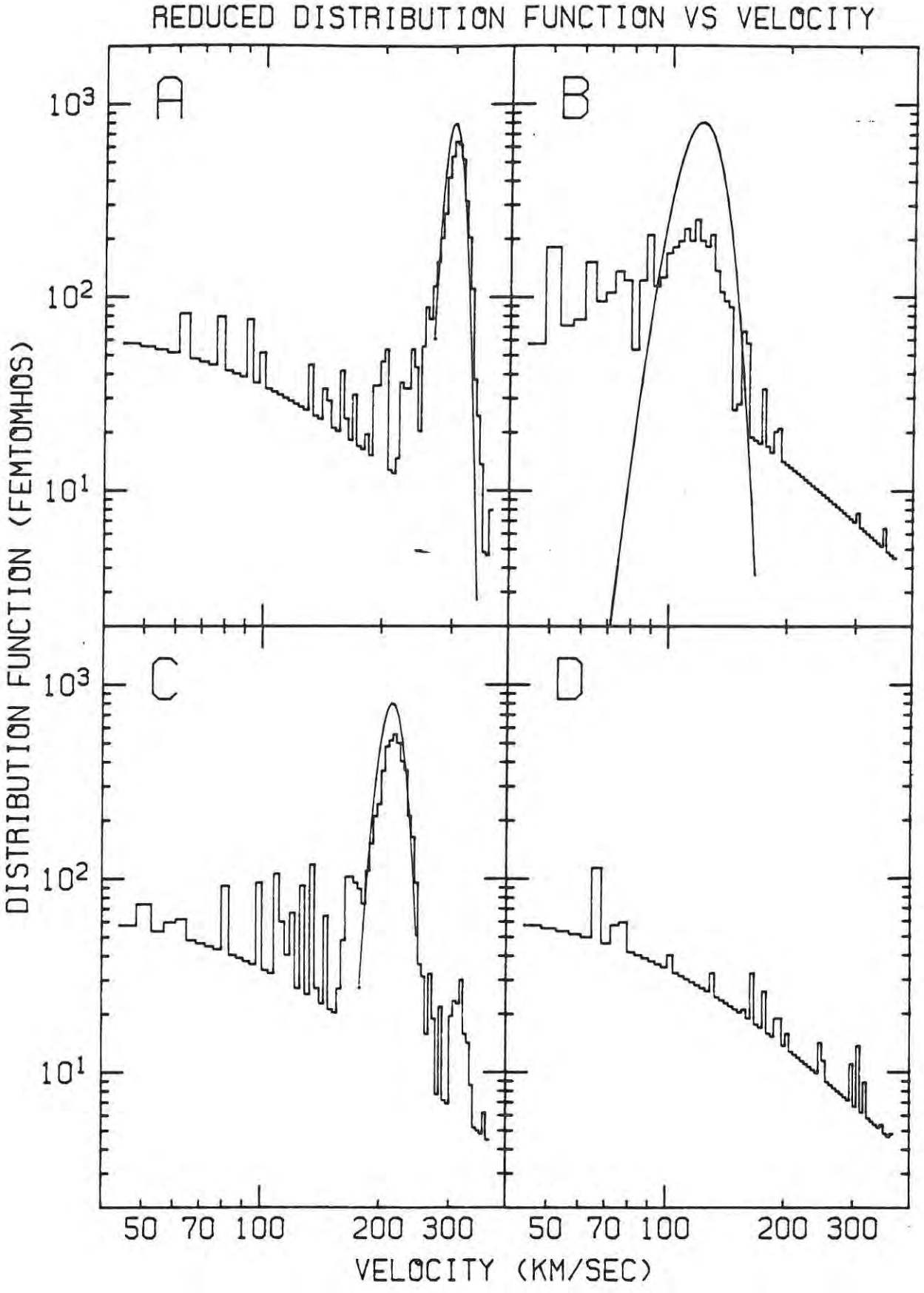
REDUCED DISTRIBUTION FUNCTION VS VELOCITY
A
B
C
D
10^3
10^2
10^1
DISTRIBUTION FUNCTION (FEMTOMHOS)
50 70 100 200 300
50 70 100 200 300
VELOCITY (KM/SEC)

Figure 16

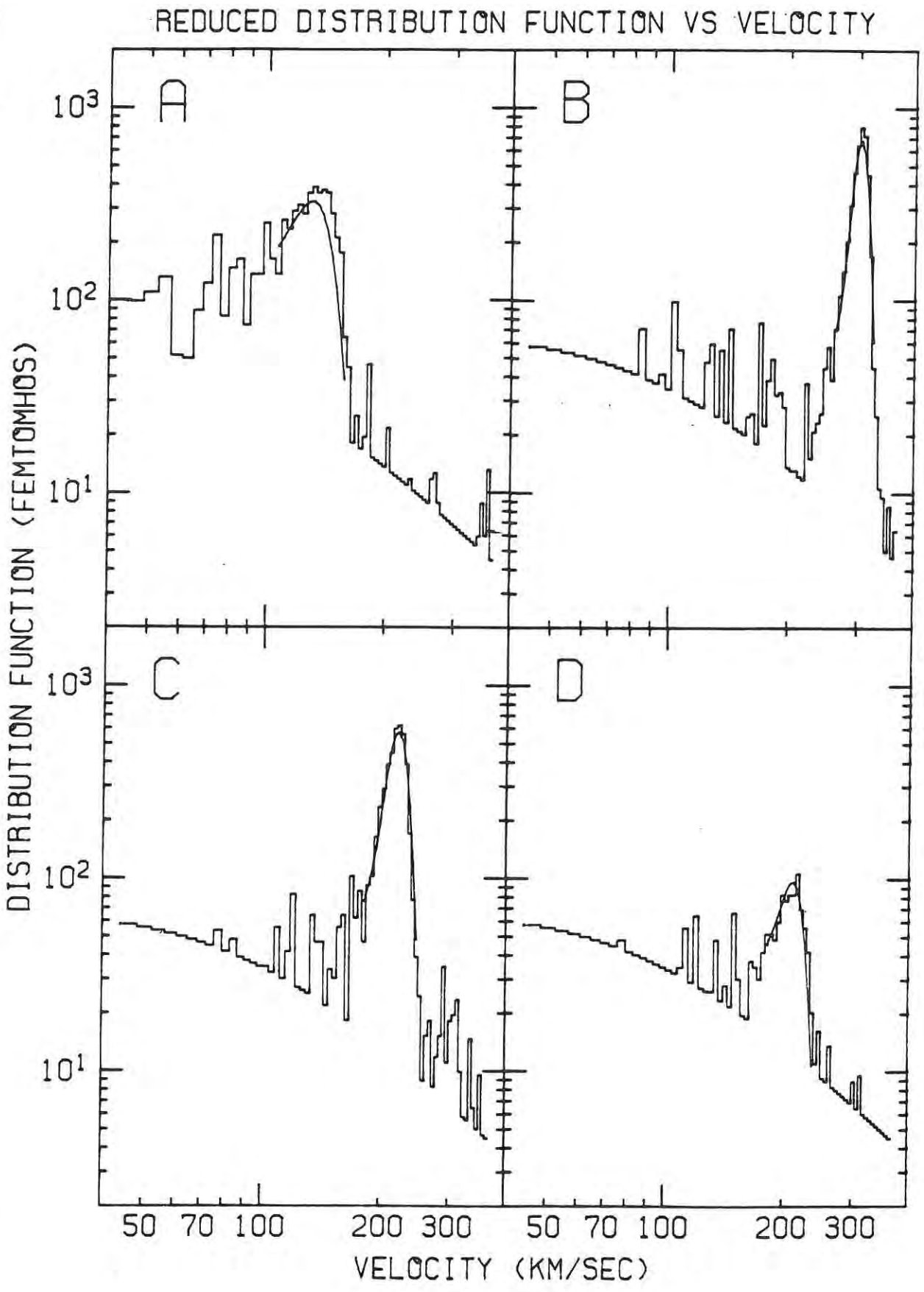
REDUCED DISTRIBUTION FUNCTION VS VELOCITY
A
B
C
D
10^3
10^2
10^1
DISTRIBUTION FUNCTION (FEMTOMHOS)
50 70 100 200 300
50 70 100 200 300
VELOCITY (KM/SEC)

Figure 17

Synopsis: PLS - Sensors Response

1. Intro: motivation and approach

2. Geometry - Modul. Voltages - Modes of Operation - Coord. Systems of PLS Sensors

3. Three basic functions describing the Response (path fct, transparency, sensitive area function)

4. Rigorous an Expressions of the overall Response Fct.s

5. Simplified Representation of Anal Approx. to the Resp. Fct.

6. Calc. currents - using Approx. Resp. Functions
   (a) Connected Maxw. (b) Conned. bi-maxw.

7. Feedthrough Problems
   (a) Electrons in (position) modes (b) pos. Ions in E_1, E_2 Mode

Response Functions of PLS-sensors of the Voyager Mission

(Brief Summary for Internal Use)

S. Olbert

1. Introduction

The design and operation of the four sensors of the Plasma Science Experiment onboard Voyager I and II spacecraft (referred to hereafter as "PLS-sensors") were reported in various papers (see, e.g., H.S. Bridge et al., Space Sci. Rev. 21, №3, pp. 259-287, (1977)). We assume that the reader is familiar with the basic concept of these detectors so that we may focus directly on the problem of their response. ~~confine ourselves to the discussion~~ Nevertheless, this report is intended to be self-contained, ~~alone the purpose of this report is a summary~~ and thus includes a brief summary of the data ~~of a tedious and lengthy effort that off and on~~ on the geometry and operation modes of the sensors. ~~occupied this author over a period of last three~~ (not) ~~summers.~~ It is offered as a "mini-manual" to anyone who is involved in the analysis of the plasma data from the magnetospheres

of Jupiter and Saturn. [9] As it will become clearer later on, the design of the sensors is such that, when the plasma flow in the spacecraft ~~coordinate system~~ frame of reference is highly supersonic (say, Mach number of the order of 10) and the direction of the convective plasma velocity lies within a narrow cone about the antinormal of any given sensor that measures substantial currents, the response function for positive ions ~~of the sen~~ is extremely simple: if properly normalized, it is a "unity function." This is the case during the entire cruise of both Voyagers in the interplanetary medium outside the interaction regions of the solar wind with the planets (i.e., magnetosheaths and magnetospheres). The unity response obtains also approximately during limited periods of time on Voyager I when the Jovian magnetospheric plasma is cold (say, Mach number larger than 4) and nearly corotating, provided the side-sensor's anti-normal or the symmetry axis of the main sensors is close to the corotation direction (i.e., along the Jovian azimuth). In these cases the data reduction is straightforward and one is spared all the cumbersome details collected below.

In all other cases (flow directions intermediate and/or the Mach number less than 4) one has to face the folding procedures of complicated expressions of the response function with the ~~sought~~ ion distribution functions in order to obtain the correct relation between the measured current and the ~~sought~~ desired plasma parameters. One is interested ~~at least~~ routinely in five scalar parameters for each ion species: three components of the mean streaming velocity, $\hat{\vec{V}}_a$, the number density, $\hat{n}_a$, and the temperature, $\hat{T}_a$ (or thermal speed). The data analysis may reveal that characterizing the ion distribution by one scalar temperature ~~is not adequate~~ (convected isotropic distribution) is not adequate and ought to be replaced by a tensor temperature $\hat{\mathbf{T}}_a$ diagonalizable along the magnetic field with two distinct elements $T_{\parallel a}$ and $T_{\perp a}$ (convected gyrotropic distribution). The task then is to find six macroscopic parameters that adequately reproduce the observed currents in the four detectors.

To cast the above remarks into a quantitative language, let us define the following quantities:

$\Delta I^{(a)}_{j,KN}$ – the electric current due to the ions of kind "a", measured in the j^{th} modulation step of the K^{th} sensor in the

N^{th} mode of operation;

$Z_a e$, — the electric charge of the "a" ion;

A_K, T_K — the free-access area and transparency of the K^{th} sensor, respectively, at normal ion incidence;

v_x, v_y, v_z, — the "a" ion velocity components with v_z pointing into the sensor's collector plate ("antinormal" direction)

$f_a(\vec{v}; p_a^{(a)})$ — the distribution function of the "a" ion; $p_a^{(a)}$ symbolizes the dependence of f_a on the macroscopic parameters, viz.: $p_a^{(a)} \to n_a, \vec{V}_a, T_{\parallel a}, T_{\perp a}$;

$R^{(a)}_{j,KN}(\vec{v})$ — the response function of K^{th} sensor at j^{th} modulation step in N^{th} mode; $R^{(a)}_{j,KN} = 1$ for $v_x = v_y = 0$;

$v^{(a)}_{j,N} \equiv \sqrt{\frac{2 Z_a e \phi_{j,N}}{m_a}}$ — the threshold value of v_z of "a" ion in j^{th} modulation step in N^{th} mode

$\phi_{j,N}$ — the threshold value of the modulation grid voltage (relative to the collector voltage) at j^{th} step operating in N^{th} mode.

As explained in the past accounts, one has then the following basic relation between $\Delta I^{(a)}_{j,KN}$ and f_a:

$$\Delta I^{(a)}_{j,KN} = Z_a e A_K T_K \left[\int_{v^{(a)}_{j,N}}^{\infty} dv_z\, v_z \iint_{-\infty}^{+\infty} R^{(a)}_{j,KN}(v_x, v_y, v_z) f_a(\bar{v}; p^{(a)}_a)\, dv_x\, dv_y \right.$$
$$\left. - \int_{v_{j+1,N}}^{\infty} dv_z\, v_z \iint_{-\infty}^{+\infty} R^{(a)}_{j+1,KN}(v_x, v_y, v_z) f_a(\bar{v}; p^{(a)}_a)\, dv_x\, dv_y \right] \quad (1)$$

The above equation shows clearly the physical meaning of $R^{(a)}_{j,KN}$: $R^{(a)}_{j,KN}$ represents the fraction of ions of kind "a", contained in an extended, uniform (monoenergetic and unidirectional) beam traveling with $\bar{v}$, intercepted by the collector plate of the k^{th} sensor when the threshold voltage is $\Phi_{j,N}$. At normal incidence ($v_x = v_y = 0$), $R^{(a)}_{j,KN}(0,0,v_z) = 1$.

Since $R^{(a)}_{j,KN}$ implies evaluation of the sensitized portion of the collecting area, Eq. (1) actually involves a five-dimensional integral. Thus a computer program for calculating directly a simulated $\Delta I^{(a)}_{j,KN}$, using some assumed f_a, is unduly time-consuming. Such direct simulation program has been in fact compulated (Vasyliunas et al) and used sporadically on a limited number of data samples of parti-

cular importance. However, the routine use of this program for extended data analysis - in particular, when best-fitting procedures are called for, — is not practicable; the duration of computer runs and the financial costs are simply too excessive. This circumstance motivated us to develop a new approach, namely, a construction of accurate but mathematically simple, empirical expressions for the response functions, R_j. The desired "simplicity" of R_j's is dictated by the requirement that the integrations in Eq. (1) be carried out explicitly for some reasonable forms of f_a, e.g., convected Maxwellian or Bi-maxwellian distributions. In what follows, the reader will find the summary of this effort. The effort, by the very nature of the problem, was tedious and often tested the endurance limits of the author. Nonetheless, we believe that it was worthwhile because the availability of tractable response functions may make the difference between a new knowledge about the dynamics of the magnetospheres of major planets and the pathos of un-interpreted data, buried somewhere in the dark recesses of the magnetic-tape racks.

2. Geometry and Operational Modes of PLS-Sensors.

(a) Location of PLS-sensors in the space-craft coordinate system.

Figure 1 shows the sketch of the cluster of ~~the~~ four PLS-sensors. The drawing is a simplified version of a photograph; the scale is 1:5 of the real size. Note the agreed-upon labeling A, B, C, D for identifying each sensor. The D sensor is cylindrical in shape and is often referred to as the "D-cup"; the term "the side sensor" is also used frequently. The A, B, C sensors are identical in shape (pentagonal) and operation and ~~these~~ are called "the main sensors"; they form "the main cluster" which has one common axis of symmetry, S. The entire system is rigidly mounted on the "science boom" of the Voyager. ~~[illegible]~~. (There are, of course, two sets, one for each Voyager; there are no physical differences between the two sets with one minor exception referring to the alignments of the grid meshes in the D-cup. For our purposes the two sets may be treated as identical.)

In discussing the response of each sensor

it is convenient to make use of four distinct cartesian coordinate systems, (x_K, y_K, z_K), where $K=(A,B,C,D)$, one for each ~~for the~~ sensor. ~~Under Consideration~~. In addition one needs a common reference frame whose coordinates do not change in time ~~relative~~ with respect to the sensor coordinate systems. This common frame is called "the space-craft (s/c) coordinate system," $(x_{s/c}, y_{s/c}, z_{s/c})$, and is defined as follows:

$\hat{z}_{s/c}$ is parallel to the Earth-Voyager line and points away from the Earth, i.e., lies along the axis of the main antenna dish.

The PLS-sensors are mounted in such a way that the symmetry axis, S, of the main cluster is parallel to $\hat{z}_{s/c}$ and the x-axis of the C-sensor, $\hat{x}_C$, is antiparallel to $\hat{x}_{s/c}$. Figure 2 shows the relative configurations of the five coordinate systems. It is important to keep in mind the following facts:

1) each of $\hat{y}_A, \hat{y}_B, \hat{y}_C$ points toward S and each $\hat{y}_K$ lies in the plane of the collector of the K^{th} sensor, respectively.

2) each of $\hat{z}_A, \hat{z}_B, \hat{z}_C$ forms an angle of 20° with $\hat{z}_{s/c}$. each $\hat{z}_K$ points into the K^{th} sensor at right angles to the collector plate re-

3) $\hat{X}_K$'s are defined by

$$\hat{X}_K = \frac{\hat{Z}_K \times \hat{Z}_{s/c}}{\sin\theta_K} \qquad K=(A,B,C,D)$$

where $\sin\theta_K = |\hat{Z}_K \times \hat{Z}_{s/c}|$

4) $\hat{Z}_D$ is "anti-normal" to the collector plate of the D-cup, ~~and~~ forms an angle of 88° with $\hat{Z}_{s/c}$, and points toward S.

If we introduce the polar and azimuth angles, $(\theta_{(K)}^{s/c}, \varphi_{(K)}^{s/c})$, in the s/c coordinate system for each $\hat{Z}_K$, then we have the following representation:

$\hat{Z}_K$	$\theta_{(K)}^{s/c}$	$\varphi_{(K)}^{s/c}$
$\hat{Z}_A$	20°	30°
$\hat{Z}_B$	20°	150°
$\hat{Z}_C$	20°	270°
$\hat{Z}_D$	88°	223°

To obtain the cartesian components of $\hat{Z}_K$ in s/c system one simply recalls that

$$\hat{Z}_{K,i} = \begin{cases} \cos\varphi_{(K)}^{s/c} \sin\theta_{(K)}^{s/c} \\ \sin\varphi_{(K)}^{s/c} \sin\theta_{(K)}^{s/c} \\ \cos\theta_{(K)}^{s/c} \end{cases} \qquad \left(i=(x_{s/c}, y_{s/c}, z_{s/c})\right)$$

The above information allows us to compute the polar and azimuth angles, (θ_K, φ_K), in the frame of the K^{th} sensor of any given unit vector if the polar and azimuth angles, $(\theta_{s/c}, \varphi_{s/c})$, of this vector are known in the s/c frame. Figures 3, 4, 5 and 6 give the graphical answer to this type of transformation. One often needs also to transform the cartesian components of a unit vector $\hat{u}$ in the s/c frame into cartesian components of $\hat{u}$ in the frame of the k^{th} sensor; viz.:

$$u_i^K = T_{ij}^K u_j^{s/c} \qquad \begin{cases} i = 1,2,3 \\ j = 1,2,3 \\ K = A,B,C,D \end{cases} \qquad (2)$$

The four matrices T_{ij}^K are given by:

$$T_{ij}^K = \hat{x}_{iK} \cdot \hat{x}_{js/c} \qquad (3)$$

where $\hat{x}_{1K} \equiv \hat{x}_K$, $\hat{x}_{2K} \equiv \hat{y}_K$, $\hat{x}_{3K} \equiv \hat{z}_K$

and $\hat{x}_{1s/c} \equiv \hat{x}_{s/c}$, $\hat{x}_{2s/c} \equiv \hat{y}_{s/c}$, $\hat{x}_{3s/c} \equiv \hat{z}_{s/c}$.

The inverse transformation is obtainable from

$$u_i^{s/c} = \tilde{T}_{ij}^K u_j^K = u_j^K T_{ji}^K$$

Table 1 below gives the numerical values of all T_{ij}^K.

TABLE 1

Transformation Matrix $T_{ij}^{K} = \hat{x}_{iK} \cdot \hat{x}_{js/c}$ for u_i^K

$u_i^K = T_{ij}^K u_j^{s/c}$

$(u_i^z = 1)$

Sensor:	u_i^K \ $u_j^{s/c}$	$u_x^{s/c}$	$u_y^{s/c}$	$u_z^{s/c}$
A	u_x^A	.500	-.865	0
	u_y^A	.813	.470	-.342
	u_z^A	.296	.171	.940
B	u_x^B	.500	.865	0
	u_y^B	-.813	.470	-.342
	u_z^B	-.296	.171	.940
C	u_x^C	1.000	0	0
	u_y^C	0	-.940	.342
	u_z^C	0	-.342	.940
D	u_x^D	-.682	.731	0
	u_y^D	-.026	-.024	-.999
	u_z^D	-.731	-.682	.035

(b) Dimensions of PLS-Sensors

Figures 7 and 8 refer to a main sensor and show, respectively, the pertinent dimensions in the (x_K, y_K)-plane and (y_K, z_K)-plane, $(K = A, B, C)$. All distances are given in cm. The sketches are self-explanatory but they deserve a few special comments. All grids and the collector are mutually parallel; the collector has a rim 0.584 cm high, which reduces the effective depth of the sensor from 4.684 cm to 4.10 cm as far as the response of the sensor to a uniform ion beam is concerned. Notice also the asymmetric positioning of the aperture relative to the collector; there is only one symmetry in the (x_K, y_K)-plane, namely, that about the y_K-axis.

4. Simplified Representation of Response Functions

The "rigorous" expressions constructed in the preceding sections are clearly too cumbersome to be of practical use in analytical evaluations of $\Delta I_j^{(a)}$. Therefore, we went through a series of trials using a variety of simple, empirical expressions containg a number of "adjustable" parameters to find analytically tractable formulas of R_j. Since the geometry of the main sensors and the D-cup are different, we have two distinct representations of R_j. Here we summarize the results of our final choice.

(a) Main Sensors

We found that we can approximate the response function R_j of a main sensor by the following expression:

$$R_{j,KN}^{(a)} = G_{j,K}^{N} P_{j,K}^{N} \qquad (K = A, B, C)$$

where N symbolizes the mode (N = L-mode; M-mode etc) and "a" identifies the ion species, and

$$G^N_{j,k} = \left[\sum_{i=1}^{2} C^N_{ik}(j)\, e^{-A^N_{ik}(i) v_x^2/v_z^2}\right]\left[\sum_{i=1}^{2} C^N_{ik}(j)\, e^{-A^N_{ik}(i) v_y^2/v_z^2}\right]$$

$$C^N_{1k}(j) + C^N_{2k}(j) = 1 \quad \text{(for all } j\text{'s and } N\text{'s)}$$

$$P^N_{j,k} = U(x) \begin{cases} \dfrac{y - y_D'}{y_D - y_D'} & \text{for } y_D' < y < y_D \\ 1 & \text{for } y_D < y < y_U \\ \dfrac{y_U' - y}{y_U' - y_U} & \text{for } y_U < y < y_U' \end{cases}$$

$$U(x) = \begin{cases} 1 & \text{for } 0 < |x| < x_c \\ \dfrac{x_c' - |x|}{x_c' - x_c}\,\xi(x) & \text{for } x_c < |x| < x_c' \end{cases}$$

$$\xi(x) = 1.257 - 0.063|x| - 0.126\sqrt{x^2 - 5.10|x| + 6.612}$$

[$U(x)$ and $P^N_{j,k}$ are zero for $|x| > x_c'$ and $y < y_D'$ or $y > y_U'$]

x_c, x_c', y_D, y_D' are dimensionless numbers:

$$x_c = 1.10 \;;\; x_c' = 4.94$$

$$y_D = -2.02 \qquad y_D' = -3.62$$

y_U and y_U' are empirical functions of $|x|$:

$$y_U = \frac{0.762 \cos(1.018|x| + 0.247)}{1 + 0.25|x|}$$

$$y_U' = 2.50 - 0.125(|x| - 1)^2$$

Finally, the variables x and y are related to v_x and v_y by the formulas:

$$x = S^N_{j,K} \frac{v_x}{v_z} \quad ; \quad y = S^N_{j,K} \frac{v_y}{v_z}$$

$S^N_{j,K}$ are the "shift functions" and are given by:

$$S^N_{j,K} = 0.338 + 0.744\left(1 - \sqrt{1-\xi_j^N}\right) + 0.394\left(\sqrt{1-\xi_s^N} - 1\right) + \frac{0.093}{\sqrt{1-\xi_j^N}}$$

where

$$\xi_j^N = \frac{2Z_a e \phi_j^N}{m_a v_z^2} \leq 1$$

$$\xi_s^N = \frac{2Z_a e \phi_s^N}{m_a v_z^2} \leq 1 \qquad (\phi_s^N \text{ is negative})$$

and $K = (A, B, C)$.

The coefficients $C^N_{iK}(j)$ and $A^N_{iK}(j)$ are tabulated for all values of j in M and L-modes in Table 3. Note that ~~the~~ each voltage interval $\phi^M_{j+1} - \phi^M_j$ in the M-mode has been divided into three sub-intervals, labeled by $s = 1, 2, 3$; thus, e.g.,

$A^M_{iK}(j,1)$ is evaluated at $\phi^N_j(1+\frac{1}{6})$

$A^M_{iK}(j,2)$ —"— at $\phi^M_j(1+\frac{3}{6})$

(b) Side Sensor

The fitted form of the response function for the side sensor is considerably simpler. We found:

$$R_{j,DN}^{(a)} = \sum_{i=1}^{3} C_{iD}\left(1 - \frac{v_x^2 + v_y^2}{v_z^2 \psi_m^N(j)}\right) e^{-A_{iD}^N(j)(v_x^2+v_y^2)/v_z^2}$$

where C_{iD} are constant numbers:

$$C_{1D} = 1.5$$
$$C_{2D} = -1.1$$
$$C_{3D} = 0.62$$

and the coefficients $\psi_m^N(j)$ and $A_{iD}^N(j)$ are tabulated in Table 3.

[redacted] SENSOR RESPONSE FUNCTION "CONSTANTS" – K = A, B, C (Main Sensors)

MODE → L-Mode

j ↓

0.055	0.038	0.032	$A^L_{1K}(j,s)$
0.077	0.044	0.039	
0.086	0.049	0.042	
0.095	0.050	0.045	
0.096	0.054	0.045	
0.106	0.055	0.040	
0.106	0.057	0.049	
0.105	0.060	0.050	
0.115	0.057	0.047	
0.115	0.056	0.047	
0.115	0.059	0.049	
0.116	0.059	0.049	
0.116	0.060	0.050	
0.116	0.060	0.050	
0.117	0.060	0.050	
0.117	0.060	0.050	
0.770	0.500	0.350	$A^L_{2K}(j,s)$
1.030	0.570	0.520	
1.120	0.620	0.550	
1.200	0.630	0.600	
1.200	0.680	0.600	
1.280	0.680	0.610	
1.290	0.700	0.640	
1.180	0.730	0.640	
1.230	0.650	0.560	
1.230	0.640	0.560	
1.230	0.670	0.580	
1.230	0.670	0.580	
1.230	0.670	0.580	
1.230	0.670	0.580	
1.230	0.670	0.580	
1.230	0.670	0.580	
0.180	0.180	0.180	$C^L_{1K}(j,s)$
0.220	0.210	0.190	
0.230	0.220	0.200	
0.260	0.240	0.200	
0.260	0.240	0.220	
0.270	0.250	0.220	
0.270	0.250	0.220	
0.280	0.250	0.220	
0.300	0.280	0.250	
0.300	0.280	0.250	
0.300	0.280	0.250	
0.300	0.280	0.250	
0.300	0.280	0.250	
0.300	0.280	0.250	
0.300	0.280	0.250	
0.300	0.280	0.250	

10-11-74 per Ster
after this – clean disconnect – feedthrough effect

MODE: M-Mode $A^M_{1K}(j)$

j	1	2	3	4	5	6	7	8
1	0.079	0.087	0.095	0.100	0.104	0.111	0.115	0.120
9	0.125	0.128	0.132	0.135	0.141	0.143	0.149	0.152
17	0.155	0.158	0.162	0.166	0.166	0.170	0.175	0.175
25	0.180	0.180	0.184	0.183	0.183	0.190	0.190	0.196
33	0.196	0.196	0.196	0.202	0.202	0.202	0.202	0.210

$A^M_{IK}(j)$ [K=ABC] [M-Mode] (cont.)

j	v1	v2 etc						
41	0.210	0.210	0.210	0.210	0.218	0.218	0.218	0.218
49	0.218	0.218	0.218	0.218	0.226	0.226	0.226	0.226
57	0.226	0.226	0.226	0.226	0.226	0.226	0.226	0.226
65	0.226	0.236	0.236	0.236	0.236	0.236	0.236	0.236
73	0.236	0.236	0.236	0.236	0.236	0.236	0.236	0.236
81	0.236	0.236	0.236	0.236	0.236	0.236	0.236	0.236
89	0.236	0.236	0.247	0.247	0.247	0.247	0.247	0.247
97	0.247	0.247	0.247	0.247	0.247	0.247	0.247	0.247
105	0.247	0.247	0.247	0.247	0.247	0.247	0.247	0.247
113	0.247	0.247	0.247	0.247	0.247	0.247	0.247	0.247
121	0.247	0.247	0.247	0.247	0.247	0.247	0.247	0.247

$A^M_{2K}(j)$

1.020	1.110	1.220	1.260	1.300	1.380	1.420	1.470
1.500	1.540	1.560	1.590	1.650	1.670	1.720	1.740
1.760	1.790	1.820	1.850	1.850	1.880	1.920	1.920
1.960	1.960	1.990	1.970	1.970	2.030	2.030	2.070
2.070	2.070	2.070	2.120	2.120	2.120	2.120	2.170
2.170	2.170	2.170	2.170	2.210	2.210	2.210	2.210
2.210	2.210	2.210	2.210	2.260	2.260	2.260	2.260
2.260	2.260	2.260	2.260	2.260	2.260	2.260	2.260
2.260	2.320	2.320	2.320	2.320	2.320	2.320	2.320
2.320	2.320	2.320	2.320	2.320	2.320	2.320	2.320
2.320	2.320	2.320	2.320	2.320	2.320	2.320	2.320
2.320	2.320	2.390	2.390	2.390	2.390	2.390	2.390
2.390	2.390	2.390	2.390	2.390	2.390	2.390	2.390
2.390	2.390	2.390	2.390	2.390	2.390	2.390	2.390
2.390	2.390	2.390	2.390	2.390	2.390	2.390	2.390
2.390	2.390	2.390	2.390	2.390	2.390	2.390	2.390

$C^M_{IK}(j)$

0.240	0.240	0.240	0.250	0.260	0.260	0.269	0.270
0.277	0.280	0.285	0.290	0.290	0.292	0.295	0.297
0.300	0.302	0.304	0.305	0.305	0.307	0.309	0.309
0.311	0.311	0.314	0.314	0.314	0.316	0.316	0.319
0.318	0.319	0.318	0.320	0.320	0.320	0.320	0.322
0.322	0.322	0.322	0.322	0.326	0.326	0.326	0.326
0.326	0.326	0.326	0.326	0.330	0.330	0.330	0.330
0.330	0.330	0.330	0.330	0.330	0.330	0.330	0.330
0.330	0.333	0.333	0.333	0.333	0.333	0.333	0.333
0.333	0.333	0.333	0.333	0.333	0.333	0.333	0.333
0.333	0.333	0.333	0.333	0.333	0.333	0.333	0.333
0.333	0.333	0.335	0.335	0.335	0.335	0.335	0.335
0.335	0.335	0.335	0.335	0.335	0.335	0.335	0.335
0.335	0.335	0.335	0.335	0.335	0.335	0.335	0.335
0.335	0.335	0.335	0.335	0.335	0.335	0.335	0.335
0.335	0.335	0.335	0.335	0.335	0.335	0.335	0.335

SENSOR RESPONSE FUNCTION CONSTANTS

K=D (side sensor)

L-mode

$A^L_{ID}(j,s)$

j \ s →	1	2	3
1	0.830	0.740	0.710
2	0.980	0.840	0.800
3	1.040	0.900	0.840
4	1.100	0.930	0.870
5	1.110	0.970	0.890
6	1.150	0.980	0.920
7	1.150	0.990	0.930
8	1.160	1.010	0.930
9	1.190	1.000	0.940
10	1.190	1.000	0.940
11	1.190	1.020	0.950
12	1.190	1.020	0.950
13	1.190	1.020	0.950

for both L & M-mode:

$C_{1D} = 1.5$

$C_{2D} = -1.1$

$C_{3D} = 0.62$

L-mode [D-cup] (cont.)

j \ s →	1	2	3
14	1.190	1.020	0.950
15	1.190	1.020	0.950
16	1.190	1.020	0.950

$A^{L}_{2D}(j,s)$

	.250	2.100	2.050
2	.550	2.350	2.300
	.700	2.500	2.400
	2.850	2.550	2.450
	2.900	2.700	2.450
3	.000	2.700	2.600
	3.000	2.700	2.650
	3.000	2.800	2.600
3	.050	2.700	2.600
	3.050	2.700	2.600
	3.050	2.750	2.700
3	.050	2.750	2.700
	3.050	2.750	2.700
	3.050	2.750	2.700
3	.050	2.750	2.700
	3.050	2.750	2.700

$A^{L}_{3D}(j,s)$

	4.800	4.500	4.300
5	.500	5.000	4.900
	5.800	5.300	5.100
	6.150	5.400	5.200
6	.300	5.600	5.100
	6.500	5.750	5.500
	6.500	5.700	5.600
6	.400	6.000	5.500
	.500	5.700	5.400
	.500	5.700	5.400
	6.500	5.700	5.700
	6.500	5.700	5.700
	6.600	5.700	5.700
	6.600	5.800	5.700
	6.600	5.800	5.700
	6.600	5.800	5.700

$\psi^{L}_{m}(j,s)$

	4.523	4.936	5.068
	4.116	4.509	4.689
	3.947	4.311	4.496
	3.851	4.196	4.379
	3.790	4.122	4.304
	3.749	4.072	4.252
	3.720	4.036	4.215
	3.700	4.011	4.189
	3.685	3.993	4.170
	3.674	3.980	4.156
	3.666	3.970	4.145
	3.660	3.963	4.138
	3.656	3.957	4.132
	3.652	3.953	4.128
	3.650	3.950	4.124
	3.648	3.949	4.122

M-mode

$A^{M}_{1D}(j)$

j \	1	2 etc						
1	0.950	0.980	1.010	1.030	1.050	1.080	1.090	1.100
9	1.120	1.140	1.150	1.160	1.170	1.180	1.190	1.200
17	1.210	1.220	1.230	1.240	1.240	1.250	1.260	1.260
etc	1.270	1.270	1.280	1.280	1.290	1.290	1.300	1.300
	1.310	1.310	1.310	1.320	1.320	1.320	1.320	1.330

[D-cup] M-mode (cont.) $A^M_{1D}(j)$

$j \rightarrow$

41	1.330	1.330	1.340	1.340	1.350	1.350	1.350	1.350
49	1.350	1.350	1.350	1.350	1.360	1.360	1.360	1.360
	1.360	1.360	1.360	1.360	1.360	1.360	1.360	1.360
etc	1.360	1.375	1.375	1.375	1.375	1.375	1.375	1.375
↓	.375	1.375	1.375	1.375	1.375	1.375	1.375	1.375
	1.375	1.375	1.375	1.375	1.375	1.375	1.375	1.375
	1.375	1.375	1.390	1.390	1.390	1.390	1.390	1.390
	1.390	1.390	1.390	1.390	1.390	1.390	1.390	1.390
	1.390	1.390	1.390	1.390	1.390	1.390	1.390	1.390
	1.390	1.390	1.390	1.390	1.390	1.390	1.390	1.390
	1.390	1.390	1.390	1.390	1.390	1.390	1.390	1.390

$A^M_{2D}(j)$

2.400	2.500	2.500	2.600	2.600	2.720	2.740	2.750
2.760	2.860	2.880	2.890	2.900	2.920	2.930	2.940
2.970	2.990	3.030	3.060	3.060	3.080	3.080	3.080
3.110	3.120	3.150	3.150	3.150	3.150	3.160	3.160
3.180	3.190	3.200	3.210	3.220	3.220	3.230	3.240
3.240	3.240	3.250	3.260	3.260	3.260	3.260	3.280
3.280	3.280	3.280	3.280	3.290	3.290	3.290	3.290
3.290	3.290	3.290	3.290	3.290	3.290	3.290	3.290
3.290	3.300	3.300	3.300	3.300	3.300	3.300	3.300
3.300	3.300	3.300	3.300	3.300	3.300	3.300	3.300
3.300	3.300	3.300	3.300	3.300	3.300	3.300	3.300
3.300	3.300	3.320	3.320	3.320	3.320	3.320	3.320
3.320	3.320	3.320	3.320	3.320	3.320	3.320	3.320
3.320	3.320	3.320	3.320	3.320	3.320	3.320	3.320
3.320	3.320	3.320	3.320	3.320	3.320	3.320	3.320
3.320	3.320	3.320	3.320	3.320	3.320	3.320	3.320

$A^M_{3D}(j)$

5.200	5.500	5.500	5.700	5.700	6.000	6.100	6.100
6.100	6.300	6.400	6.400	6.450	6.500	6.550	6.570
6.600	6.650	6.750	6.850	6.850	6.900	6.900	6.900
7.000	7.000	7.000	7.050	7.100	7.100	7.100	7.100
7.150	7.200	7.200	7.200	7.290	7.290	7.300	7.340
7.340	7.340	7.340	7.350	7.350	7.350	7.350	7.430
7.430	7.430	7.430	7.430	7.450	7.450	7.450	7.450
7.450	7.450	7.450	7.450	7.450	7.450	7.450	7.450
7.450	7.500	7.500	7.500	7.500	7.500	7.500	7.500
7.500	7.500	7.500	7.500	7.500	7.500	7.500	7.500
7.500	7.500	7.500	7.500	7.500	7.500	7.500	7.500
7.500	7.500	7.500	7.500	7.500	7.500	7.500	7.500
7.500	7.500	7.500	7.500	7.500	7.500	7.500	7.500
7.500	7.500	7.500	7.500	7.500	7.500	7.500	7.500
7.500	7.500	7.500	7.500	7.500	7.500	7.500	7.500
7.500	7.500	7.500	7.500	7.500	7.500	7.500	7.500

$q^M_m(i)$

$i \rightarrow$	1	2						
1	4.210	4.130	4.070	4.020	3.970	3.930	3.900	3.870
9	3.840	3.820	3.800	3.780	3.760	3.750	3.730	3.720
↓	3.700	3.690	3.680	3.670	3.660	3.650	3.640	3.630
⋮	3.620	3.620	3.610	3.600	3.600	3.590	3.580	3.580
	3.570	3.570	3.570	3.560	3.560	3.550	3.550	3.550
	3.540	3.540	3.530	3.530	3.530	3.530	3.520	3.520
	3.520	3.520	3.510	3.510	3.510	3.510	3.510	3.500
	3.500	3.500	3.500	3.500	3.490	3.490	3.490	3.490
	3.490	3.490	3.490	3.490	3.480	3.480	3.480	3.480
	3.480	3.480	3.480	3.480	3.480	3.480	3.480	3.470
	3.470	3.470	3.470	3.470	3.470	3.470	3.470	3.470
	3.470	3.470	3.470	3.470	3.470	3.470	3.470	3.470
	3.470	3.460	3.460	3.460	3.460	3.460	3.460	3.460
	3.460	3.460	3.460	3.460	3.460	3.460	3.460	3.460
	3.460	3.460	3.460	3.460	3.460	3.460	3.460	3.460
	3.46	3.46	3.46	3.46	3.46	3.46	3.46	3.46

Main Sensor, Transparency, Positive Ions.

$$\epsilon = \sqrt{\frac{1}{\zeta} - 1} \quad ; \quad N = \frac{\phi_N}{|\phi_s|} \quad ; \quad \zeta = z\frac{2e\phi_n}{m_n v_z^2} \quad ; \quad \frac{1}{\zeta} - 1 = \epsilon^2 \; ; \; \zeta = \frac{1}{1+\epsilon^2}$$

$$\tau_x = \frac{v_x}{v_z} \qquad \psi = \frac{v_x^2}{v_z^2}$$

$$G(\tau_x, \tau_y) = G_1(\tau_x^2) G_1(\tau_y^2)$$

$$G_1(\psi) = \frac{1}{(1-c)^9}\left(1 - c\sqrt{1+\psi}\right)^5 \left(1 - c\sqrt{1+\frac{\psi}{1-\zeta}}\right)^3 \left(1 - c\sqrt{1+\frac{\psi}{1+\zeta/N}}\right)$$

For $\psi \ll (1-\zeta)$:

~~$G \approx G_0\left(1 - 5c\left(1+\frac{1}{2}\psi\right)\right)\left(1 - 3c - \frac{3c\psi}{2(1-\zeta)}\right)\left(1 - c - \frac{c\psi}{2(1+\zeta/N)}\right)$~~

~~$\approx 1 - \frac{5\psi c}{2(1-3c)}$~~

$$G \cong \left(\frac{1 - c - \frac{1}{2}c\psi}{1-c}\right)^5 \left(\frac{1 - c - \frac{c\psi}{2(1-\zeta)}}{1-c}\right)^3 \left(\frac{1 - c - \frac{c\psi}{2(1+\zeta/N)}}{1-c}\right)$$

$$\approx \left(1 - \frac{5}{2}\frac{c}{1-c}\psi - \frac{3}{2}\frac{c}{1-c}\frac{\psi}{1-\zeta} - \frac{c}{2(1-c)}\frac{\psi}{1+\zeta/N}\right)$$

$$= 1 - a_0\psi \quad ; \quad \boxed{a_0 = \frac{c}{2(1-c)}\left(5 + \frac{3}{1-\zeta} + \frac{1}{1+\zeta/N}\right)}$$

$$\frac{c}{2(1-c)} = \frac{1}{42 \times 2\left(1 - \frac{1}{42}\right)} = \frac{1}{2(41)} = .0122$$

ϵ	ζ	a_0 $N=.3$	$N=1$	$N=3$	$N=10$	$N=\infty$	$5+\frac{3}{1-\zeta}$
.10	.990	3.72				3.73	305
.15	.978	1.72				1.73	141
.2	.962	1.03				1.04	83.9 41.1
.3	.917	.504				.514	~~41.1~~
.4	.862	.329				.338	26.7
.5	.800	.247				.256	20
.6	.735	.202				.211	16.3
.8	.610	.161				.167	12.7
1.0	.500	.139				.146	11.0

$$1 - \zeta = \frac{\epsilon^2}{1+\epsilon^2}$$

$$\frac{1}{1-\zeta} = 1 + \frac{1}{\epsilon^2}$$

(N=1)

$$\boxed{a_0 \cong \frac{c}{2(1-c)}\left(8.5 + \frac{3}{\epsilon^2}\right)}$$

$$a_0(\epsilon = \infty) \cong .110$$

Main Sensor (pos. ions)

(N=1)

$$G = g_2(\psi, \epsilon)\, g_1$$

ψ	$g_1(\psi)$	ϵ=.15	ϵ=.2	.3	.4	.5	.6	.8	1.0
0	1.000	1	1	1	1	1	1	1	1
0.01	1.101	.985	.991	.995	.997	.998	.998	.999	.999
.05	1.098	.939	.959	.978	.985	.988	.990	.992	.993
.10	1.095	.898	.929	.959	.971	.977	.981	.985	.987
.25	1.085	.814	.863	.913	.936	.948	.956	.963	.976
.50	1.071	.720	.787	.857	.890	.909	.921	.933	.940
.75	1.059	.652	.730	.813	.854	.877	.892	.908	.916
1.0	1.047	.598	.682	.776	.822	.848	.865	.884	.894
1.5	1.025	.512	.606	.714	.768	.799	.820	.843	.856
2.0	1.006	.447	.547	.664	.723	.759	.782	.809	.823
3.0	.973	.351	.457	.585	.652	.693	.719	.751	.767
4.0	.945	.282	.389	.523	.595	.640	.669	.703	.722
5.0	.920	.231	.336	.473	.548	.595	.626	.663	.683
6.0	.897	.190	.293	.431	.508	.556	.589	.628	.649
7.0	.877	.158	.257	.395	.473	.523	.557	.597	.619
8.0	.857	.132	.227	.363	.442	.493	.527	.568	.591
9.0	.840	.110	.200	.335	.415	.466	.501	.543	.567
$1-\tau$		.022	.038	.083	.138	.200	.265	.390	.500
$1+\tau$		1.978	1.962	1.917	1.862	1.800	1.735	1.610	1.50

$$g_1 = \frac{1}{(1-\epsilon)^9}\left(1-\tfrac{1}{\sqrt{2}}\sqrt{1+\psi}\right)^5 = .805\left(1-\tfrac{1}{\sqrt{2}}\sqrt{1+\psi}\right)^5$$

$$g_2 = \left(1-\tfrac{1}{\sqrt{2}}\sqrt{1+\frac{\psi}{1-\tau}}\right)^3\left(1-\tfrac{1}{\sqrt{2}}\sqrt{1+\frac{\psi}{1+\tau}}\right)$$

$g_2 = 0$ for $\psi \geq 2.48$

$g_1(1.4) = .766$

$\epsilon=1$ $g_2(1.4) = .612$ $G(1.4) = .469$

$$\ln G(1)/G(2) = a\Delta\psi \qquad a_1 = \frac{\ln G_1/G_2}{\Delta\psi}$$

ψ	$\Delta\psi$	ϵ=.15	.2	.3	.4	.5	.6	.8	1.0	
0	.05	1.26	.837	.445	.302	.241	.201	.161	.140	a_1
.05	.10	1.08	.736	.419	.294	.233	.192	.151	.131	
.10										
3	1	.219	.161	.112	.0915	.0801	.0721	.066	.029	a_2
4										

$$G \cong C_1 e^{-a_1\psi} + C_2 e^{-a_2\psi} = Cy_1 + (1-C)y_2 = C(y_1 - y_2) + y_2$$

($y_1 = e^{-a_1\psi}$, $y_2 = e^{-a_2\psi}$)

$$C = \frac{G - y_2}{y_1 - y_2} = \frac{y_2 - G}{y_2 - y_1}$$

$\psi = 4$: $\epsilon = 1$

$e^{-a_1\psi} = .57 = y_1$

$e^{-a_2\psi} = .890 = y_2$

$$C = \frac{.89 - .745}{.89 - .57} = .45$$

$G(1) = .45e^{-.140} + .55e^{-.029} = .925$ +3%

$G(9) = .551$ -3%

$G(.5) = .962$ +2%

($\psi = 4$)

	ϵ=.15	.2	.3	.4	.5	.6	.8	1.0	
y_1	.0065	.0352	.169	.299	.381	.448	.525	.571	
y_2	.416	.525	.639	.694	.726	.749	.77	.89	
G	.282	.389	.529	.595	.640	.669	.703	.745	
C	.327	.278	.247	.250	.250	.266	.273	.450	
a_1	1.26	.837	.445	.302	.241	.201	.160	.140	
a_2	.219	.161	.112	.092	.080	.072	.066	.029	
G(1)	.541 .634	.615 .735	.673 .831					.925	fit
	.598	.682	.776	.822	.848			.894	analytic
G(4)	.280 .282								

Aug 11, 1980

Dear Ed,

Here is the Response Function for the Voyager Main Sensors (A, B, C cups):

1) Definition for M-Mode:

$$\Delta I_j^{(a)} = A_{eff}\, Ze\, \bar{v}_{zj}\, \Delta v_{zj} \iint \underbrace{R_j(v_x, v_y)}_{\text{Response function}} \underbrace{f_a(\vec{v})}_{\text{distribution function}} dv_x\, dv_y$$

$\Delta I_j^{(a)}$: current in j^{th} channel due to species "a" ($j = 1, \ldots, 128$)

$$A_{eff} = 102\,cm^2 \times .64^{\dagger} = 66\,cm^2$$

† Transparency at normal incidence

$$\bar{v}_{zj} = \sqrt{\frac{2Ze\bar{\phi}_j}{A m_p}}$$

(m_p = proton mass, A = atomic weight)

Δv_{zj} = "rel. window width" (see your tables) for j^{th} channel

R_j is normalized such that $R_j(0,0) = 1$

2) Cup coordinates

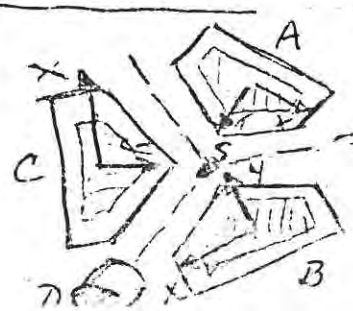

S = sym. axis and s/c z-axis pointing into paper

z-axes for A, B, C cups point into paper

$$\cos\theta_{A,B,C} \equiv \hat{z}_{s/c} \cdot \hat{z}_{A,B,C}; \quad \theta_{A,B,C} = 20°$$

$$\hat{x}_{A,B,C} \cdot \hat{z}_{s/c} = 0$$

"Negative Cup Normals", $\hat{z}_{A,B,C}$, in s/c coord. system:

$(\hat{i}_{s/c}, \hat{j}_{s/c}, \hat{k}_{s/c})$

$$\hat{z}_A = (.296, .171, .940)$$

$$\hat{z}_B = (-.296, .171, .940)$$

$$\hat{z}_C = (0, -.342, .940)$$

{ also $\hat{z}_D = (-.731, -.682, .035)$ just for your information }

---

3) Analytical Approx. for R_j:

$$R_j = \underbrace{G_j\left(\frac{v_x}{\bar{v}_{zj}}\right) G_j\left(\frac{v_y}{\bar{v}_{zj}}\right)}_{\text{Transpar. fcts}} \underbrace{P_j(x,y)}_{\text{Sensitive Area function}}$$

$$G_j(\psi) = c_j e^{-a_j \psi^2} + (1-c_j) e^{-b_j \psi^2}$$

(ψ = either $v_x/\bar{v}_{zj}$ or $v_y/\bar{v}_{zj}$)

a_j, b_j, c_j depend on channel width and are given by:

$$a_j = \frac{2.16\times10^{-2}}{\epsilon_j^{2.22}}\left(1+25.6\epsilon_j^{1.86}\right)$$

$$b_j = \frac{4.16\times10^{-3}}{\epsilon_j^{1.91}}\left(1+9.73\epsilon_j^{1.68}\right)$$

$$c_j = \frac{0.141}{\epsilon_j^{.401}}\left(1+0.125\epsilon_j^{8.92}\right)$$

Only valid for antisymmetric form

where $\epsilon_j = \sqrt{\frac{Am_p\bar{v}_{zj}^2}{2Ze\bar{\phi}_j^{max}} - 1} = \sqrt{\frac{\bar{\phi}_j}{\phi_j} - 1} = \sqrt{\frac{\Delta\phi_j}{2\phi_j}}$

(where ϕ_j is threshold voltage, $\bar{\phi}_j = \frac{\phi_{j+1}+\phi_j}{2}$ (See Figure))

The arguments in $P_j(x,y)$ are defined as follows:

$$x \equiv S_j\frac{v_x}{\bar{v}_{zj}} \quad ; y \equiv S_j\frac{v_y}{\bar{v}_{zj}}$$

where S_j is the "shift function" and is given, to an excell. approx., by:

$$S_j = \frac{.093\sqrt{1+\epsilon_j^2}}{\epsilon_j} + \frac{.741\sqrt{1+\epsilon_j^2}}{\epsilon_j+\sqrt{1+\epsilon_j^2}} + .535$$

In so-called Trapezoidal ("poor man's approx") Approx we have (with better than 6% accur. for $R_j > .06$)

$$P_j(x,y) \cong P(x) \begin{cases} \dfrac{y - y_D'}{y_D - y_D'} & y_D' < y < y_D \\ 1 & y_D < y < y_U \\ \dfrac{y_U' - y}{y_U' - y_U} & y_U < y < y_U' \end{cases}$$

($P_j = 0$ elsewhere)

where $$P(x) = \begin{cases} 1 & 0 < |x| < x_C \\ \dfrac{x_C' - |x|}{x_C' - x_C} & x_C < |x| < x_C' \\ 0 \text{ elsewhere} \end{cases}$$

Note:

(a) y_D', y_D, x_C, x_C' are fixed dimensionless numbers, viz:

$$y_D' = -3.63 \quad , \quad y_D = -2.02$$

$$x_C = 1.10 \quad , \quad x_C' = 4.94$$

(b) y_U and y_U' are functions of x:

$$y_U(x) = \frac{.762 \cos(1.018|x| + .247)}{1 + 0.25|x|}$$

(cos-argument in radians)

$$y_U'(x) = 2.50 - 0.125(|x|+1)^2$$

Best regards,

Stan

P.S. See figure 2 for graph. representation of $P_j(x,y)$ and Fig. 3 (an example for $\epsilon_j = .15$) for $R_j(x,y)$

TH-mode

Fig. 1

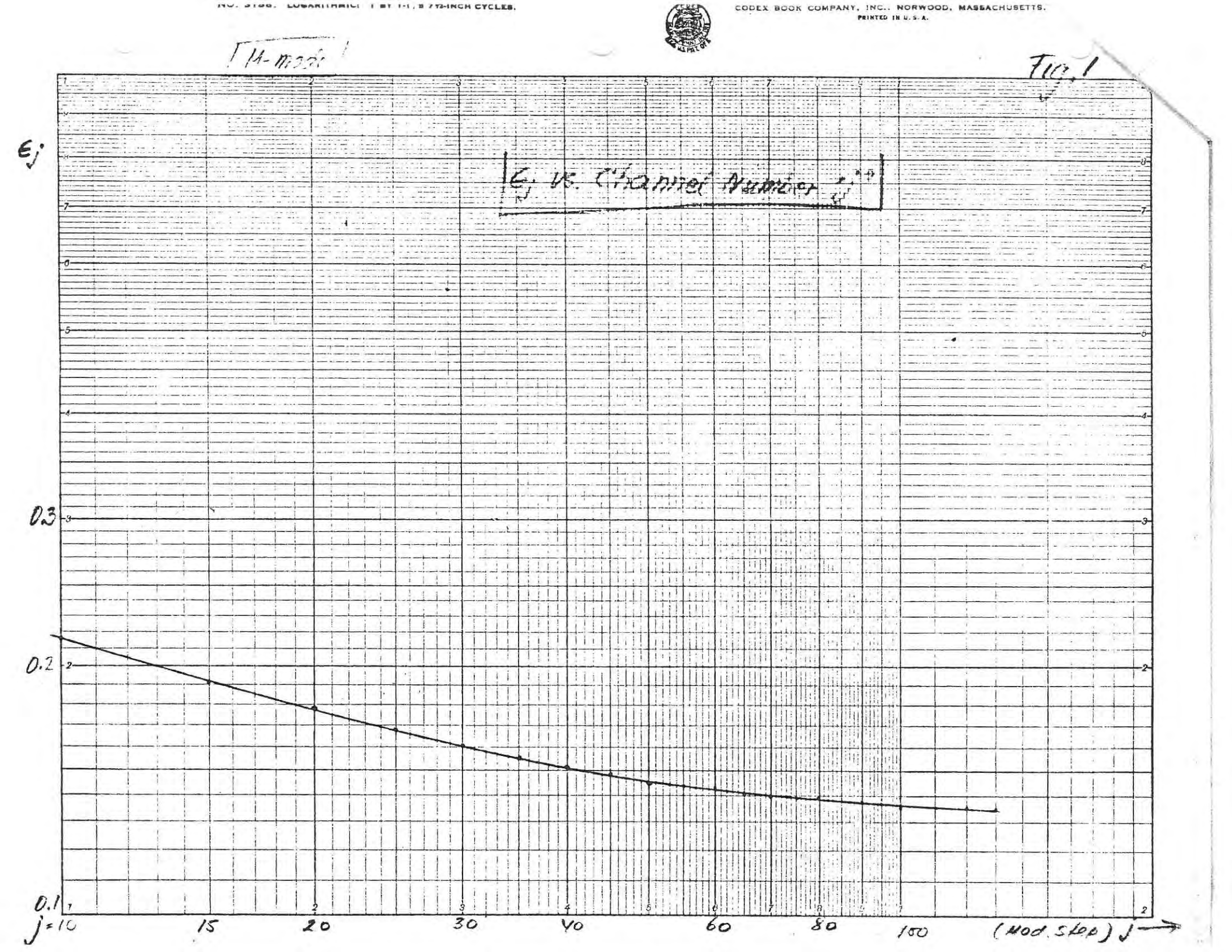

32 dia

GSG 13:59:27 Thursday, 31st January, 1980

Fig. 2
$P_i(x,y)$

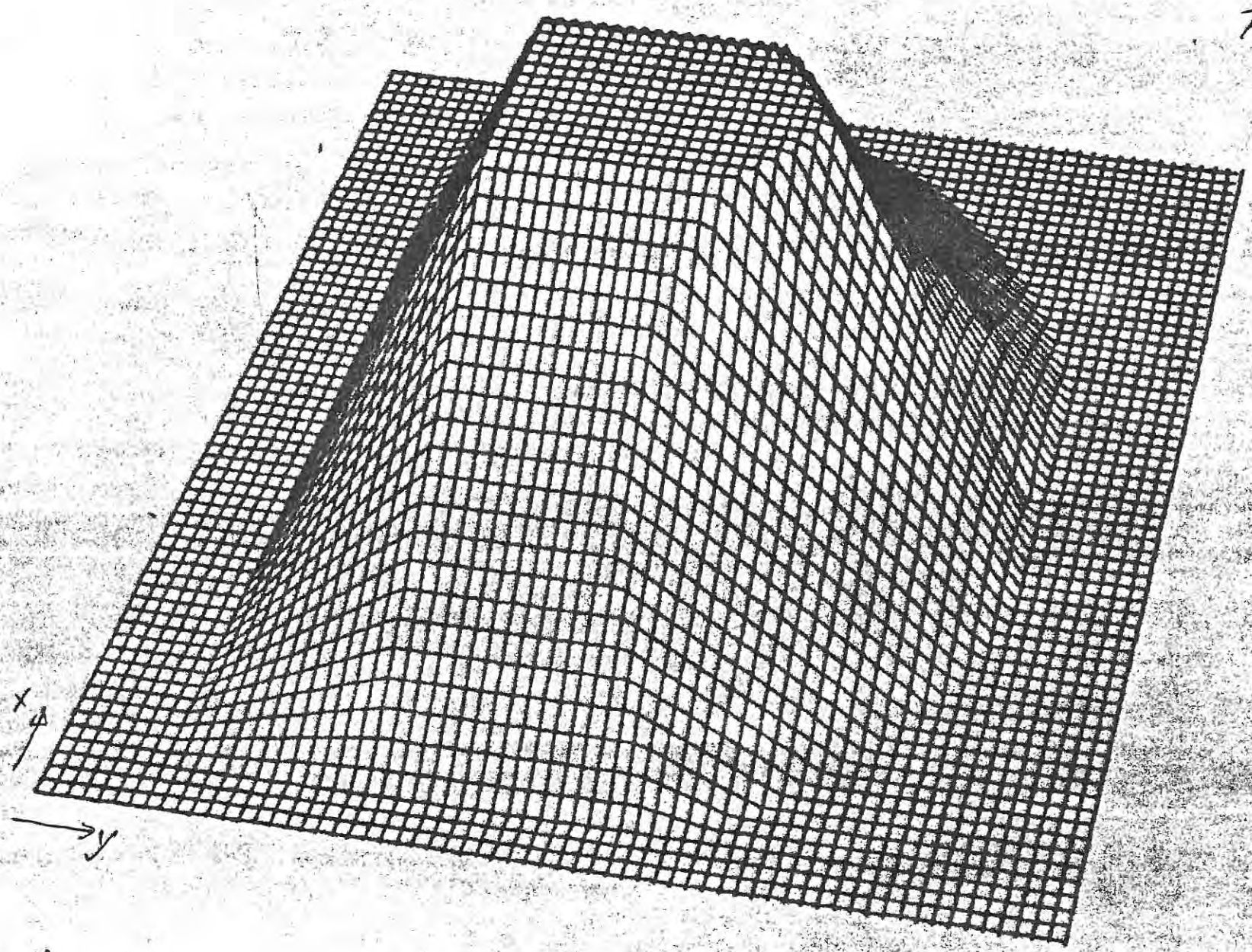

50, 10, 10

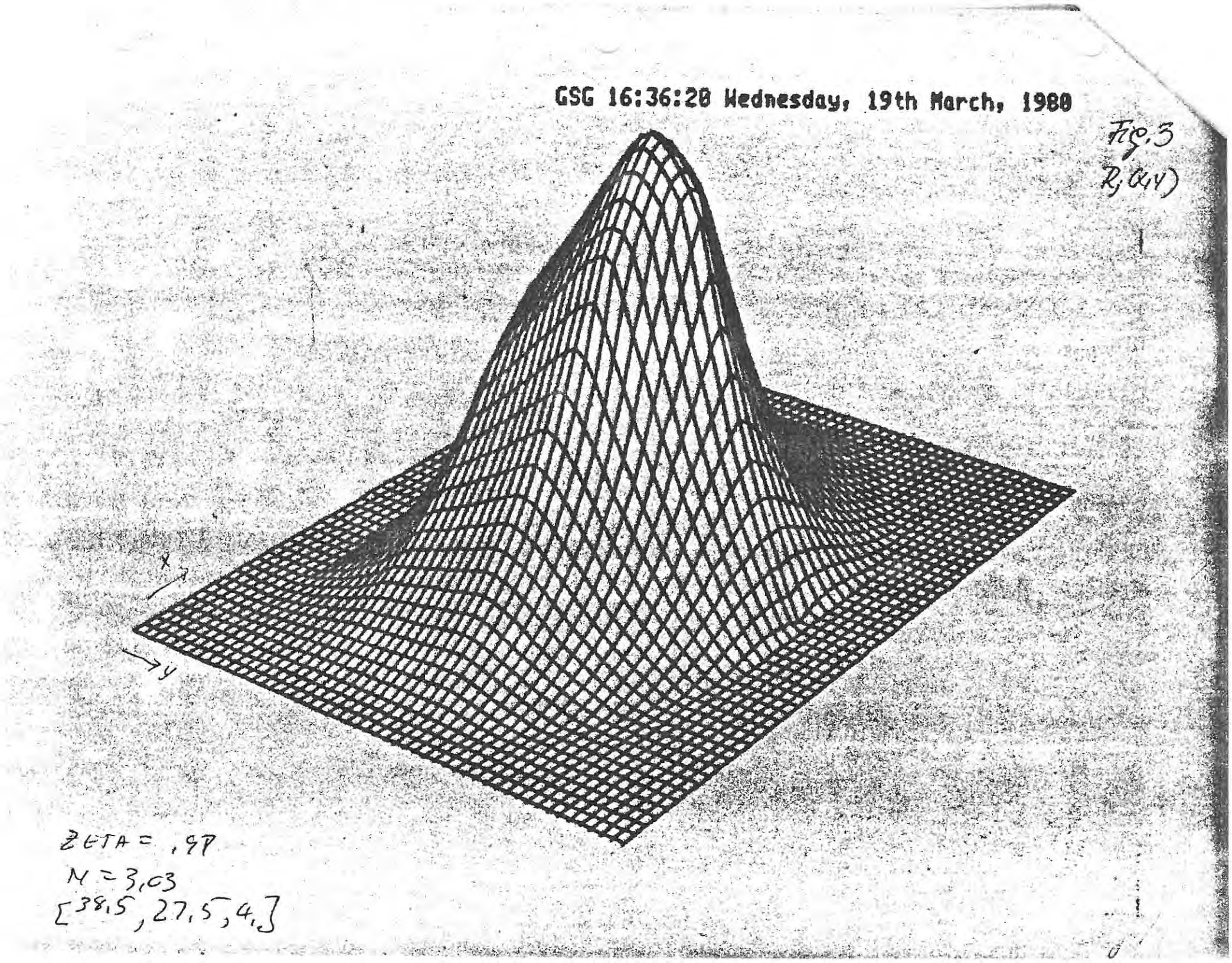
GSG 16:36:20 Wednesday, 19th March, 1980
Fig. 3
$R_j(x,y)$
x
y
BETA = .97
N = 3,03
[38.5, 27.5, 4.]